REGULATION OF CXC CHEMOKINE RECEPTOR FUNCTION THROUGH INTRACELLULAR TRAFFICKING AND NOVEL RECEPTOR-INTERACTING PROTEINS

By

Nicole Fowler Neel

Dissertation

Submitted to the Faculty of the

Graduate School of Vanderbilt University

In partial fulfillment of the requirements

for the degree of

DOCTOR OF PHILOSOPHY

in

Cancer Biology

May, 2008

Nashville, Tennessee

Approved:

Professor Albert B. Reynolds

Professor Ann Richmond

Professor James R. Goldenring

Professor Alissa M. Weaver

Professor Raymond L. Mernaugh

To my parents, for their immeasurable love

and their unwavering belief in me always

and

To my husband, Mike, for all his love, patience and kindness

ACKNOWLEDGEMENTS

I would first like to thank Dr. Ann Richmond for all her support and guidance over the past few years. Her mentoring has contributed so much to my development as a scientist during my graduate research experience. She has supplied immense energy and excitement regarding my research. While always providing support she has promoted my abilities as an independent thinker and her confidence in my abilities allowed me to accomplish so much. I must also extend my sincere gratitude to all the members of the Richmond laboratory who are truly a fantastic group of people. Jiqing Sai has offered tremendous help over the years with techniques and scientific discussion. Sarah Short was an enormous help with the animal studies and Snjezana Milatovic performed the immunohistochemical staining for the in vivo studies. In particular, my thanks to Linda Horton, whose vigor is truly an inspiration and whose support and friendship over the years have kept me motivated.

I want to next thank all the members of my committee. Dr. Jim Goldenring has been an outstanding resource as a collaborator on the RhoB trafficking and proteomics studies. In addition, the RhoB studies would not have been possible without the help of Dr. Lynne Lapierre in his laboratory. Dr. Ray Mernaugh was instrumental in the development of the protocol used for the proteomics analyses as well as the biochemical techniques utilized to characterize the protein-protein interactions. He has also been an incredible mentor for me providing support and encouragement. I would also like to thank Dr. David Blum in his laboratory

for his help with the protein biochemistry. Dr. Reynolds has also been a terrific mentor and advocate providing career advice and constructive criticism that has greatly aided in my scientific development. Dr. Weaver has provided great motivation through her energetic feedback on data.

I would like to thank Dr. Amy Ham and the Vanderbilt Proteomics core for their collaboration on the proteomics studies. In addition, Dr. Dawn Kilkenny-Rocheleau and Dr. Sam Wells and the Vanderbilt Cell Imaging Shared Resource Core must also be thanked for all their assistance with imaging and analysis over the years. I must also acknowledge the VA Flow Cytometry Special Resource Center for all their assistance with FACS analysis over the years.

I must also acknowledge Dr. Frank Gertler at Massachusetts Institute of Technology and members of his laboratory particularly Dr. Melanie Barzik and Dr. Elaine Pinheiro for their terrific collaboration on the VASP studies. This work would not have been possible without the contribution of their expertise.

Finally, I must thank my wonderful family for their unconditional love and support over the years. My parents have believed in my abilities and for that I am eternally grateful. They have always instilled in me a passion for learning, the value of perseverance, and the importance of impacting the lives of others with hard work. I owe my husband Mike a special thank you for his incredible love, backing, and partnership without which none of this would have been possible. He has always given me the freedom to pursue my goals whole-heartedly. This has been indispensable for my motivation and passion for the science.

I would like to acknowledge the Multidisciplinary Basic Research Training in Cancer grant T32CA09592, NCI grant CA34590 to A.R., Vanderbilt-Ingram Cancer Center Support grant CA68485, Eli Lilly, and Ingram Professorship to A.R. for the funding that allowed me to do this work.

Elements of this work have been previously published in peer-reviewed journals in the following references:

Neel NF, Lapierre L, Goldenring J, Richmond A (2007). RhoB plays an essential role in CXCR2 sorting decisions. *Journal of Cell Science* **120**:1559-1571.

Ueda Y, **Neel NF**, Schutyser E, Raman D, Richmond A (2006). Deletion of the Carboxyl Terminal Domain of CXCR4 Leads to the Down-regulation of Cell-Cell Contact, Enhanced Motility and Proliferation in Breast Carcinoma Cells. *Cancer Research* **66**:5665-5675.

Neel NF, Schutyser E, Sai J, Fan GH, Richmond A. 2005. Chemokine receptor internalization and intracellular trafficking. *Cytokine and Growth Factor Reviews* **16**:637-658.

TABLE OF CONTENTS

LIST OF TABLES

Table Page

LIST OF FIGURES

LIST OF ABBREVIATIONS

ABTS	2,2’-azino-bis (3-ethylbenzothiazoline-6-sulfonic acid)
Akt	AKR mouse thymoma serine kinase
ANOVA	Analysis of variance
AP-2	Adaptin-2
APC	Adenomatous polyposis coli
Arp 2/3	Actin-related protein 2/3
CHIPS	Complete Hierarchical Integration of Protein Searches
CLIP-170	Cytoplasmic linker protein-170
COCO	Coiled-coil
CTD	Carboxyl-terminally deleted
cAMP	Cyclic adenosine monophosphate
DMEM	Dulbecco's modified Eagle's medium
DMSO	Dimethyl sulfoxide
EEA-1	Early endosomal antigen-1
EGF	Epidermal growth factor
EGTA	Ethylene glycol tetraacetic acid
EMT	Epithelial-to-mesenchymal
ERK	Extracellular signal-regulated kinase
EVH	Ena/VASP homology
EVL	Ena-VASP-like
FAB	F-actin binding

FACS	Fluorescence-activated cell sorting
FBS	Fetal bovine serum
FGF	Fibroblast growth factor
fMLP	Formyl-met-leu-phe
FPR	N-Formyl peptide receptor
GAP	GTPase-activating protein
GDI	GDP dissociation inhibitor
GDP	Guanosine diphosphate
GEF	Guanine nucleotide exchange factor
GPCR	G protein-coupled receptor
GRK	G protein-coupled receptor kinases
GST	Glutathione *S*-transferase
GTP	Guanosine triphosphate
HER2	Human epidermal growth factor receptor
IPTG	Isopropyl b-D-thiogalactopyranoside
IQGAP1	IQ motif containing GTPase activating protein 1
LAMP-1	Lysosome-associated membrane protein 1
Lasp-1	LIM and SH3 domain protein-1
LC/MS/MS	Liquid chromatography-mass spectrometry-mass spectrometry
MAPK	Mitogen activated protein kinase
Mena	Mammalian enabled
MMP	Matrix metalloproteinase
MPO	Myeloperoxidase

MPR	Mannose-6-phosphate receptor
MTOC	Microtubule-organizing-center
PCR	Polymerase chain reaction
PDZ	Post synaptic density protein (PSD95)/Disc Large (DlgA)/Zonula occludens (ZO-1)
PH	Pleckstrin homology
PI3K	Phosphatidylinositol 3-kinase
PI(3)P	Phosphatidylinositol 3-phosphate
PKA/C/G	Protein kinase A/C/G
PLC	Phospholipase C
PP2A	Protein phosphatase 2A
PRK1	Protein kinase C-related kinase 1
PRR	Proline-rich region
PTD	Protein transduction domain
PtdIns(3,4,5)P3	Phosphatidylinositol-3,4,5-tripshosphate
Rab11-FIP2	Rab11-Family Interacting Protein 2
RGS	Regulators of G-protein signaling
RNAi	RNA interference
RPMI	Roswell Park Memorial Institute media
SDF-1α	Stromal-derived factor-1 alpha
SH3	Src homology 3
siRNA	Small interfering RNA
SNAP	Synaptosomal-associated protein

TAT	Transactivator of transcription
TfnR	Transferrin receptor
TRBD	Rhotekin Rho-binding domain
VASP	Vasodilator-stimulated phosphoprotein
WASP	Wiskott-Aldrich syndrome protein
WAVE	WASP family verprolin-homologous proteins
WHIM	Warts, hypogammaglobulinemia, infections, and myelokathexis
ZO-1	Zonula occludens

CHAPTER I

INTRODUCTION

Chemokines are a family of chemotactic cytokines that bind seven transmembrane G protein-coupled receptors. Chemokines are classified based on the position of conserved cysteine residues in the amino-terminus into the CC, CXC, CX3C, and C subfamilies (Murphy et al., 2000). The corresponding chemokine receptors can be somewhat specific in the binding of chemokines, as is the case for CXCL12 which binds only CXCR4 and CXCR7, or receptors can be more promiscuous in chemokine binding, such as CXCR2 for example, which binds CXCL1, 2, 3, 5, 6, 7, and 8. In recent years chemokines have gained greater recognition as mediators of tumorigenesis and metastasis. Newly characterized roles in inflammation-mediated tumorigenesis, angiogenesis, and metastasis have established chemokines as therapeutic targets for cancer treatment. Therefore, understanding the biology of chemokines and their receptors is crucial for the development of novel therapeutics. The cellular responses elicited by chemokines are in part regulated through the internalization and intracellular trafficking of chemokine receptors. In addition, the chemotactic response is regulated through previously identified adaptor proteins and likely through novel proteins complexes that interact with the cytoplasmic domains of the receptors. Understanding the intracellular trafficking mechanisms and the identification of components of the cytoplasmic protein complexes that regulate

the chemotactic response will greatly impact the field and aid in the identification of potential therapeutic targets for the treatment of malignancies.

Internalization and trafficking of chemokine receptors

Regulation and functional significance of internalization

Chemokine receptors undergo a basal level of internalization, followed by degradation or recycling, in the absence of ligand. Ligand binding can greatly enhance the internalization and trafficking of these G protein-coupled receptors (GPCRs) and can increase the dynamics of receptor sensitization versus desensitization and of receptor recycling versus degradation. The receptor trafficking pathways may vary depending on the presence or absence of ligand. Two major choices are available for this trafficking: clathrin-mediated endocytosis and/or lipid raft/caveolae-dependent internalization. Some receptors take advantage of both of these pathways, while others may follow one pathway the majority of the time. The cell type in which the receptor is expressed may in part determine the likelihood of utilization of one pathway as compared to another. This may be due to the ratio of specific adaptor proteins, the lipid composition of the membrane in proximity to the domain to which the receptor is localized, or other poorly characterized determinates. The fate of the receptor after ligand stimulation (to traffic or not to traffic) may affect the length, strength, or type of intracellular signals generated. Moreover, the type of post-translational

modifications of the receptor can also have major effects on ligand mediated signaling.

A major mechanism by which chemokine receptors undergo ligand-induced internalization is through clathrin-mediated endocytosis (Figure 1) (Signoret et al., 2005; Venkatesan et al., 2003; Vila-Coro et al., 1999; Weber et al., 2004; Yang et al., 1999). The binding of ligand results in phosphorylation of Ser and Thr residues in the intracellular loops and carboxyl-terminus of the chemokine receptor by G protein-coupled receptor kinases (GRKs) (Ferguson, 2001; Ferguson et al., 1998; Freedman and Lefkowitz, 1996; Krupnick and Benovic, 1998). Phosphorylation results in the uncoupling of the G protein subunits from the receptor and receptor desensitization in some cases (Ferguson et al., 1996; Krupnick and Benovic, 1998). In addition, the phosphorylation of these residues and/or the presence of di-leucine motifs in the carboxyl-terminal domain of chemokine receptors are important for the recruitment of adaptor molecules that link the receptor to a lattice of clathrin that facilitates receptor internalization. Two adaptor molecules that play important roles in G protein-coupled receptor internalization are adaptin-2 (AP-2) and β-arrestin. β-arrestin binds with high affinity to the phosphorylated receptor, to the β2-adaptin subunit of the AP-2 heterotrimeric protein complex, and to clathrin to mediate endocytosis (Benovic et al., 1987; Fan et al., 2001b; Goodman et al., 1996; Laporte et al., 1999; Lohse et al., 1990; Pippig et al., 1993). It was originally thought that β-arrestin binding to GPCRs was only mediated through phosphorylated residues in the carboxyl-terminus. However, more recent

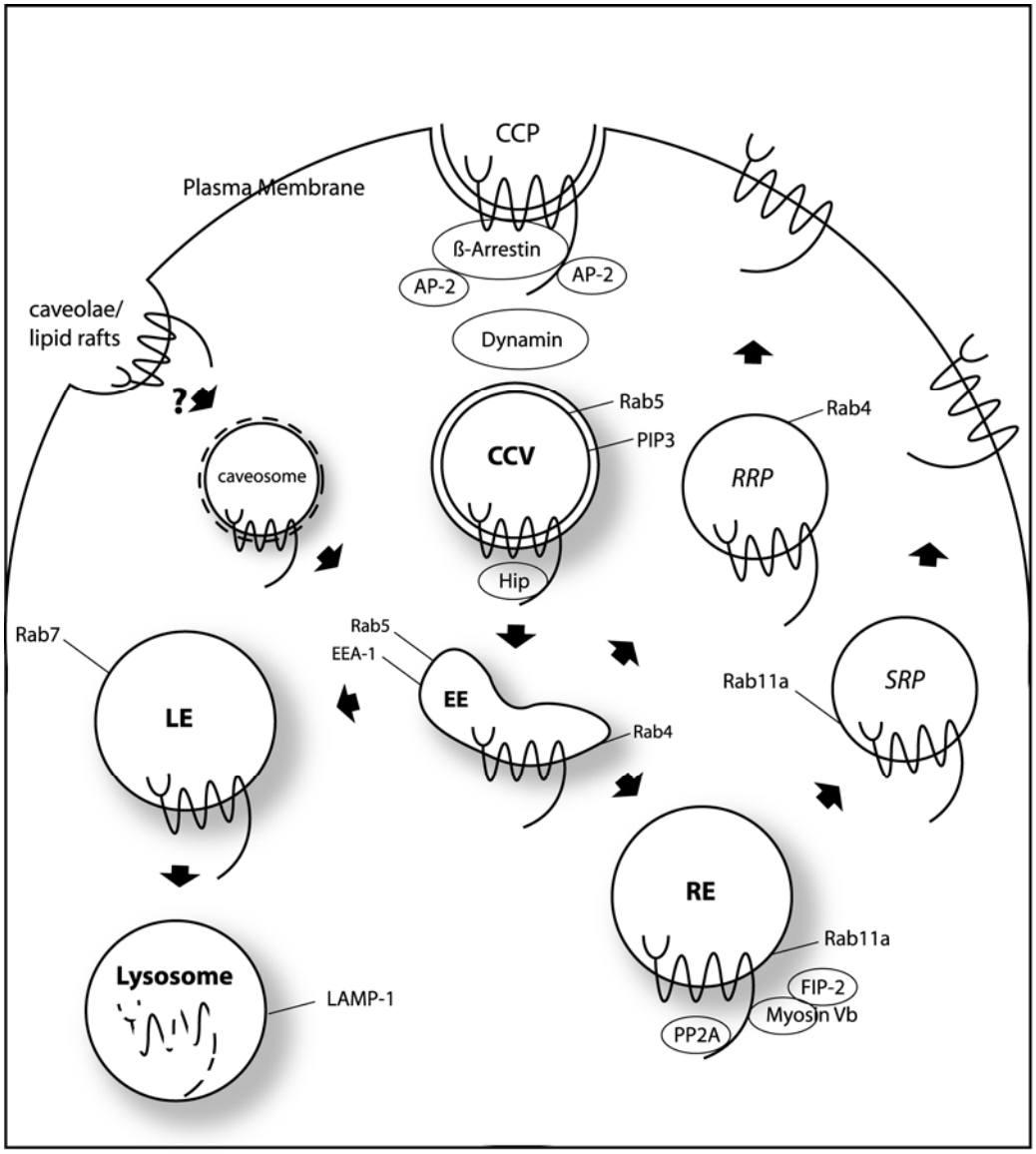

Figure 1: Schematic of chemokine receptor endocytosis and intracellular trafficking.
CCP: clathrin-coated pit, CCV: clathrin-coated vesicle, EE: early endosome, LE: late endosome, RE: recycling endosome, RRP: rapid recycling pathway, SRP: slow recycling pathway, EEA-1: early endosomal antigen-1, FIP-2: Rab11-family interacting protein-2, LAMP-1: lysosomal-associated membrane protein-1.

chemokine receptor studies suggest that binding can also occur through the intracellular loops. Studies on CCR5 demonstrate that phosphorylated Ser residues in the carboxyl-terminus and a conserved Asp-Arg-Tyr sequence motif in the second intracellular loop are necessary for β-arrestin association (Huttenrauch et al., 2002). Moreover, β-arrestin binds to both the carboxyl-terminus and the third intracellular loop of CXCR4 (Cheng et al., 2000). AP-2 binds directly to some chemokine receptors, including CXCR2 and CXCR4, through highly conserved Leu-Leu, Ile-Leu, Leu-Ile motifs in the carboxyl-terminus (Fan et al., 2001b; Heilker et al., 1996). The association of receptors with these adaptor molecules results in recruitment of clathrin and formation of clathrin-coated pits which 'pinch off' from the membrane through the action of dynamin and become clathrin-coated vesicles (Barlic et al., 1999; Colvin et al., 2004; Droese et al., 2004; Jimenez-Sainz et al., 2003; Orsini et al., 1999; van der Bliek et al., 1993; Vila-Coro et al., 1999; Weber et al., 2004; Yang et al., 1999). The clathrin-coated vesicle is then uncoated and the receptor-ligand complex enters the early endosomal compartment. Recent findings suggest that β-arrestin not only plays an important role in the desensitization and internalization of chemokine receptors, but also in the intracellular trafficking of chemokine receptors. According to immunofluorescence staining and confocal microscopy, β-arrestin accompanies CXCR4 to the early endosome following CXCL12-induced internalization (Orsini et al., 1999). However, it remains unclear whether this endosomal colocalization points to an active contribution of β-arrestin to the endosomal trafficking of CXCR4 or whether it is just a consequence of the

binding of β-arrestin to both clathrin and CXCR4 during internalization. The chemokine receptor can then either enter the perinuclear recycling compartment and traffic back to the plasma membrane to be re-exposed to ligand, or it can enter the late endosomal compartment where it will be sorted to the lysosomal compartment for degradation.

Regulation of chemokine receptor trafficking by Rab GTPases

Rabs are small GTPases that cycle between GDP-bound (inactive) and GTP-bound (active) states and regulate a number of cellular trafficking events. The exchange of GDP for GTP, GTP hydrolysis, and GDP displacement are regulated by guanine nucleotide exchange factors (GEFs), GTPase-activating proteins (GAPs), and GDP dissociation inhibitors (GDIs), respectively. Rabs are post-translationally modified with geranyl-geranyl groups at their carboxyl-termini (Pereira-Leal and Seabra, 2000; Zerial and McBride, 2001). This modification allows Rabs to associate with intracellular membrane-bound compartments. Interestingly, individual Rab family members associate with particular endocytic compartments. For example, Rab4 and Rab5 associate with the early endocytic compartment (Bucci et al., 1992; Gorvel et al., 1991; van der Sluijs et al., 1992) and Rab11 associates with the perinuclear recycling compartment (Casanova et al., 1999; Green et al., 1997; Ren et al., 1998), and Rab7 associates with the late endosomal compartment (Meresse et al., 1995; Soldati et al., 1995) (Figure 1).

Rab5 is an important mediator of the early endocytic response. The fusion of early endosomes *in vitro* requires Rab5 (Gorvel et al., 1991) and expression of

a dominant negative Rab5 (S34N mutant) results in a decrease of transferrin receptor endocytosis (transferrin co-localization is a marker for early endosomes) (Stenmark et al., 1994). Rab5 binds to type I phosphatidylinositol 3-kinase (PI3K) and promotes production of phosphatidylinositol 3-phosphate (PI(3)P) (Miaczynska and Zerial, 2002). Rab5 and PI(3)P then recruit EEA-1 (early endosomal antigen-1) and other proteins that stimulate fusion with early endosomes (Nielsen et al., 2000). Rab5 appears to be important in chemokine receptor endocytosis and trafficking as well. CXCR2 localizes to Rab5-positive endosomes during early time points of ligand stimulation. Moreover, ligand-stimulated CXCR2 internalization requires rab5 GTP hydrolysis. Expression of a Rab5 dominant negative mutant (Rab5-S34N) significantly attenuates CXCR2 internalization (Fan et al., 2003). In addition, internalization of CXCR4 and CCR5 is also inhibited by expression of a dominant-negative Rab5 mutant (Venkatesan et al., 2003).

There are two main endosomal recycling pathways, a slow and a rapid recycling process to which Rab11a and Rab4 can contribute, respectively. Rab11a localizes to the perinuclear recycling compartment and plays a prominent role in the slow recycling process (Ullrich et al., 1996). The recycling pathway involving Rab11a is important for the intracellular trafficking of and the responses mediated by chemokine receptors. Following ligand stimulation, CXCR2 localizes to the Rab11a-positive compartment. The expression of a dominant negative (Rab11a-S25N) mutant results in significantly reduced CXCR2 recycling (Fan et al., 2003). Two proteins that interact with Rab11a and

play a role in recycling of CXCR2 are myosin Vb (Lapierre et al., 2001) and Rab11-Family Interacting Protein 2 (FIP2) (Hales et al., 2002). Expression of the myosin Vb tail (mutant that lacks the motor domain) and Rab11-FIP2 (129-512) truncated mutant inhibits recycling of CXCR2 and impairs its resensitization. In addition, expression of the myosin Vb tail impairs CXCR2- and CXCR4-mediated chemotaxis (Fan et al., 2003). These studies demonstrate the importance of recycling in chemokine receptor function.

The second pathway bypasses the Rab11a-positive perinuclear endosomes and mediates rapid recycling of receptors through Rab4-positive endosomes (Sheff et al., 1999; Sonnichsen et al., 2000). This occurs in a PI3K-dependent manner (Hunyady et al., 2002). It remains unclear what mechanisms mediate these different recycling pathways. Recent studies suggest that the low-affinity N-Formyl peptide receptor (FPR) utilizes both the rapid and slow recycling pathways. The receptor shows extensive co-localization with Rab4 and partial co-localization with Rab11, suggesting that the receptor primarily recycles through the rapid pathway, but also utilizes the slower recycling pathway (Ernst et al., 2004).

Rab7 mediates the movement of late endosomes to the lysosome by interacting with microtubule motor proteins (Jordens et al., 2001). Prolonged exposure of chemokine receptors to ligand results in their lysosomal degradation (Marchese and Benovic, 2001; Mueller et al., 1997; Yang et al., 1999). Rab7 appears to be involved in the lysosomal sorting of chemokine receptors. Expression of a dominant negative mutant of Rab7 (Rab7-T22N) results in

decreased localization of CXCR2 to the lysosomal compartment (LAMP-1-positive) after prolonged ligand treatment. CXCR2 localization to Rab5- and Rab11a-positive endosomes increased with expression of Rab7-T22N. These data suggest that Rab7 regulates the transfer of CXCR2 to the lysosome and blocking its activity results in accumulation of CXCR2 in early and recycling endosomes (Fan et al., 2003).

Regulation of chemokine receptor trafficking

Little is known about chemokine receptor recycling and what factors mediate the fate of the chemokine receptor once it is internalized. It is likely that many factors contribute to differential recycling of chemokine receptors. These factors may include the duration and concentration of ligand stimulation as well as sorting motifs located in the intracellular domains of the receptor. It does appear that the length of stimulation with ligand plays a role in the recycling/degradation sorting decision. For example, CCR5 exhibits plasma membrane and recycling endosome localization at early time points of ligand stimulation and localization to the late endosomal compartments at later time points (Signoret et al., 2000). At early time periods after CXCL8 stimulation of CXCR2, the receptor enters the recycling compartment. Following extended periods of stimulation, the receptor enters the late endosomal and lysosomal compartments (Fan et al., 2003). The ability of internalized CXCR2 to recycle is crucial for continued gradient sensing and chemotactic response to ligand. When CXCR2 recycling is inhibited, chemotaxis and signaling are impaired (Fan et al.,

2003; Fan et al., 2004). It is not yet known what other sorting molecules bind to chemokine receptors and how they may mediate trafficking.

Chemokine receptor signaling and the chemotactic response

The process of directional cell migration involves multiple steps including cell polarization, protrusion of lamellipodial protrusion, leading edge adhesion formation, and rear retraction. Despite extensive investigation, the mechanisms that regulate the coordination of these various processes remain elusive. Of particular interest is the communication between chemokine receptors, the cytoskeleton, and the signaling pathways that mediate polarization in the direction of a chemotactic gradient.

Since there is no clear evidence for the assymetrical distribution of chemokine receptors during chemotaxis, it seems likely that gradient sensing polarization results from polarized distribution of intracellular signaling mediators. One of these mediators is phosphatidylinositol-3 kinase (PI3K), more specifically the PI3Kγ isoform. During cell migration, the PI3K product, phosphatidylinositol-3,4,5-tripshosphate (PtdIns(3,4,5)P3) accumulates at the leading edge in neutrophils as indicated by localization of the PI(3)P binding probe, GFP fused to the PH domain of protein kinase B (Akt) (Merlot and Firtel, 2003). In addition, it appears that PI3Kγ is important but not essential for an efficient chemotactic response in leukocytes, as bone marrow-derived neutrophils and macrophages from PI3Kγ-/- mice exhibit impaired but not ablated chemotaxis (Hirsch et al., 2000). The necessity of PI3K for efficient leukocyte chemotaxis is likely due to its

role in Rac activation (Akasaki et al., 1999; Weiner, 2002) although the partial inhibition of Rac activation indicates that PI3K-independent signaling pathways for Rac activation do exist (Akasaki et al., 1999; Fukui et al., 2001; Reif and Cyster, 2002).

The reorganization of the actin and microtubule components of the cytoskeleton in response to chemokines play critical roles in polarization and chemotaxis. The Rho family of small GTPases are critically involved in these processes. Formation of productive lamellipodia at the leading edge during cell migration requires the actin-related protein (Arp) 2/3 complex, which mediates actin filament nucleation and the formation of branched actin networks. Arp 2/3 activity is indirectly regulated by the small GTPases Rac and Cdc42 through the Wiskott-Aldrich syndrome proteins (WASP) and WASP family verprolin-homologous proteins (WAVE) proteins (reviewed in (Stradal et al., 2004; Takenawa and Suetsugu, 2007)). Additionally, Rac and Cdc42 play a role in the reorientation of the microtubule-organizing-center (MTOC) in gradient-sensing cells, an event that is critical for the establishment of cell polarization. This effect is mediated through the adaptor molecule IQ motif containing GTPase activating protein 1 (IQGAP1), cytoplasmic linker protein-170 (CLIP-170), and Adenomatous polyposis coli (APC) (Fukata et al., 2002; Watanabe et al., 2004). In contrast to Rac and Cdc42 which localize to the leading edge in the migrating cell, RhoA localizes to the rear of the cell during migration (del Pozo et al., 1999) and has a role in the actomyosin-based contraction which is important for rear

retraction, a necessary step for the translocation of the cell body (Worthylake et al., 2001).

Despite all the current literature regarding regulation of the chemotactic response, direct links connecting activated chemokine receptors to the actin cytoskeleton, mediators of intracellular trafficking, and signaling scaffolds are limited. It is hypothesized that these chemokine receptor-interacting proteins are essential for the mediation of the chemotactic response. Furthermore, the identification of these interactions reveals potential novel therapeutic targets for the treatment of cancer.

The role of chemokines in tumorigenesis and metastasis

The contributions of chemokines to the process of tumorigenesis are both positive and negative. It is critical to understand the various roles of chemokines in tumor biology as they represent attractive therapeutic targets. First, chemokines have a role in the anti-tumorigenic and in some cases tumor-promoting immune responses. Chemokines produced by tumor cells regulate the recruitment of dendritic cells, cytotoxic T lymphocytes, and natural killer cells into the tumor site, which can promote anti-tumorigenic immune responses (Rosenberg, 2001; Vicari et al., 2004). These properties are the basis of current efforts directed toward cell-based immunotherapeutic strategies. Conversely, tumor-produced CCL2 can promote trafficking of macrophages, which can release angiogenic factors and have immunosuppressive effects (Coussens et al., 1999; Loberg et al., 2007; Negus et al., 1995; Pollard, 2004; Polverini et al.,

1977). In addition, production of CCL22 by tumor cells can recruit immunosuppressive T-regulatory cells into the tumor, which can aid in tumor promotion (Curiel et al., 2004; Zou, 2005). Finally, recent evidence suggests that chronic inflammation may promote tumorigenesis in some instances, such as hepatocellular, gastric, and colon carcinomas (reviewed in (Balkwill et al., 2005; Dalgleish and O'Byrne, 2006; Moss and Blaser, 2005)) and chemokines play a central role in the inflammatory process.

There is also a substantial contribution of the CXC chemokine family to angiogenesis, which is an important component of tumorigenesis. Although there are exceptions, in general chemokines that contain a glutamic acid-leucine-arginine (ELR) motif on the amino-terminus are angiogenesis promoters while those that lack this motif are angiostatic (Belperio et al., 2000; Strieter et al., 1995). The angiogenic activity of ELR+ chemokines is mediated through CXCR2 (Addison et al., 2000). The importance of CXCR2 in mediating tumor-associated angiogenesis is demonstrated by studies using murine lung cancer model in CXCR2 -/- mice and neutralizing antibodies against CXCR2 (Keane et al., 2004). These studies revealed a significant inhibition of tumor angiogenesis, tumor growth, and metastasis (Keane et al., 2004). Additionally, in a mouse xenograft model using transgenic mice that specifically overexpress CXCR2 on endothelial cells, melanoma tumor growth and angiogenesis is significantly increased (Horton et al., 2007).

Chemokines also have a role in targeting of metastatic spread to specific organs. The CXCR4 chemokine receptor has recently been shown to be

important in tumor metastasis, including breast cancer. The expression of this receptor on tumor cells may mediate preferential metastasis to target organs that express the ligand for this receptor, stromal-derived factor-1 alpha (SDF-1α), also known as CXCL12. CXCR4 is upregulated in metastatic breast cancer cells and neutralization of the CXCR4/SDF-1α interaction with CXCR4-specific antibodies impairs the metastasis of breast cancer cell lines (Muller et al., 2001). In addition, both RNAi of CXCR4 and the synthetic polypeptide TN14003 that mimics SDF-1α but blocks activation of CXCR4 have been shown to individually inhibit primary tumor growth and metastasis of the highly metastatic MDA-MB-231 breast cancer cell line (Chen et al., 2003b; Lapteva et al., 2005; Liang et al., 2005).

CHAPTER II

RHOB PLAYS AN ESSENTIAL ROLE IN CXCR2 SORTING DECISIONS

Introduction

A major mechanism by which chemokine receptors undergo ligand-induced internalization is through clathrin-mediated endocytosis (Signoret et al., 2000; Venkatesan et al., 2003; Vila-Coro et al., 1999; Weber et al., 2004; Yang et al., 1999). The binding of ligand results in phosphorylation of Ser and Thr residues in the intracellular loops and carboxyl-terminus of the chemokine receptor by G protein-coupled receptor kinases (GRKs) (Ferguson, 2001; Ferguson et al., 1998; Freedman and Lefkowitz, 1996; Krupnick and Benovic, 1998). Receptor phosphorylation results in the uncoupling of the G protein subunits from the receptor and receptor desensitization in some cases (Ferguson, 2001; Ferguson et al., 1996; Krupnick and Benovic, 1998). In addition, the phosphorylation of these residues and/or the presence of di-leucine motifs in the carboxyl-terminal domain of chemokine receptors are important for the recruitment of adaptor molecules that link the receptor to a lattice of clathrin that facilitates receptor internalization. The association of receptors with these adaptor molecules results in recruitment of clathrin and formation of clathrin-coated pits which “pinch off’ from the membrane through the action of dynamin and become clathrin-coated vesicles (Barlic et al., 1999; Colvin et al., 2004; Droese et al., 2004; Jimenez-Sainz et al., 2003; Orsini et al., 1999; van der Bliek

et al., 1993; Vila-Coro et al., 1999; Weber et al., 2004; Yang et al., 1999). Indeed, chemokine receptors may concentrate and internalize through preformed clathrin lattices where endocytic machinery is accumulated (Signoret et al., 2005). The clathrin-coated vesicle is uncoated and the receptor-ligand complex enters the early endosome. The receptor can either enter the recycling compartment and traffic back to the plasma membrane to bind ligand, or enter the late endosome where it will be sorted to the lysosome for degradation. The factors that mediate the trafficking fate of internalized chemokine receptors are largely unknown.

Prior studies show that the length of stimulation with ligand plays a role in the recycling/degradation sorting decision (Fan et al., 2003; Neel et al., 2005; Signoret et al., 2000). At early time periods after CXCL8 stimulation of CXCR2, the receptor enters the recycling compartment; conversely, following extended periods of stimulation, the receptor enters the late endosome and lysosome (Fan et al., 2003). The ability of internalized CXCR2 to recycle is crucial for continued gradient sensing and chemotactic response to ligand. When CXCR2 recycling is inhibited, chemotaxis and signaling are impaired (Fan et al., 2003; Fan et al., 2004; Zaslaver et al., 2001).

Rabs are small GTPases that are post-translationally modified with geranyl-geranyl groups at their carboxyl-termini (Pereira-Leal and Seabra, 2000; Zerial and McBride, 2001) which allows them to associate with particular intracellular membrane-bound compartments and regulate a number of cellular trafficking events. Rab5, a mediator of the early endocytic response, is important

for CXCR2 trafficking. CXCR2 localizes to Rab5-positive endosomes during early time points of ligand stimulation and expression of a Rab5 dominant negative mutant attenuates CXCR2 internalization (Fan et al., 2003). The recycling pathway involving Rab11a is important in the intracellular trafficking of chemokine receptors and the responses mediated by these receptors. Following ligand stimulation, CXCR2 localizes to the Rab11a-positive compartment. Expression of a dominant negative mutant reduces CXCR2 recycling (Fan et al., 2003). Rab7 appears to be involved in the lysosomal sorting of chemokine receptors. Expression of dominant negative Rab7 decreases localization of CXCR2 to the lysosome (LAMP-1-positive) and increases localization to Rab5- and Rab11a-positive endosomes after prolonged ligand stimulation (Fan et al., 2003). These data suggest that Rab7 regulates the transfer of CXCR2 to the lysosome.

Although the small GTPase RhoB has nearly 85% sequence homology to the extensively characterized isoform RhoA, a number of studies suggest a unique function for RhoB (Ridley, 2001; Wennerberg and Der, 2004; Wheeler and Ridley, 2004). RhoB can be prenylated with either a farnesyl or a geranylgeranyl group, where RhoA and RhoC are only geranylgeranylated. These differences in post-translational modification may be responsible for the unique cellular functions and localization of RhoB from other isoforms. The majority of RhoB is localized to endosomes but its precise localization remains controversial. Studies have reported it to be localized to the plasma membrane (Michaelson et al., 2001), late endosomes (Wherlock et al., 2004), and more

recently to early endosomes (Rojas et al., 2004). Despite the ambiguity of its localization, it does appear that RhoB plays an important role in intracellular trafficking (Gampel et al., 1999; Mellor et al., 1998).

In the current study, we utilized dominant negative (T19N) and GTPase-deficient activated (Q63L) RhoB mutants as well as siRNA directed against RhoB to investigate the potential role of RhoB in CXCR2 chemokine receptor trafficking. We have found that the RhoB T19N mutant, RhoB Q63L mutant, and siRNA directed against RhoB impair CXCR2-mediated chemotaxis and disrupt the intracellular trafficking of CXCR2. In addition, we have shown for the first time that CXCR2 may recycle through alternative pathways when RhoB function is disrupted. These data suggest that RhoB plays a key role in the recycling/degradation sorting decision in CXCR2 receptor trafficking.

Materials and Methods

Materials and Antibodies

Anti-CXCR2 affinity purified polyclonal antibody was generated in our laboratory and described previously (Mueller et al., 1994). Anti-CXCR2, anti-CD63 monoclonal, and anti-Actin rabbit polyclonal antibodies were purchased from Santa Cruz, Biotechnology, Inc. (Santa Cruz, CA). Anti-RhoB polyclonal rabbit antibody was acquired from Bethyl Laboratories, Inc. (Montgomery, TX). Anti-EEA-1 and Anti-LAMP-1 (CD107a) monoclonal antibodies were obtained from Becton Dickinson Biosciences (Franklin Lakes, NJ). Anti-Rab11a polyclonal

antibody was used for immunofluorescence staining. Anti-Calreticulin polyclonal antibody and anti-Rab4 rabbit polyclonal antibody were purchased from Abcam (Cambridge, MA). Anti-Golgin-97 and anti-CD71 monoclonal antibodies and Oregon Green 488 phalloidin were obtained from Invitrogen (Carlsbad, CA). Anti-Na^+/K^+ ATPase monoclonal antibody was purchased from Upstate (α-1, clone 464.6, Lake Placid, NY). Anti-mannose-6-phosphate polyclonal antibody was a generous gift from Dr. Lisa Matovcik and was described previously (Goldenring et al., 1999). Species specific Cy2 (donkey anti-rabbit), Cy5 (donkey anti-mouse), and Cy3 (donkey anti-goat) conjugated secondary antibodies were acquired from Jackson Immunoresearch Laboratories, Inc. (West Grove, PA). Anti-β-tubulin monoclonal antibody was purchased from Sigma-Aldrich (St. Louis, MO).

Plasmids

The human CXCR2 plasmid was constructed and described previously (Mueller et al., 1997). The human myc-tagged wild type, T19N, and Q63L RhoB constructs were a generous gift from Dr. Harry Mellor (University of Bristol). The EGFP-Rab7 construct was described previously (Fan et al., 2003) and was a gift from Dr. Angela Wandinger-Ness (University of New Mexico School of Medicine). The EGFP-Rab11a construct was described previously (Lapierre et al., 2001).

Cell Culture and Transfection

Human embryonic kidney (HEK) 293 cells were cultured in DMEM (Dulbecco's modified Eagle's medium) supplemented with penicillin (50 units/ml)/streptomycin (50 µg/ml), 3 mM glutamine, 10% heat-inactivated fetal bovine serum (FBS) (Atlanta Biologicals, Lawrenceville, GA) at 37°C, 5% CO_2 and transfected with human CXCR2 plasmid using Fugene6 transfection reagent following the manufacturer's protocol (Roche Applied Science, Indianapolis, IN). Neomycin-resistant cells were selected and surface expression of CXCR2 was confirmed using FACS analysis. Cells were transfected with Fugene6 for transient transfections and experiments were performed after 48 hours. All experiments conducted using myc-tagged RhoB mutants and EGFP-Rab7 or –Rab11a were transiently transfected into cells stably expressing hCXCR2.

RhoB RNA Interference

Pre-designed Cy-3 labeled siRNA oligomers containing 21 nucleotides were purchased from Ambion (Austin, TX). siRNA identification numbers 42060 or 120362 were used to specifically target human RhoB with sequences 5'gccuacgacuaccucgagutt 3' and 5'gcaugaacaggacuugacctt 3', respectively. Nonspecific Cy-3 labeled siRNA (#4621) was also purchased from Ambion and used as a negative control in these studies. Transfections were performed using Oligofectamine reagent (Invitrogen, Carlsbad, CA). Experiments were performed 48 hours after transfection.

Isolation of GST-TRBD

GST-TRBD fusion protein was isolated from *E.coli* as previously described (Ren and Schwartz, 2000). Briefly, cells were grown in LB/Amp and protein expression was induced with 0.5mM isopropyl b-D-thiogalactopyranoside (IPTG) for 2 hours at 37˚C. The cells were harvested, resuspended in 50mM Tris-HCl, pH 7.4, 0.5% Triton X-100, 150mM NaCl, 5mM $MgCl_2$ containing bacterial protease inhibitor cocktail (Sigma-Aldrich, St. Louis, MO), disrupted by sonication, and debris removed by centrifugation. GST-TRBD protein was purified by incubating lysates with Glutathione-Agarose (Sigma-Aldrich, St. Louis, MO).

RhoB Activation Assay

GST-TRBD expression construct and pull-down assay were previously described (Ren and Schwartz, 2000) and adapted for RhoB (Gampel and Mellor, 2002). Approximately 1.5 X 10^7 HEK293 cells stably expressing CXCR2 were transiently transfected with myc-RhoB WT or myc-RhoB Q63L 48 hours prior to experiment. Cells were serum-starved overnight, stimulated with vehicle (0.1% BSA/PBS) for 60 minutes, 100 ng/ml EGF for 60 minutes, or 100 ng/ml CXCL8 for 5 minutes, 30 minutes, or 60 minutes, and lysed in 50mM Tris-HCl, pH 7.4, 1% Triton X-100, 0.1% SDS, 500mM NaCl, 10mM MgCl2 containing mammalian protease inhibitor cocktail and phosphatase inhibitor cocktails I and II (Sigma-Aldrich, St. Louis, MO). Lysates were cleared by centrifugation and an aliquot was removed from each and used as total RhoB for western blot. GST-TRBD

agarose beads were incubated with lysates at 4˚C and washed three times with 50mM Tris-HCl, pH 7.4, 1% Triton X-100, 150mM NaCl, 10mM $MgCl_2$.

Immunofluorescence and Confocal Microscopy

Cells were grown on glass coverslips coated with 0.1 mg/ml poly-L-lysine (Sigma-Aldrich) and transfected with indicated constructs. Cells were serum starved 4 hours and stimulated with vehicle (0.1% BSA/PBS) or 100 ng/ml CXCL8 at 37˚C for indicated times. Cells were fixed in 4% paraformaldehyde for 10 minutes, permeabilized in 0.2% Triton X-100/PBS for 5 minutes, blocked in 10% normal donkey serum for 30 minutes (Jackson Immunoresearch Laboratories, Inc., West Grove, PA), and incubated with primary antibodies for 2 hours at room temperature. After washing three times with 0.1% Tween 20/PBS, the coverslips were incubated with fluorescence-conjugated secondary antibodies for 1 hour. After three washes with 0.1% Tween 20/PBS, coverslips were mounted with ProLong Gold antifade reagent (Invitrogen, Carlsbad, CA). Confocal images were acquired using a LSM-510 Meta laser scanning microscope (Carl Zeiss, Thornwood, NY) with a 63X 1.3 numerical aperture oil immersion lens and images were processed by Photoshop software (Adobe Systems, San Jose, CA).

Quantitation of Co-localization in Confocal Images

Co-localization of CXCR2 with endosomal markers was quantitated using Metamorph Imaging System software package (Molecular Devices Corporation,

Sunnyvale, CA). Threshold levels for all images were kept consistent among vector and mutant transduced cells. At least twenty fields were quantitated for each time point. The percent co-localization is indicative of the area of CXCR2-stained fluorescent pixels overlapping that of endocytic markers.

Fractionation of Endosomal Compartments

Cells were lysed mechanically in detergent-free homogenization buffer. Nuclei and cell debris were removed by centrifuging at 3000 X g. The cell homogenates were then mixed with iodixanol media to bring the final concentration to 12.5%. The compartments were then fractionated on the self-generated density gradient by centrifuging at 350,000 X g in vertical rotor. Fractions were then collected and endosomal compartments were collected by centrifuging at 300,000 X g. Fractions were separated by SDS-PAGE and subjected to western blot analysis. The Golgin-97 antibody was used to detect Golgi, the Calreticulin antibody was used to detect ER, the Na+/K+ ATPase antibody was used to detect plasma membrane, and Rablla and LAMP-1 antibodies were used to detect the recycling and lysosomal compartments, respectively.

Measurement of endosome motility

Velocity and distance traveled by individual endosomes were measured using Metamorph Imaging System software package (Molecular Devices Corporation, Sunnyvale, CA). A series of 60 images at 1 second time intervals

was taken for cells stimulated with vehicle or CXCL8 for 30 minutes. Because it is difficult to distinguish directional linear movement with random movement of endosomes, maximum distance traveled from point of origin (frame 1 of the time lapse series) was also measured. The average velocities and distances were measured for at least thirty individual endosomes in at least ten randomly selected cells.

Chemotaxis Assay

96-well chemotaxis chamber (Neuroprobe, Gaithersburg, MD) was used for chemotaxis assays as described previously (Fan et al., 2004). The number of cells were counted in 20 microscope fields (20X objective).

CXCR2 degradation by western blot analysis

Cells were transfected 48 hours prior to experiments with vector, myc-RhoB WT, T19N, or Q63L. Cells were pretreated for 30 minutes at 37˚C with 20 μg/ml cycloheximide to inhibit new receptor synthesis, stimulated with vehicle (0.1% BSA/PBS) or 100 ng/ml CXCL8 for 30 minutes, 180 minutes, or 360 minutes, and lysed in 50mM Tris-Cl, pH 7.5, 150mM NaCl, 0.1% SDS, 1% NP-40, 0.5% sodium deoxycholate. Lysates were subjected to SDS-PAGE and CXCR2 and actin were detected by western blot analysis. The densities of the CXCR2 and actin protein bands were measured using Odyssey 2.1 software package (Li-COR Biosciences, Lincoln, NE). The densities of the CXCR2 bands were normalized to total protein by dividing by the actin band densities. Percent

receptor remaining values were calculated by dividing the normalized densities of the treated samples by the normalized density of the vehicle treated samples and multiplying by 100.

CXCR2 Recycling using ^{125}I-CXCL8 Binding

Cells were transfected 48 hours prior to experiments with vector, myc-RhoB WT, T19N, or Q63L. Cells were pretreated for 30 minutes at 37˚C with 20 μg/ml cycloheximide to inhibit new receptor synthesis then stimulated with vehicle (0.1% BSA/PBS) or 100 ng/ml CXCL8 for 30 minutes, washed twice with DMEM/10% FBS and CXCR2 surface expression was recovered by placing cells in DMEM/10% FBS containing 20 μg/ml cycloheximide for 0 minutes, 30 minutes, or 60 minutes at 37˚C. Cells were washed three times with ice-cold binding buffer (DMEM/1% BSA). 0.1 nM ^{125}I-CXCL8 prepared in binding buffer containing 20 μg/ml cycloheximide was added and incubated for 2 hours on ice. Following binding, cells were washed three times with ice-cold binding buffer and lysed in 1% SDS/0.1 N NaOH, collected, and the level of radioactivity quantitated by γ-counter. Experiments were performed in triplicate and percent total binding was calculated by dividing the average radioactive counts for each recovery time by the radioactive counts for the vehicle treated cells (Total Binding).

Preparation of Triton-soluble and –insoluble fractions

Triton-soluble and –insoluble fractions were prepared as described previously (Minamide et al., 1997). Briefly, HEK293 cells stably expressing

CXCR2 and transiently transfected with empty vector, myc-RhoB T19N, or myc-RhoB Q63L were washed four times with ice-cold PBS and lysed in 10mM Tris-HCl, pH 7.5, 2mM $MgCl_2$, 0.5mM DTT, 2mM Ethyleneglycol-*bis*(2-aminoethylether)-N,N,N′,N′-tetraacetic Acid (EGTA), 1% Triton X-100, and 7.5% glycerol containing protease and phosphatase inhibitors. Soluble and insoluble fractions were prepared by centrifugation at 170,000 X g for 20 minutes. Actin in each fraction was detected by western blot analysis.

Statistical Analysis

Statistically significant differences between two groups with the same treatment were determined using the non-parametric two-tailed Mann Whitney U test (Wilcoxin rank sum test). Significant differences between two groups with several treatments were determined using non-parametric analysis of variance (ANOVA) (Kruskal-Wallis test). Individual p-values were calculated using the Dunn's post test. All statistical analysis was performed using GraphPad Prism 5 software (GraphPad software, Inc., San Diego, CA).

Results

RhoB is activated upon CXCL8 stimulation

In order to determine whether RhoB is activated upon stimulation with the CXCR2 ligand CXCL8, we utilized the Rho-binding domain of rhotekin (TRBD) GST-fusion protein to isolate GTP-bound (active) RhoB from HEK293 cells stably

expressing CXCR2. It has been previously demonstrated that Epidermal growth factor (EGF) activates RhoB (Gampel et al., 1999); therefore EGF was used as a positive control for RhoB activation. The GTPase-deficient activated (Q63L) RhoB mutant was used as an additional positive control for GTP-bound RhoB. Cells were transfected with WT myc-RhoB or with Q63L myc-RhoB and either stimulated with vehicle (untreated), EGF for 60 minutes, or CXCL8 for 5 minutes, 30 minutes, or 60 minutes. Following stimulation, GTP-bound RhoB was isolated using GST-TRBD and analyzed by SDS-PAGE and western blot with detection using RhoB antibody. Activation of exogenous RhoB was detected after CXCL8 stimulation (Figure 2). These experiments were repeated numerous times and the activation of RhoB after 5 minutes of CXCL8 stimulation was statistically significant ($p \leq 0.05$, Mann Whitney U test). Activation of RhoB after 30 minutes and 60 minutes of CXCL8 stimulation was also observed in some experiments. It is expected that the localized activation of RhoB stronger and more biologically relevant than the overall detection observed by the pull-down assay. Discrepancies in specific time point of activation may be due to the two differentially localized forms of RhoB and variations among different preparations of the GST-TRBD fusion protein.

Dominant negative (T19N) and GTPase-deficient activated (Q63L) RhoB mutants impair CXCR2-mediated chemotaxis

To assess whether CXCR2 function is regulated by RhoB, CXCR2-mediated chemotaxis was investigated using the Boyden chamber chemotaxis assay in cells stably expressing CXCR2. Cells were transiently transfected with

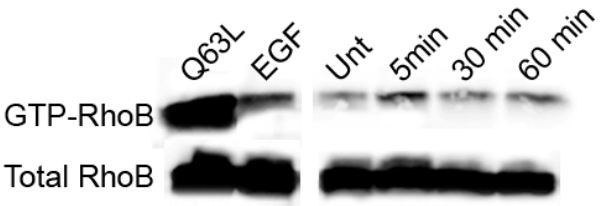

Figure 2: RhoB is activated upon CXCL8 stimulation.
Western blot analysis with anti-RhoB antibody of input lysates (Total RhoB) and GST-TRBD bound RhoB (GTP-RhoB) separated by SDS-PAGE. HEK293 cells stably expressing CXCR2 were transiently transfected with myc-WT RhoB or myc-Q63L RhoB mutant. Cells transfected with myc-Q63L RhoB were stimulated with vehicle. Cells transfected with myc-WT RhoB were stimulated with 100ng/ml EGF for 60 minutes (EGF), vehicle (Unt), or 100 ng/ml CXCL8 for 5 minutes, 30 minutes, or 60 minutes. Lysates were incubated with GST-TRBD (rhotekin Rho binding domain) to isolate GTP-bound RhoB. Data shown are representative from three separate experiments. The fold induction at the 5 minute and 60 minute time points when normalized to total RhoB was 1.6 and 1.1, respectively in the experiment shown here.

empty pcDNA3 vector, myc-RhoB T19N (dominant negative) or myc-RhoB Q63L mutants (activated). Cells transfected with the empty vector demonstrate a characteristic bell-shaped chemotactic response. In contrast, cells expressing either the myc-RhoB T19N or myc-RhoB Q63L mutants exhibit a two-fold reduction in the number of migrated cells (Figure 3A,B). We also examined CXCR2-mediated chemotaxis in cells expressing myc-RhoB WT and found that there was no effect on chemotaxis when WT RhoB is expressed (Figure 3C). To investigate whether the decrease in chemotaxis was a result of impaired actin polymerization, we examined F-actin by phalloidin staining and confocal microscopy and prepared Triton-soluble and –insoluble fractions and performed western blot analysis for actin. Expression of RhoB T19N or Q63L did not alter the appearance of F-actin staining or actin levels in Triton-soluble and –insoluble fractions (Figure 4). These data suggest that the effect of altering RhoB GTPase activity on CXCR2 function is not due to a more general impairment of actin polymerization. The RhoB T19N mutant is GTP binding-deficient and acts as a dominant negative by binding and sequestering guanine nucleotide exchange factors (GEFs) and making them unavailable to endogenous RhoB. Therefore, in order to rule out the possibility that the phenotype associated with this mutant is nonspecific, we examined the effect of knocking down endogenous RhoB on chemotaxis. Knocking down endogenous RhoB expression using siRNA also results in impaired CXCR2-mediated chemotaxis (Figure 5).

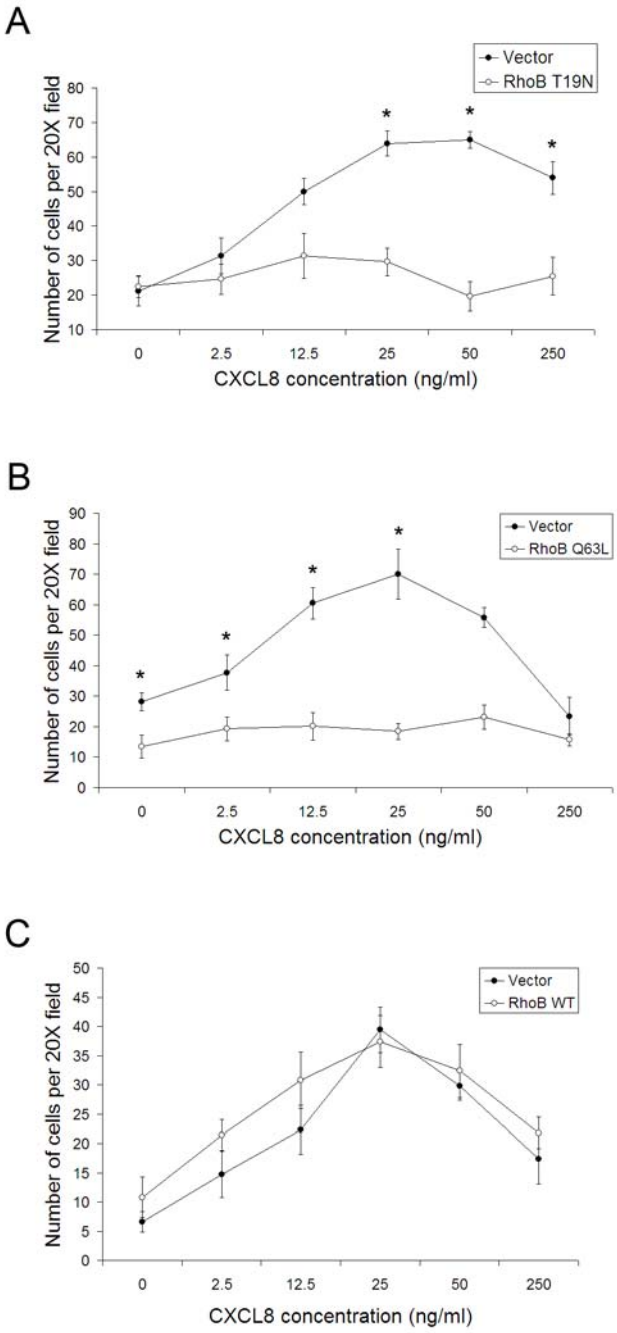

Figure 3: RhoB T19N and Q63L mutants impair CXCR2-mediated chemotaxis.

Boyden chamber assay assessing chemotaxis of HEK293 cells stably expressing CXCR2 and transiently transfected with empty vector, myc-RhoB T19N, or myc-RhoB Q63L. A two-fold reduction in CXCR2-mediated chemotaxis was observed when myc-RhoB T19N and myc-RhoB Q63L mutants were expressed. No effect on chemotaxis was observed when myc-RhoB WT was expressed. CXCR2-mediated chemotaxis of cells expressing myc-RhoB T19N (A), myc-RhoB Q63L (B), and myc-RhoB WT (C). The graphs display number of cells from twenty

Figure 3, continued
separate fields using the 20X objective lens ± S.E.M. Significant differences of vector versus myc-RhoB T19N or -RhoB Q63L transfected cells are indicated by asterisks (p-value < 0.05, ANOVA). Data shown are representative from three separate experiments.

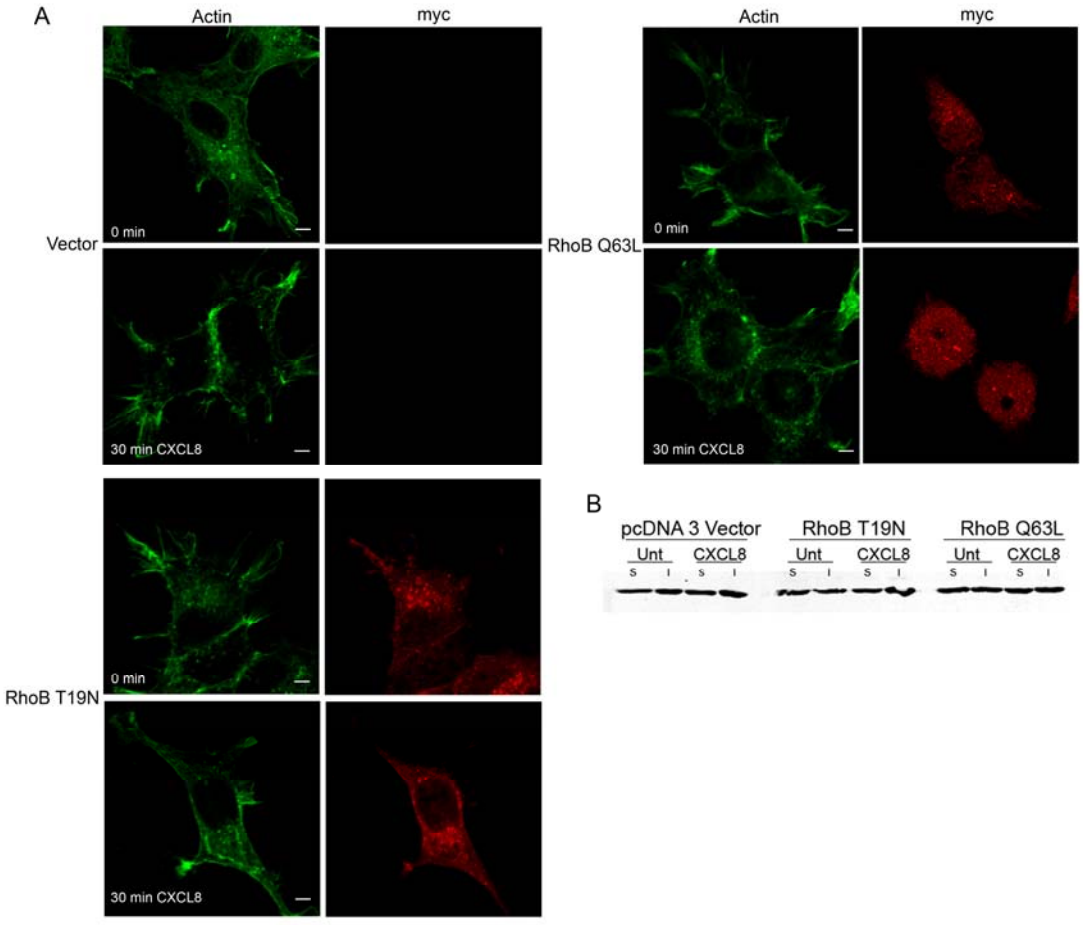

Figure 4: Expression of myc-RhoB T19N or Q63L mutants does not alter F-actin staining with phalloidin or actin content in Triton-soluble and –insoluble fractions.
(A) Confocal images of F-actin staining with Oregon Green 488 phalloidin in HEK293 cells stably expressing CXCR2 and transfected with empty vector, myc-RhoB T19N, or myc-RhoB Q63L. Cells were stimulated with vehicle (0 min) or 100 ng/ml CXCL8 for 30 minutes. Transfected cells were identified by staining with anti-myc antibody. Bars, 5 μm (B) Western blot analysis of Triton-soluble (S) and –insoluble (I) actin isolated from cells expressing empty pcDNA 3 vector, myc-RhoB T19N, or myc-RhoB Q63L mutants that were stimulated with vehicle (Unt) or 100 ng/ml CXCL8 for 30 minutes.

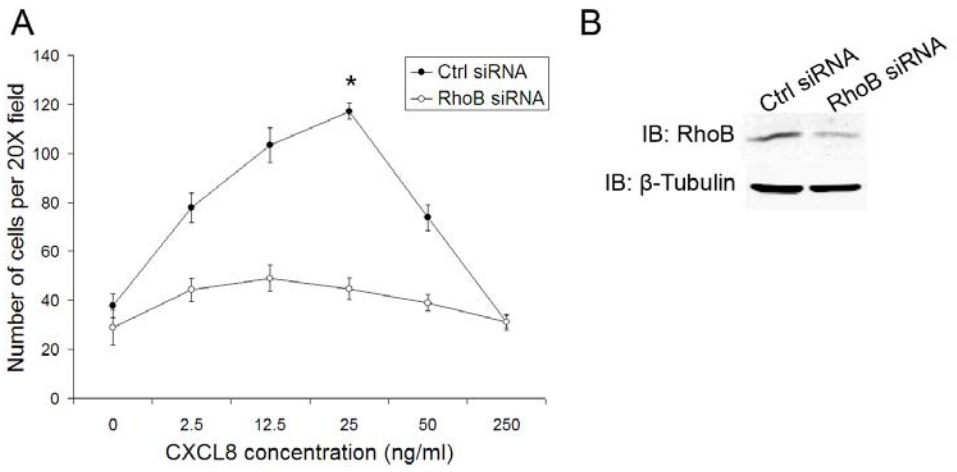

Figure 5: RhoB siRNA impairs CXCR2-mediated chemotaxis.
(A)Boyden chamber chemotaxis assay used to assess chemotaxis of HEK293 cells stably expressing CXCR2 and transiently transfected with either control (Ctrl) siRNA or RhoB-specific siRNA. The graphs display number of cells from twenty separate fields using the 20X objective lens ± S.E.M. Significant differences between Ctrl siRNA transfected cells versus RhoB-specific siRNA transfected cells are indicated asterisks (p-value < 0.05, ANOVA). (B) Western blot analysis of RhoB protein levels from Ctrl siRNA or RhoB-specific siRNA transfected cells used in Boyden chamber assay. β-tubulin western blot is shown as a control to monitor equal loading of protein. Data shown are representative from three separate experiments.

Expression of dominant negative (T19N) RhoB alters trafficking of CXCR2 following 3 hours of CXCL8 stimulation

Because RhoB activation occurs upon EGF stimulation and is involved in the intracellular trafficking of the EGF receptor (Gampel et al., 1999; Wherlock et al., 2004), we sought to investigate whether RhoB similarly regulates the trafficking of CXCR2. In order to investigate, we transiently expressed empty vector or myc-RhoB T19N in HEK293 cells stably expressing CXCR2. CXCR2 trafficking was evaluated by immunofluorescence staining and confocal microscopy. Previous studies in our laboratory revealed that the majority of CXCR2 enters the perinuclear Rab11a-positive recycling compartment and recycles back to the plasma membrane after periods of CXCL8 stimulation greater than 30 minutes and less than 1 hour. However, upon longer periods of stimulation with saturating concentrations of CXCL8, the majority of CXCR2 no longer enters the recycling compartment and instead traffics to the late endosomal compartment where it is then transferred to the lysosome for degradation (Fan et al., 2003). In the current study, CXCR2 substantially co-localized with the lysosomal marker LAMP-1 upon 3 hours of CXCL8 stimulation in vector transfected cells (44.4 ± 15.8 %) and cells transfected with myc-RhoB WT (56.6 ± 22.6 %) (Figure 6A,C and Figure 7). In contrast, HEK293 cells expressing the myc-RhoB T19N mutant exhibited minimal co-localization of CXCR2 with the lysosomal marker LAMP-1 (12.9 ± 8 %) after 3 hours of CXCL8 stimulation (Figure 6B,C). Similarly, knocking down endogenous RhoB with siRNA also resulted in a significant decrease in co-localization of CXCR2 with LAMP-1 after 3 hours of CXCL8 stimulation (12.8 ± 3% co-localization) when

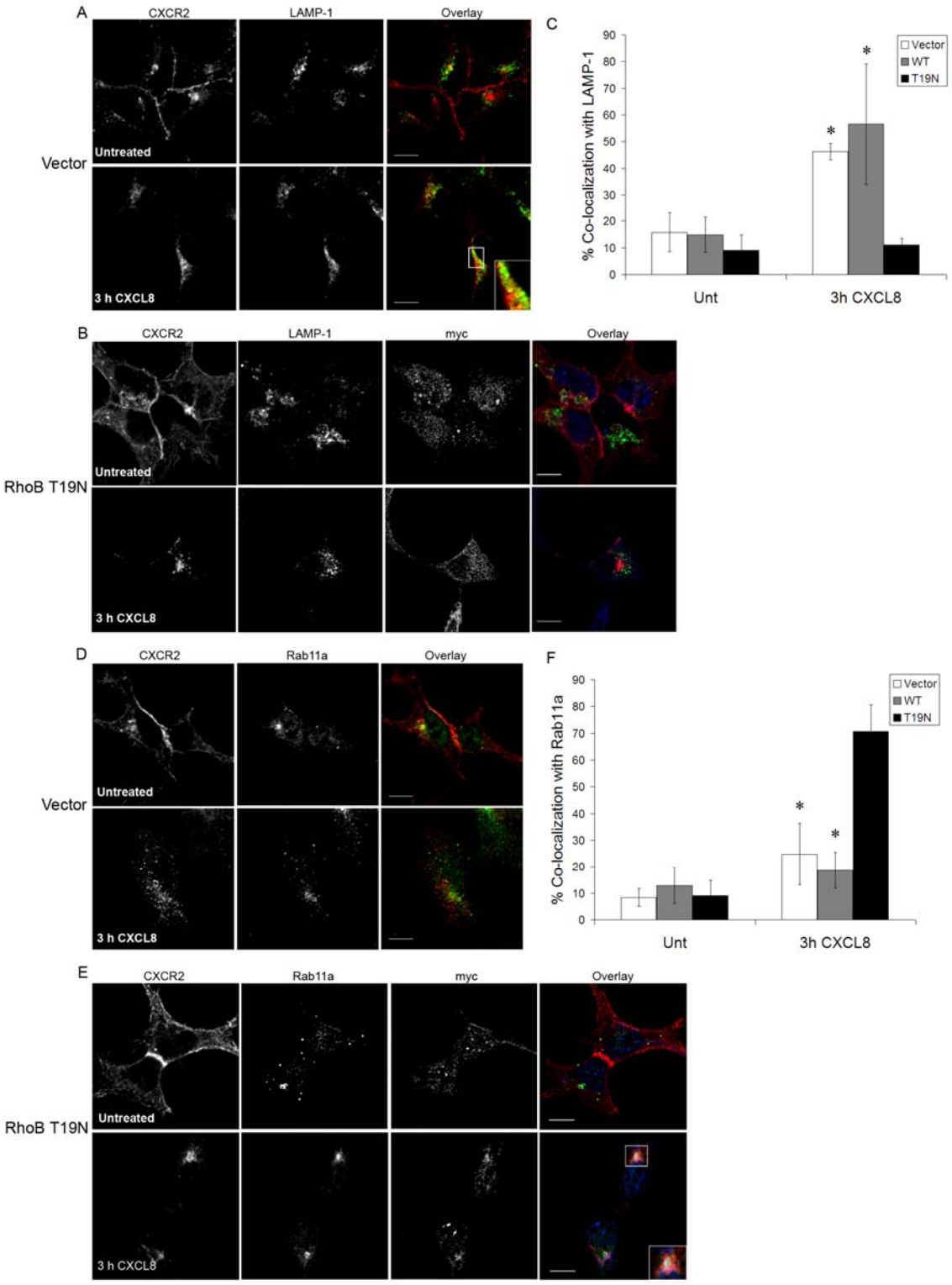
A
CXCR2
LAMP-1
Overlay
Vector
Untreated
3 h CXCL8
C
% Co-localization with LAMP-1
Vector
WT
T19N
Unt
3h CXCL8
B
CXCR2
LAMP-1
myc
Overlay
RhoB T19N
Untreated
3 h CXCL8
D
CXCR2
Rab11a
Overlay
Vector
Untreated
3 h CXCL8
F
% Co-localization with Rab11a
Vector
WT
T19N
Unt
3h CXCL8
E
CXCR2
Rab11a
myc
Overlay
RhoB T19N
Untreated
3 h CXCL8

Figure 6: Expression of dominant negative (T19N) RhoB alters trafficking of CXCR2 following 3 hours of CXCL8 stimulation.
Confocal images of immunofluorescence staining of HEK293 cells stably expressing CXCR2. CXCR2 and LAMP-1 staining in cells transfected with vector (A) or myc-RhoB T19N (B) and stimulated with vehicle (Untreated) or 100 ng/ml CXCL8 for 3 hours. Transfected cells were identified by staining with anti-myc antibody. Overlay images are pseudocolored where red is CXCR2, green is LAMP-1, and blue is myc-RhoB T19N. Bars, 10 μm (C) Quantitation of co-localization of CXCR2 with LAMP-1 in cells transfected with vector, myc-RhoB WT, or myc-RhoB T19N. Values are shown as mean ± S.E.M. Significant differences of vector or myc-RhoB WT versus myc-RhoB T19N transfected cells are indicated by asterisks (p-value ≤ 0.05, Mann Whitney U test). CXCR2 and Rab11a staining in cells transfected with empty vector (D) or myc-RhoB T19N (E) stimulated with vehicle (Untreated) or 100 ng/ml CXCL8 for 3 hours. Transfected cells were identified by staining with anti-myc antibody. Overlay images are pseudocolored where red is CXCR2, green is Rab11a, and blue is myc-RhoB T19N. Bars, 10 μm (F) Quantitation of co-localization of CXCR2 with Rab11a in cells transfected with vector, myc-RhoB WT, or myc-RhoB T19N. Values are shown as mean ± S.E.M. Significant differences of vector or myc-RhoB WT versus myc-RhoB T19N transfected cells are indicated by asterisks (p-value < 0.05, Mann Whitney U test). Quantitation of the percentage of CXCR2 co-localized with LAMP-1 or Rab11a in 20 fields was performed using the MetaMorph Imaging system (Universal Imaging). Images were processed using Photoshop (Adobe Systems, San Jose, CA). Data shown are representative from three separate experiments.

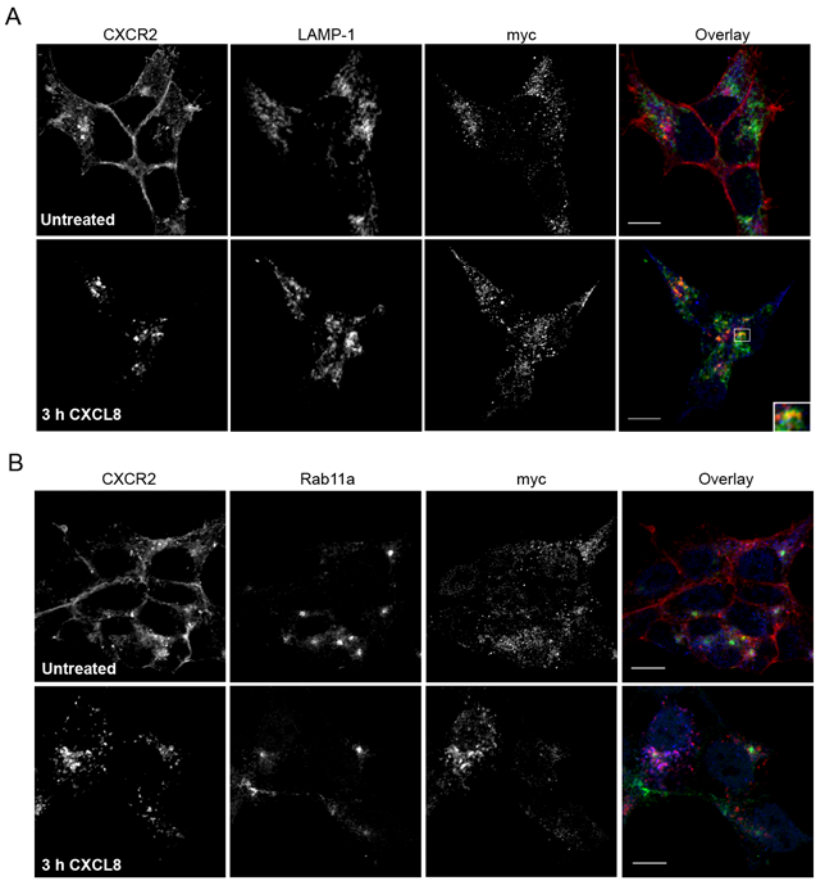

Figure 7: Confocal images of immunofluorescence staining of HEK293 cells stably expressing CXCR2 and transfected with myc-RhoB WT.
CXCR2 and LAMP-1 staining (A) or Rab11a staining (B) in cells stimulated with vehicle (Untreated) or 100 ng/ml CXCL8 for 3 hours. Transfected cells were identified by staining with anti-myc antibody. Overlay images are pseudocolored where red is CXCR2, green is LAMP-1 (A) or Rab11a (B), and blue is myc-RhoB WT. Bars, 10 μm

compared to control siRNA (36.5 ± 7.6 % co-localization) (Figure 8). Furthermore, there was minimal co-localization of CXCR2 with Rab11a after 3 hours of CXCL8 stimulation in cells expressing empty vector (24.8 ± 11.6 %) or myc-RhoB WT (18.7 ± 6.8 %) (Figure 6D,F and Figure 7). In contrast to vector and myc-RhoB WT transfected cells, HEK293 cells expressing myc-RhoB T19N exhibited extensive CXCR2 accumulation in the Rab11a compartment (70.7 ± 9.9 %) (Figure 6E,F). At earlier time periods of CXCL8 stimulation there was no difference observed in CXCR2 localization in myc-RhoB T19N transfected cells when compared to vector transfected cells.

Expression of dominant Negative RhoB T19N leads to co-fractionation of CXCR2 with the Rab11a compartment in density gradients

In order to determine whether expression of RhoB T19N effects a change in the movement of CXCR2 through endosomal compartments that can be observed biochemically, iodixanol density gradients were used to fractionate endosomal compartments of HEK293 cells stably expressing CXCR2 and transiently expressing either empty vector or myc-RhoB T19N mutant following 3 hours of CXCL8 stimulation. As shown by western blot in Figure 9A, CXCR2 co-fractionates with the lysosomal marker LAMP-1 following 3 hours of CXCL8 stimulation in cells expressing the empty vector. However, in cells expressing the RhoB T19N mutant, there is substantial co-fractionation of CXCR2 with the Rab11a compartment after 3 hours of CXCL8 stimulation (Figure 9B). These data suggest that RhoB activity is required for the movement of CXCR2 into the lysosomal compartment after prolonged ligand stimulation.

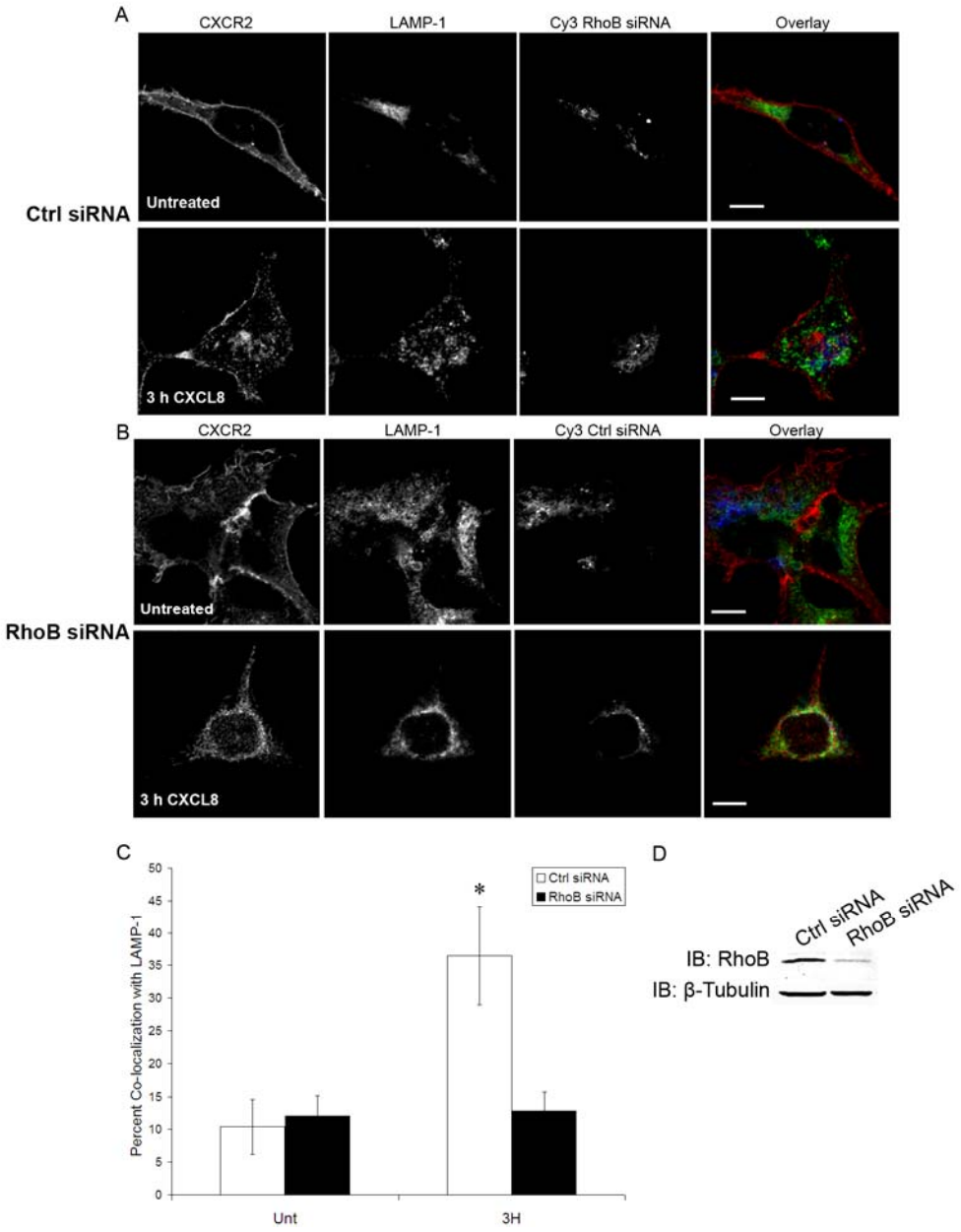

Figure 8: Transfection of cells with RhoB-specific siRNA decreases co-localization of CXCR2 with LAMP-1 following 3 hours of CXCL8 stimulation. Confocal images of immunofluorescence staining of HEK293 cells stably expressing CXCR2. CXCR2 and LAMP-1 staining in cells transfected with Ctrl siRNA (A) or RhoB-specific siRNA (B) and stimulated with vehicle (Untreated) or 100 ng/ml CXCL8 for 3 hours. Transfected cells were identified by Cy3-siRNA. Overlay images are pseudocolored where red is CXCR2, green is LAMP-1, and blue Cy3-siRNA. Images were processed using Photoshop (Adobe Systems, San Jose, CA). Bars, 10 μm (C) Quantitation of co-localization of CXCR2 with LAMP-1 in cells stimulated with vehicle and cells stimulated with CXCL8 for 3 hours. Values are shown as mean ± S.E.M. Quantitation of the percentage of CXCR2

Figure 8, continued
co-localized with LAMP-1 in 20 fields was performed using the MetaMorph Imaging system (Universal Imaging). Significant differences of Ctrl siRNA transfected cells versus RhoB-specific transfected cells are indicated by asterisks (p-value < 0.05, Mann Whitney U test). (D) Western blot analysis of RhoB protein levels from Ctrl siRNA or RhoB-specific siRNA transfected cells used for immunofluorescence staining. β-tubulin western blot is shown as a control to monitor equal loading of protein. Data shown are representative from three separate experiments.

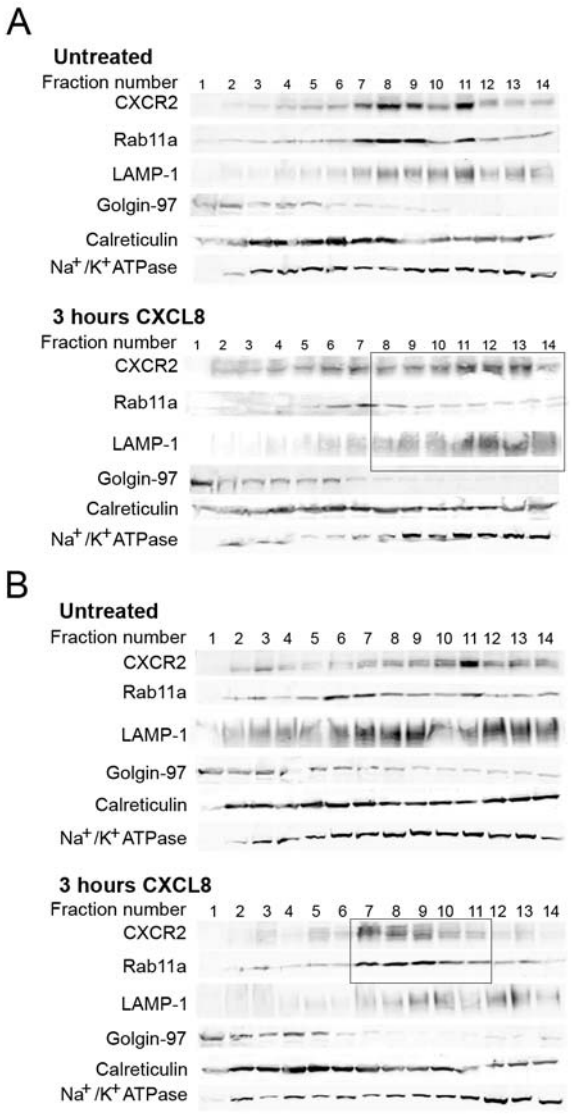

Figure 9: Expression of dominant negative RhoB T19N leads to co-fractionation of CXCR2 with the Rab11a compartment in density gradients after 3 hours of CXCL8 stimulation.

Western blot analysis of fractions collected from iodixanol density gradients from cells stimulated with vehicle (Untreated) or 100 ng/ml CXCL8 for 3 hours. (A) Fractionation of HEK293 cells stably expressing CXCR2 and transiently transfected with empty pcDNA3 vector. Top: fractionation of compartments from vehicle stimulated (Untreated) cells, Bottom: fractionation of compartments from cells stimulated with CXCL8 for 3 hours. The boxed region indicates the fractions that contain CXCR2 and LAMP-1 (B) Fractionation of HEK293 cells stably expressing CXCR2 and transiently transfected with myc-RhoB T19N. Top: fractionation of compartments from vehicle stimulated (Untreated) cells, Bottom: fractionation of compartments from cells stimulated with CXCL8 for 3 hours. The boxed region indicates the fractions that contain CXCR2 and Rab11a. Data shown are representative from at least three separate experiments.

Expression of RhoB T19N does not alter Rab11a-positive endosome motility

To evaluate whether the accumulation of CXCR2 in the Rab11a compartment is related to endosome motility and actin polymerization, the effects of actin disrupting agents on CXCR2 trafficking were examined. Indeed, it has been previously demonstrated that cytochalasin D impairs CXCR2 recycling (Zaslaver et al., 2001). HEK293 cells stably expressing CXCR2 were stimulated with vehicle or CXCL8 for 30 minutes and treated with either Latrunculin B or Cytochalasin D. CXCR2 and Rab11a were then examined by immunofluorescence staining and confocal microscopy. Both Latrunculin B and Cytochalasin D treatment resulted in accumulation of CXCR2 in the Rab11a compartment (Figure 10). These data suggest that actin polymerization is not required for movement of CXCR2 into the perinuclear recycling compartment but it may be required for the exiting of the receptor from that compartment.

We hypothesized that the accumulation of CXCR2 in the Rab11a compartment in cells expressing RhoB T19N is a result of a defect in actin-dependent endosome motility. In order to test this hypothesis, we examined Rab11a-GFP endosomes in live cells using time-lapse confocal microscopy. HEK293 cells stably expressing CXCR2 were either transiently co-transfected with a EGFP-Rab11a construct and the myc-RhoB T19N mutant or the EGFP-Rab11a construct and the empty vector. Cells were then stimulated with vehicle or 100ng/ml CXCL8 for 30 minutes and examined using time-lapse confocal microscopy. The movement of the EGFP-Rab11a-positive endosomal structures was manually tracked as described in Materials and Methods. The average

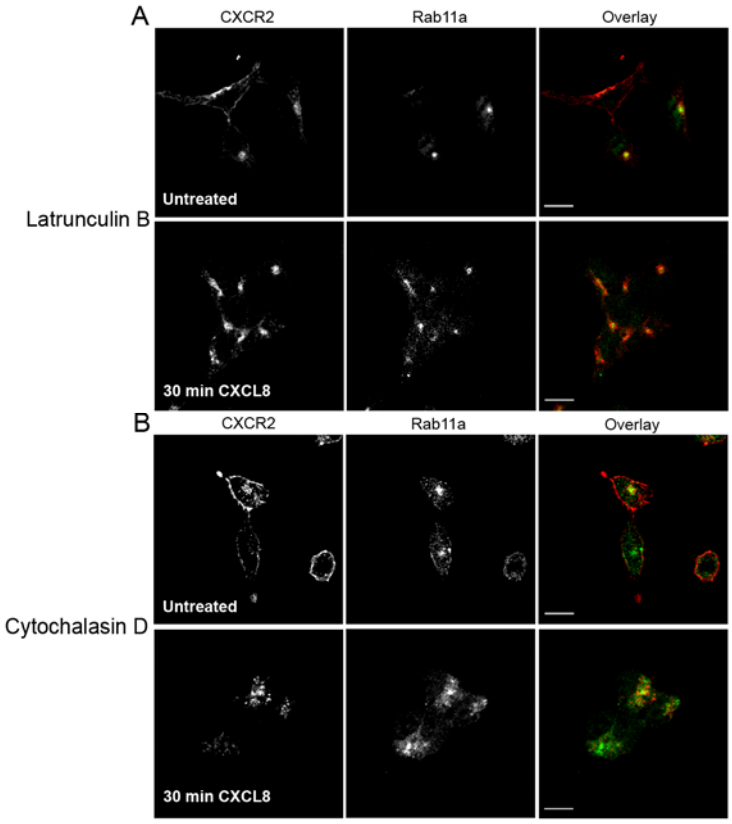

Figure 10: Actin disrupting agents Latrunculin B and Cytochalasin D cause CXCR2 accumulation in the Rab11a compartment.
Confocal images of immunofluorescence staining of CXCR2 and Rab11a in HEK293 cells stably expressing CXCR2. Overlay images are pseudocolored where red is CXCR2 and green is Rab11a. (A) Cells stimulated with vehicle (Untreated) or 100 ng/ml CXCL8 for 30 minutes and treated with 0.1 μM Latrunculin B for 10 minutes. (B) Cells stimulated with vehicle (Untreated) or 100 ng/ml CXCL8 for 30 minutes and treated with 2 μM Cytochalasin D for 60 minutes. Images were processed using Photoshop (Adobe Systems, San Jose, CA). Bars, 10 μm. Images shown are representative of at least twenty cells from three separate experiments.

velocities and distances traveled are displayed in Table 1. No detectable differences were observed in untreated or 30 minutes CXCL8 stimulation between vector- and myc-RhoB T19N-transduced cells in either Rab11a-positive endosome velocity or the maximum distance traveled from the point of origin. These results indicate that RhoB GTPase activity is not required for Rab11a-positive endosome motility.

We also examined receptor recovery to the plasma membrane after ligand stimulation using radioligand binding to determine if expression of myc-RhoB T19N impaired return of CXCR2 to the plasma membrane. We found that the reappearance of CXCR2 at the plasma membrane following ligand stimulation in the presence of cycloheximide was not impaired in cells expressing myc-RhoB T19N (Figure 11). Receptor recycling was also assessed using FACS analysis and no defect in recycling was observed using this method (data not shown). These data suggest that the expression of the RhoB T19N mutant did not result in the accumulation of CXCR2 in the Rab11a compartment, but rather the enhanced recycling of CXCR2 even after long-term ligand stimulation.

Expression of RhoB T19N impairs CXCR2 degradation following 3 hours of CXCL8 stimulation

Upon long-term stimulation with CXCL8, CXCR2 traffics to the lysosome and is degraded. Because very little CXCR2 co-localized with LAMP-1 after 3 hours of CXCL8 in HEK293 cells expressing myc-RhoB T19N, we suspected that degradation of the receptor was impaired. In order to examine whether expression of myc-RhoB T19N impairs CXCL8-induced CXCR2 degradation, we

Table 1: Average velocities and maximum distance traveled from origin of Rab11a-positive endosomes in untreated and CXCL8 stimulated cells

		Average velocity (nm/second)	Maximum distance from origin (nm)
Untreated	Vector	81.3 ± 6.9	846.9 ± 162.6
	T19N RhoB	72.1 ± 18.6	773.5 ± 384.9
*CXCL8	Vector	90.1 ± 12.5	972.6 ± 165.1
	T19N RhoB	86.8 ± 15.5	823.3 ± 359.3

*CXCL8 treatment was for 30 minutes

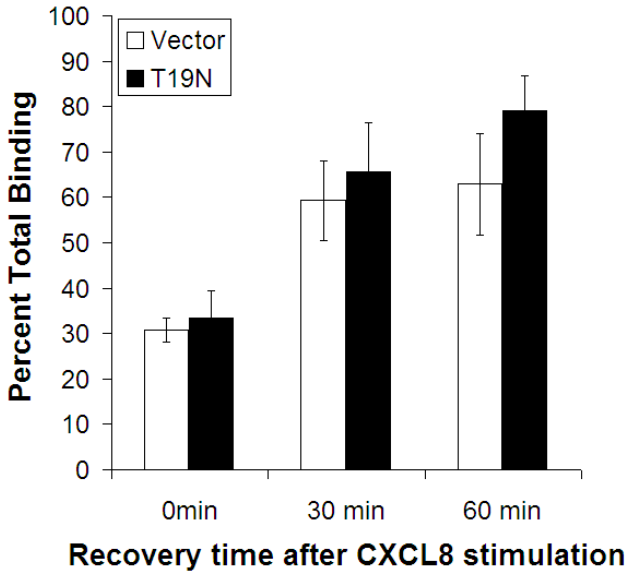

Figure 11: Expression of myc-RhoB T19N does not impair CXCR2 recycling.
^{125}I-CXCL8 binding in HEK293 cells stably expressing CXCR2 and transfected with empty vector or myc-RhoB T19N. Cells were pretreated with 20 µg/ml cycloheximide for 30 minutes and placed in the presence of 20 µg/ml cycloheximide throughout the experiment. Cells were stimulated with vehicle (Total Binding) or 100 ng/ml CXCL8 for 30 minutes, CXCL8 was removed, and cells were allowed to recover for 0 minutes, 30 minutes, or 60 minutes. Cells were incubated with 0.1 nM ^{125}I-CXCL8 (specific activity = 2200 Ci/mmol) for 2 hours, washed to remove non-specific binding, and subjected to gamma counting as described in Materials and Methods. Values represent three independent experiments and are shown as percent of Total Binding ± S.E.M. Data shown are representative from three separate experiments.

examined CXCR2 protein levels following 30 minutes, 180 minutes, and 360 minutes of CXCL8 stimulation in the presence of cycloheximide. The CXCR2 band runs at a slightly higher molecular weight following stimulation due to phosphorylation. In addition, CXCR2 is glycosylated and these forms of the receptor are visible by western blot analysis. In vector transfected cells, a significant amount of CXCR2 is degraded after 180 minutes (69.1 ± 6.3% remaining) and 360 minutes of CXCL8 stimulation (48.9 ± 9.2% remaining). Expression of myc-WT RhoB did not inhibit CXCL8-induced CXCR2 degradation (Figure 12). Expression of the RhoB T19N mutant severely impairs CXCR2 degradation after 180 minutes (94 ± 7.3% remaining) and 360 minutes of CXCL8 stimulation (97.1 ± 3.1% remaining) (Figure 13). This is presumably because of enhanced CXCR2 recycling and marked reduction in receptor trafficking to the lysosome.

Expression of GTPase-deficient activated (Q63L) RhoB mutant alters trafficking of CXCR2 following 30 minutes of CXCL8 stimulation

We have previously demonstrated that CXCR2 is recycled back to the plasma membrane when stimulated with CXCL8 for short periods of time (Fan et al., 2003). In order to characterize more extensively the role of RhoB in CXCR2 trafficking, we examined the effects of a GTPase-deficient RhoB-mutant (Q63L) on CXCR2 trafficking using immunofluorescence and confocal microscopy. CXCR2 co-localizes with the recycling endosomal marker Rab11a following 30 minutes of CXCL8 stimulation in CXCR2-expressing HEK293 cells transfected with empty vector (53.3 ± 17.6 %) or myc RhoB WT (40.9 ± 1.0 %) (Figure 14A,C

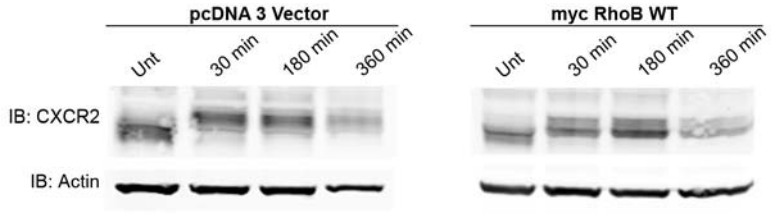

Figure 12: CXCL8-induced CXCR2 degradation following 3 hours of CXCL8 stimulation in HEK293 cells stably expressing CXCR2 and transfected with myc-RhoB WT.
Representative western blot analysis of CXCR2 expression in vector and myc-RhoB WT transfected cells in the presence of 20 µg/ml cycloheximide following stimulation with vehicle (Unt) or 100 ng/ml CXCL8 for 30 minutes, 180 minutes, or 360 minutes. Actin western blot is shown as a control to monitor for equal loading of protein. Data shown are representative from three separate experiments.

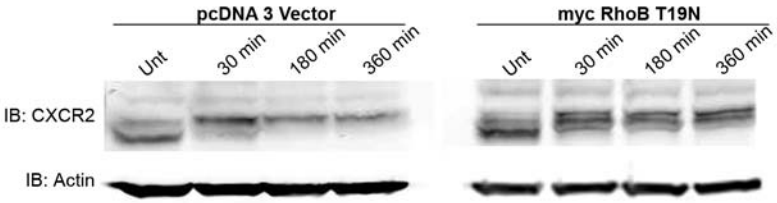

Figure 13: **Expression of myc-RhoB T19N impairs CXCL8-induced CXCR2 degradation following 3 hours of CXCL8 stimulation.**
Representative western blot analysis of CXCR2 expression in vector and myc-RhoB T19N transfected cells in the presence of 20 µg/ml cycloheximide following stimulation with vehicle (Unt) or 100 ng/ml CXCL8 for 30 minutes, 180 minutes, or 360 minutes. Actin western blot is shown as a control to monitor for equal loading of protein. Data shown are representative from three separate experiments.

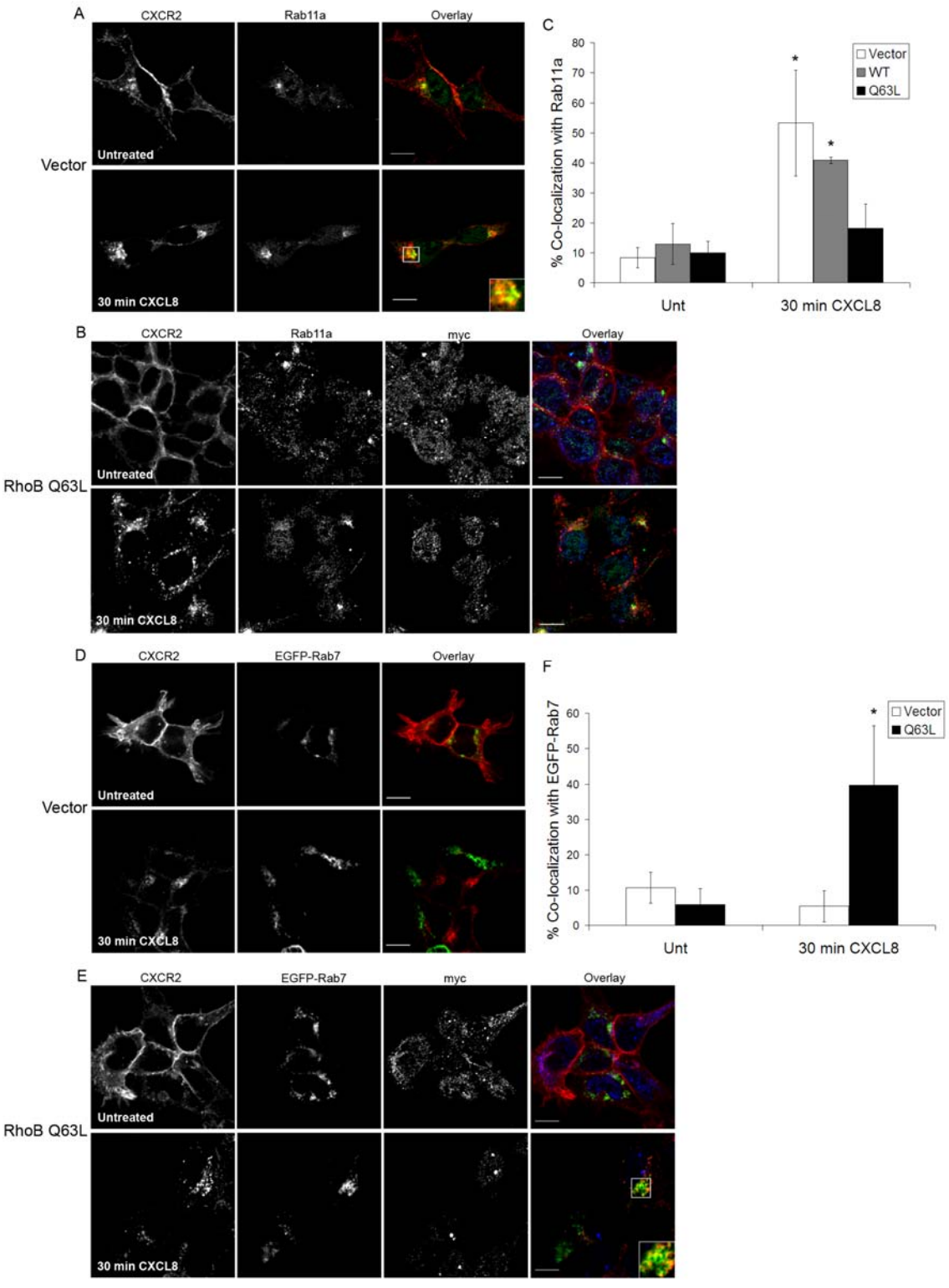
A
CXCR2
Rab11a
Overlay
Vector
Untreated
30 min CXCL8
C
% Co-localization with Rab11a
Vector
WT
Q63L
Unt
30 min CXCL8
B
CXCR2
Rab11a
myc
Overlay
RhoB Q63L
Untreated
30 min CXCL8
D
CXCR2
EGFP-Rab7
Overlay
Vector
Untreated
30 min CXCL8
F
% Co-localization with EGFP-Rab7
Vector
Q63L
Unt
30 min CXCL8
E
CXCR2
EGFP-Rab7
myc
Overlay
RhoB Q63L
Untreated
30 min CXCL8

Figure 14: Expression of GTPase-deficient RhoB (Q63L) mutant alters trafficking of CXCR2 following 30 minutes of CXCL8 stimulation.
Confocal images of immunofluorescence stained HEK293 cells stably expressing CXCR2. CXCR2 and Rab11a staining in cells transfected with empty vector (A) or myc-RhoB Q63L (B) and stimulated with vehicle (Untreated) or 100 ng/ml CXCL8 for 30 minutes. Transfected cells were identified by staining with anti-myc antibody. Overlay images are pseudocolored where red is CXCR2, green is Rab11a, and blue is myc-RhoB Q63L. Bars, 10 μm (C) Quantitation of co-localization of CXCR2 with Rab11a in cells transfected with vector, myc-RhoB WT, or myc-RhoB Q63L. Values are shown as mean ± S.E.M. Significant differences of vector or myc-RhoB WT versus myc-RhoB Q63L transfected cells are indicated by asterisks (p-value ≤ 0.05, Mann Whitney U test). CXCR2 staining and EGFP-Rab7 in cells transfected with empty vector (D) and myc-RhoB Q63L (E) and stimulated with vehicle (Untreated) or 100 ng/ml CXCL8 for 30 minutes. Transfected cells were identified by staining with anti-myc antibody. Overlay images are pseudocolored where red is CXCR2, green is EGFP-Rab7, and blue is myc-RhoB Q63L. Bars, 10 μm (F) Quantitation of co-localization of CXCR2 with EGFP-Rab7. Values are shown as mean ± S.E.M. Significant differences of myc-RhoB Q63L transfected cells versus vector are indicated by asterisks (p-value < 0.05, Mann Whitney U test). Quantitation of the percentage of CXCR2 co-localized with Rab11a or EGFP-Rab7 in 20 fields was performed using the MetaMorph Imaging system (Universal Imaging). Images were processed using Photoshop (Adobe Systems, San Jose, CA). Data shown are representative from three separate experiments.

and Figure 15).When cells were transfected with the myc-RhoB Q63L mutant, less co-localization with Rab11a is observed (18.2 ± 8.2 %) (Figure 14B,C). There is very little co-localization with the EGFP-Rab7, a late endosomal marker, in vector transfected cells (5.4 ± 8.1 %) (Figure 14D,F). In contrast, there is substantial co-localization with EGFP-Rab7 (39.7 ± 16.7 %) (Figure 14E,F) in cells transfected with myc-RhoB Q63L.

One interpretation of the data obtained showing altered trafficking of CXCR2 in RhoB T19N or RhoB Q63L transfected cells is that RhoB plays a general role in the sorting of internalized receptors and that alteration of its activity disturbs the composition/function of the respective endosomal compartments. For example, it is possible that the Rab7 endosomal compartment is mislocalized in cells expressing myc-RhoB Q63L. To clarify these issues, we investigated whether expression of the myc-RhoB-Q63L mutant alters the trafficking of the transferrin receptor (TfnR), which normally recycles through the Rab11a compartment and is not sorted to the late endosome. We utilized immunofluorescence and confocal microscopy to observe the co-localization of TfnR with EGFP-Rab7 in cells transfected with either empty vector or myc-RhoB Q63L. Expression of myc-RhoB Q63L did not result in co-localization of the TfnR with EGFP-Rab7 (Figure 16). These results suggest that CXCR2 sorting occurs in a RhoB-dependent manner while TfnR sorting occurs through a RhoB-independent mechanism. Moreover, these results argue against a generalized effect that mutant RhoB alters the localization of various Rabs in the endosomal compartments.

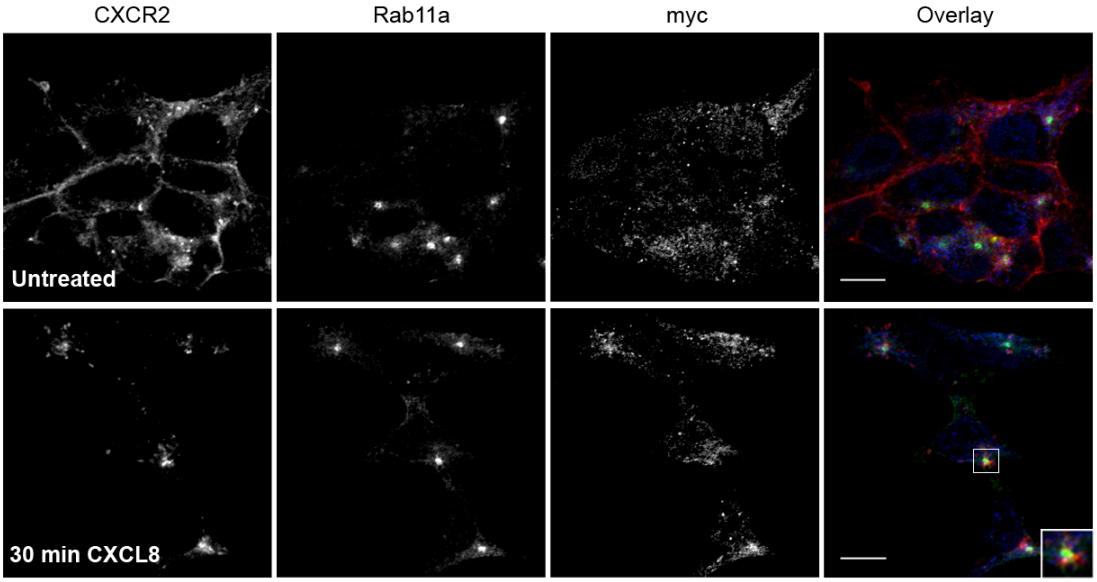

Figure 15: Confocal images of immunofluorescence staining of HEK293 cells stably expressing CXCR2 and transfected with myc-RhoB WT.
CXCR2 and Rab11a staining in cells stimulated with vehicle (Untreated) or 100 ng/ml CXCL8 for 30 minutes. Transfected cells were identified by staining with anti-myc antibody. Overlay images are pseudocolored where red is CXCR2, green is Rab11a, and blue is myc-RhoB WT. Bars, 10 μm. Data shown are representative from three separate experiments.

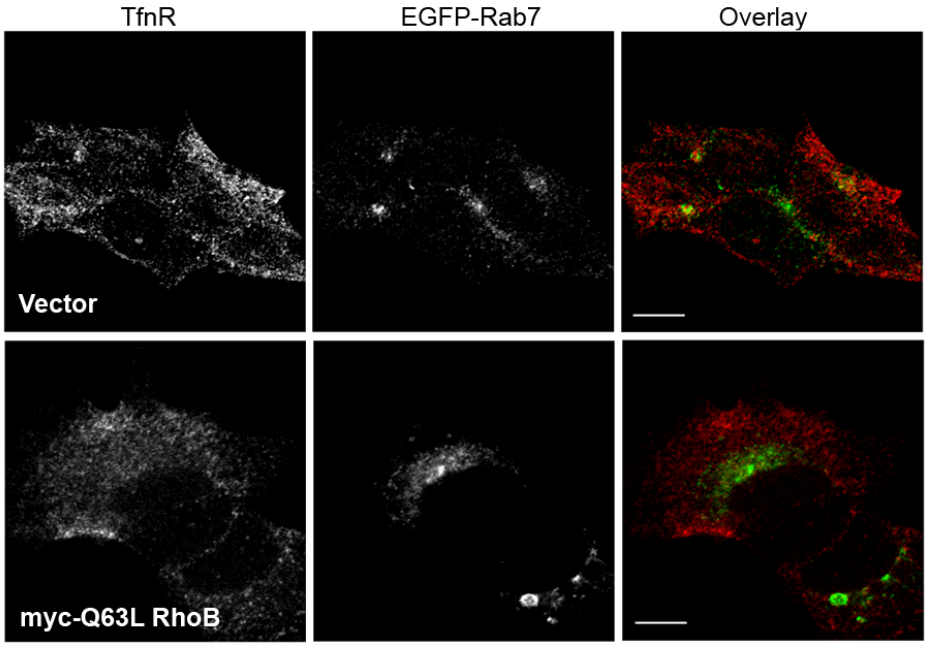

Figure 16: Expression of myc-RhoB Q63L does not cause transferrin receptor to co-localize with EGFP-Rab7.
Confocal images of immunofluorescence stained transferrin receptor and EGFP-Rab7 in HEK293 cells stably expressing CXCR2 and transiently transfected with EGFP-Rab7 and empty vector or myc-RhoB Q63L. Overlay images are pseudocolored where transferrin receptor is red and EGFP-Rab7 is green. Images were processed using Photoshop (Adobe Systems, San Jose, CA) and are representative of thirty fields. Bars, 10 μm. Data shown are representative from three separate experiments.

Expression of RhoB Q63L does not impair CXCR2 recycling

Because CXCR2 traffics to the late endosomal compartment following 30 minutes of CXCL8 stimulation in RhoB Q63L transfected cells, we expected that the receptor would not efficiently recycle back to the plasma membrane in these cells. We examined receptor recovery to the plasma membrane after ligand stimulation using radioligand binding. Surprisingly, we found that the reappearance of CXCR2 at the plasma membrane following ligand stimulation in the presence of cycloheximide was not impaired in cells expressing myc-RhoB Q63L (Figure 17). Receptor recycling was also examined using FACS analysis and results were similar (data not shown). This indicates that CXCR2 can return to the plasma membrane without entering the Rab11a perinuclear recycling compartment.

Expression of RhoB Q63L impairs CXCR2 degradation and co-localization with lysosomal markers

To determine whether CXCR2 degradation occurs at early time periods of CXCL8 stimulation in RhoB Q63L transfected cells where it is prematurely sorted to the late endosomal compartment, CXCR2 levels were determined by western blot in the presence of cycloheximide in vehicle treated cells and cells stimulated with CXCL8 for 30 minutes, 180 minutes, or 360 minutes. This experiment revealed that CXCR2 is degraded upon 180 minutes (69.1 ± 6.3% remaining) and 360 minutes (48.9 ± 9.2% remaining) of CXCL8 stimulation in vector transfected cells. Unexpectedly, CXCR2 degradation was actually impaired in cells expressing myc-RhoB Q63L after 180 minutes (97.5 ± 8% remaining) and

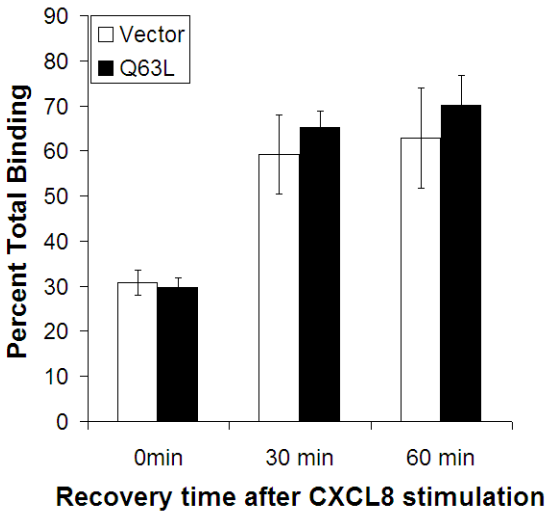

Figure 17: Expression of myc-RhoB Q63L does not impair CXCR2 recycling.
^{125}I-CXCL8 binding in HEK293 cells stably expressing CXCR2 and transfected with empty vector or myc-RhoB Q63L. Cells were pretreated with 20 µg/ml cycloheximide for 30 minutes and placed in the presence of 20 µg/ml cycloheximide throughout the experiment. Cells were stimulated with vehicle (Total Binding), 100 ng/ml CXCL8 for 30 minutes, CXCL8 was removed, and cells were allowed to recover for 0 minutes, 30 minutes, or 60 minutes. Cells were incubated with 0.1nM ^{125}I-CXCL8 (specific activity = 2220 Ci/mmol) for 2 hours, washed to remove non-specific binding, and subjected to gamma counting as described in Materials and Methods. Values represent three independent experiments and are shown as percent of Total Binding ± S.E.M. Data shown are representative from three separate experiments.

360 minutes (94.2 ± 5% remaining) of CXCL8 stimulation (Figure 18A). These results suggest that CXCR2 traffics to the late endosomal (Rab7-positive) compartment in myc-RhoB Q63L expressing cells, but it is unable to transfer to the lysosome for degradation. The ability of CXCR2 to enter the lysosome in cells expressing the RhoB Q63L mutant was also examined by immunofluorescence staining of CXCR2 and the LAMP-1 and CD63 lysosomal markers. CXCR2 did not co-localize with either the LAMP-1 or CD63 lysosomal markers in cells transfected with RhoB Q63L (Figure 18B).

Expression of Q63L RhoB results in co-localization of CXCR2 with Rab4 and Mannose-6-phosphate receptor

Our data showing that CXCR2 is unable to enter the Rab11a-positive perinuclear recycling compartment or the lysosome in cells expressing myc-RhoB Q63L suggest that CXCR2 utilizes an alternative recycling pathway to return to the plasma membrane. Therefore, we sought to investigate the mechanism by which CXCR2 returns to the plasma membrane in cell expressing myc-RhoB Q63L. There are two main endosomal recycling pathways, a slow and a rapid recycling process to which Rab11a and Rab4 can contribute, respectively. The second pathway bypasses the Rab11a-positive perinuclear endosomes and mediates rapid recycling of receptors through Rab4-positive endosomes (Sheff et al., 1999; Sonnichsen et al., 2000). We examined whether CXCR2 co-localized with Rab4 following 30 minutes of CXCL8 stimulation in vector transfected and myc-RhoB Q63L transfected cells. There was only 4.1 ± 2.4 % co-localization of CXCR2 with Rab4 in vector transfected cells

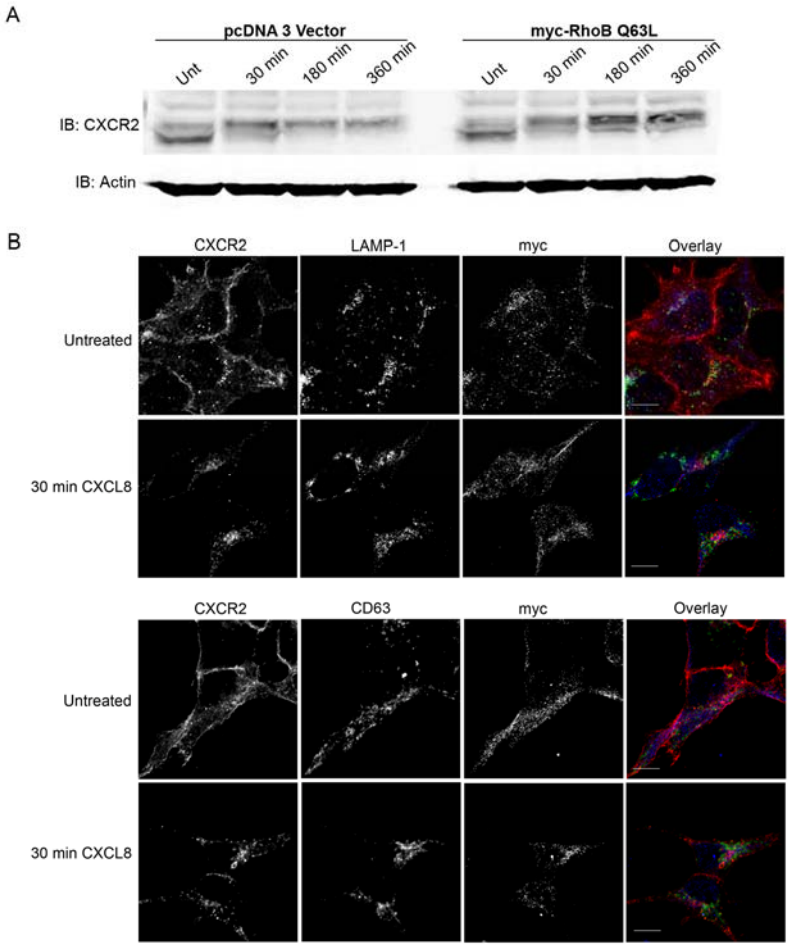

Figure 18: Expression of myc-RhoB Q63L impairs CXCL8-induced CXCR2 degradation and does not result in co-localization with lysosomal markers. (A)Western blot analysis of CXCR2 expression in vector and myc-RhoB Q63L transfected cells in the presence of 20 μg/ml cycloheximide following stimulation with vehicle (Unt) or 100 ng/ml CXCL8 for 30 minutes, 180 minutes, or 360 minutes. Actin western blot is shown as a control to monitor for equal loading of protein. (B) Confocal images from three independent experiments of immunofluorescence stained HEK293 cells stably expressing CXCR2 and transiently transfected with myc-RhoB Q63L. Transfected cells were identified by staining with anti-myc antibody. CXCR2 and LAMP-1 (Top) or CD63 (Bottom) staining in cells stimulated with vehicle (Untreated) or 100ng/ml CXCL8 for 30 minutes. Overlay images are pseudocolored where red is CXCR2, green is LAMP-1 or CD63, and blue is myc-RhoB Q63L. Images were processed using Photoshop (Adobe Systems, San Jose, CA). Bars, 10μm. Data shown are representative from three separate experiments.

(Figure 19A,C). In contrast, there was substantial co-localization of CXCR2 with Rab4 in cells transfected with myc-RhoB Q63L (49.7 ± 18 % co-localization) following 30 minutes of CXCL8 stimulation (Figure 19B,C). These data suggest that in part, myc-RhoB Q63L transfected cells utilize the rapid recycling pathway to return CXCR2 to the membrane following ligand stimulation.

An alternative but hypothetical pathway for recycling to the plasma membrane might involve the trans-Golgi. The cation-dependent mannose-6-phosphate receptor (MPR) delivers acid hydrolases from the trans-Golgi network to the late endosomal system. The receptor binds its cargo and traffics from the Golgi to the endosome and is then recycled back after the release of the hydrolases into late endosomes (reviewed in (Ghosh et al., 2003; Hille-Rehfeld, 1995; Le Borgne and Hoflack, 1998)). We examined whether CXCR2 co-localized with this receptor in cells expressing myc-RhoB Q63L. In vector transfected cells CXCR2 only minimally co-localizes with MPR after 30 minutes of CXCL8 stimulation (13.2 ± 7.8 % co-localization) (Figure 19D,F). Surprisingly, CXCR2 significantly co-localized with MPR in cells expressing myc-RhoB Q63L after 30 minutes of CXCL8 stimulation (74.1 ± 11.1 % co-localization) (Figure 19E,F). Therefore, it is possible that in myc-RhoB Q63L transfected cells CXCR2 enters the Golgi from the sorting endosome and returns to the plasma membrane from the trans-Golgi. These data suggest that CXCR2 may utilize alternative recycling pathways when it is unable to enter the Rab11a perinuclear recycling pathway in cells expressing myc-RhoB Q63L.

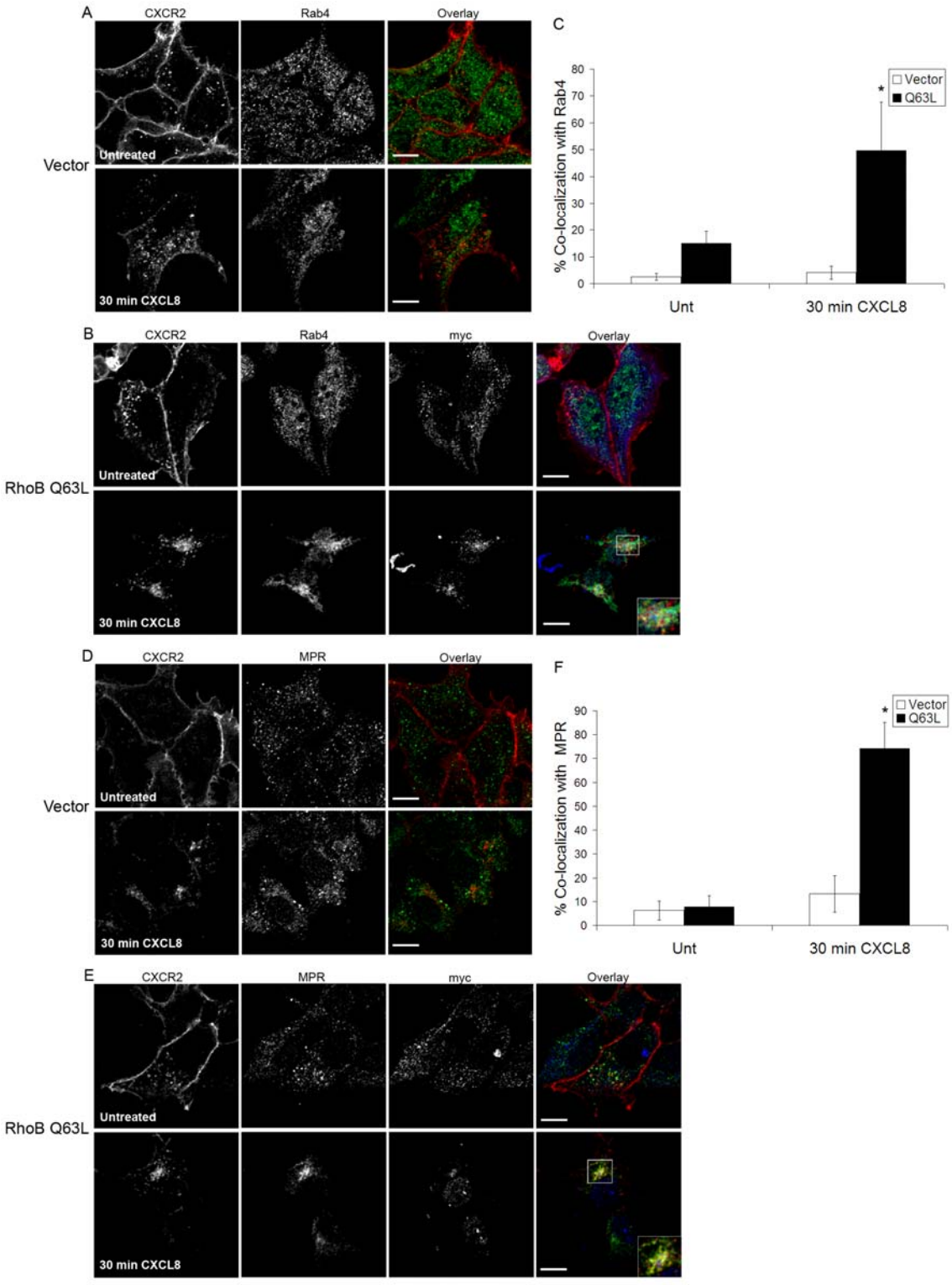
A
CXCR2
Rab4
Overlay
Vector
Untreated
30 min CXCL8
C
% Co-localization with Rab4
Vector
Q63L
Unt
30 min CXCL8
B
CXCR2
Rab4
myc
Overlay
RhoB Q63L
Untreated
30 min CXCL8
D
CXCR2
MPR
Overlay
Vector
Untreated
30 min CXCL8
F
% Co-localization with MPR
Vector
Q63L
Unt
30 min CXCL8
E
CXCR2
MPR
myc
Overlay
RhoB Q63L
Untreated
30 min CXCL8

Figure 19: Expression of Q63L RhoB results in co-localization of CXCR2 with Rab4 and Mannose-6-phosphate receptor (MPR).
Confocal images of immunofluorescence stained HEK293 cells stably expressing CXCR2. CXCR2 and Rab4 staining in cells transfected with empty vector (A) or myc-RhoB Q63L (B) and stimulated with vehicle (Untreated) or 100 ng/ml CXCL8 for 30 minutes. Transfected cells were identified by staining with anti-myc antibody. Overlay images are pseudocolored where red is CXCR2, green is Rab4, and blue is myc-RhoB Q63L. Bars, 10 μm (C) Quantitation of co-localization of CXCR2 with Rab4. Values are shown as mean ± S.E.M. Significant differences of myc-RhoB Q63L versus vector transfected cells are indicated by asterisks (p-value <0.0005, Student's *t*-test). CXCR2
and MPR staining in cells transfected with empty vector (D) or myc-RhoB Q63L (E) and stimulated with vehicle (Untreated) or 100 ng/ml CXCL8 for 30 minutes. Transfected cells were identified by staining with anti-myc antibody. Overlay images are pseudocolored where red is CXCR2, green is M6PR, and blue is myc-RhoB Q63L. Bars, 10 μm (F) Quantitation of co-localization of CXCR2 with MPR. Values are shown as mean ± S.E.M. Significant differences of myc-RhoB Q63L versus vector transfected cells are indicated by asterisks (p-value <0.0005, Student's *t*-test). Quantitation of the percentage of CXCR2 co-localized with Rab4 or MPR in 20 fields was performed using the MetaMorph Imaging system (Universal Imaging). Images were processed using Photoshop (Adobe Systems, San Jose, CA). Data shown are representative from three separate experiments.

Discussion

Early studies revealed that RhoB regulates the transport of the EGF receptor from late endosomes to the lysosome (Mellor et al., 1998). Because RhoB interacts with a number of proteins that are not isoform-specific, the function of RhoB has been difficult to establish. One possibility is that RhoB may regulate signaling events by recruiting effectors to the endosomal compartments. For example, Protein kinase C-related kinase 1 (PRK1) co-localizes with RhoB on endosomal compartments and expression of the kinase-dead mutant PRK1 antagonizes the effect of RhoB on EGF receptor trafficking (Gampel et al., 1999; Mellor et al., 1998). Recent work identified RhoB-positive endosomes as a source of new actin polymerization through the action of Scar1 (WAVE1) in a src-dependent manner (Sandilands et al., 2004). We have shown here that RhoB plays a role in the intracellular CXCR2 sorting decision and that interference with RhoB function alters CXCR2-mediated chemotaxis.

The RhoB T19N and myc-RhoB Q63L mutants as well as RhoB siRNA severely impair CXCR2-mediated chemotaxis. Although the membranes were coated with Collagen IV for these experiments, it does not appear that differences in invasion contribute significantly to the inhibition. We did not observe any difference in the migration of vector and myc-RhoB T19N transduced cells in the absence of CXCL8, suggesting that there is no difference in the ligand independent invasiveness of these two cell lines. Although there is a decrease in the number of migrated cells in the absence of CXCL8 when myc-RhoB Q63L is expressed, this would not account for the significant inhibition of

CXCL8-mediated chemotaxis. We did not observe any significant differences in activation of the MAPK or PI3K signaling pathways over a 30 minute time course as measured by phosphorylation of ERK1/2 and Akt, respectively, when either mutant was expressed. However, it is possible that localized signaling is affected when these mutants are expressed.

Expression of the dominant negative (T19N) RhoB mutant results in accumulation of CXCR2 in the perinuclear recycling compartment and enhanced recycling to the plasma membrane after long-term ligand stimulation (Figure 20). Also, CXCR2 degradation is impaired when this mutant is expressed. These results suggest that RhoB GTPase activity is required for CXCR2 entry to the lysosome after long-term ligand stimulation. However, this accumulation of CXCR2 in the perinuclear recycling compartment and failure to enter the lysosome and degrade are not a result of the inability of CXCR2 to exit the recycling compartment and return to the cell surface, since ^{125}I-CXCL8 binding studies reveal that the receptor does return to the plasma membrane and bind ligand. We hypothesize that the accumulation of CXCR2 in the Rab11a compartment is a result of the system being “overloaded” due to the fact that virtually all of the CXCR2 in the cells is passing through this compartment to return to the plasma membrane. CXCR2 is likely rapidly re-internalized upon return to the plasma membrane, reducing the time that it resides at the plasma membrane. This may contribute to the inability to visualize the receptor at the plasma membrane by microscopy. Moreover, there are no differences in EGFP-Rab11a endosome motility so differences in the rate of movement of the

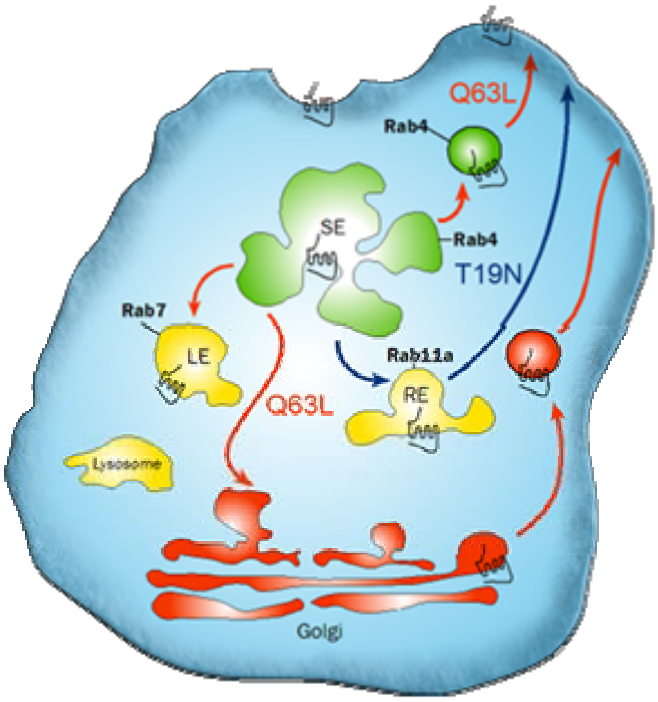

Figure 20: Schematic representation of T19N and Q63L RhoB mutant effects on CXCR2 trafficking.
After 30 minutes of CXCL8 stimulation CXCR2 traffics to the Rab11a perinuclear recycling compartment and recycles back to the plasma membrane. CXCR2 traffics to the lysosome and is degraded after 3 hours of CXCL8 stimulation. Expression of T19N RhoB mutant results in constitutive recycling of CXCR2 through the Rab11a perinuclear recycling compartment after 3 hours of CXCL8 stimulation (blue arrows). Expression of Q63L RhoB mutant results in the inability of CXCR2 to enter the Rab11a perinuclear recycling compartment after 30 minutes of CXCL8 stimulation and leads to CXCR2 recycling to the plasma membrane by alternative pathways (red arrows).

endosomes cannot account for the failure to enter the lysosome. Thus, it appears that expression of myc-RhoB T19N impairs the ability of CXCR2 to enter the lysosome and causes prolonged CXCR2 recycling.

Because expression of the RhoB T19N mutant results in decreased degradation and increased recycling of CXCR2, we expected that chemotaxis might be enhanced in cells expressing this mutant. Surprisingly, the opposite effect was observed and chemotaxis was impaired in cells expressing RhoB T19N. Although CXCR2 is efficiently recycled in these cells, the recycled receptor may not be functional upon return to the plasma membrane. For example, the dephosphorylation of the receptor is thought to be necessary for subsequent resensitization of CXCR2. Prior studies have shown that when the CCR5 receptor is stimulated with an amino-terminally modified CCL5 ligand, the receptor fails to efficiently respond to subsequent ligand challenge (Mack et al., 1998; Proudfoot et al., 1999). Further investigation revealed that when stimulated with this modified ligand, CCR5 is not dephosphorylated and therefore has only a very brief period of residency at the plasma membrane before being re-internalized (Signoret et al., 2000). In addition, studies examining the interaction of protein phosphatase 2A (PP2A) and CXCR2 demonstrated that inhibition of PP2A activity by treatment with okadaic acid impairs CXCR2-mediated chemotaxis and calcium mobilization in response to CXCL8 (Fan et al., 2001b). These studies suggest that receptor dephosphorylation may not be required for recycling but for establishing a functional receptor back at the plasma membrane. Interestingly, a novel interaction between RhoB and the

catalytic subunit of PP2A was recently identified, further suggesting a potential link between dephosphorylation and RhoB (Lee et al., 2007). It is not clear where in the endosomal trafficking pathway CXCR2 is dephosphorylated. In the future it will be of interest to examine whether CXCR2 dephosphorylation is affected in cells expressing RhoB T19N.

Treatment of cells with the actin disrupting drugs Cytochalasin D and Latrunculin B resulted in a similar accumulation of CXCR2 in the Rab11a compartment as the RhoB T19N mutant. Since RhoB coordinates actin polymerization on endosomes (Fernandez-Borja et al., 2005; Sandilands et al., 2004), we suspected that RhoB was regulating the motility of the Rab11a-positive endosomes in an actin-dependent manner. To explore this possibility we examined the motility of EGFP-Rab11a-positive endosomes using time-lapse confocal microscopy. The overall velocity of these endosomes and maximum distance traveled did not significantly differ between the vector and RhoB T19N transfected cells. These results indicate that the Rab11a-positive endosomes are able to exit the perinuclear region and return to the plasma membrane when RhoB T19N is expressed.

It is not clear whether the RhoB T19N mutant actually promotes the trafficking of CXCR2 to the Rab11a compartment or merely inhibits the ability of the receptor to enter the lysosome for degradation, which results in receptor recycling by default. Moreover, it is unclear whether the RhoB Q63L mutant inhibits entry into the perinuclear recycling compartment or actually promotes accumulation in the sorting endosome and co-localization with Rab4, mannose-

6-phoshate receptor, and Rab7. Similarly, expression of activated RhoB Q63L enhances localization of rhophilin-2 to late endosomes but not to the lysosome (Steuve et al., 2006). Studies with the EGF receptor combined with our results suggest a broad role for RhoB in receptor sorting which is not limited to a specific sorting decision. Alternatively, RhoB may play a variant role in the trafficking of receptors such as CXCR2 that can be differentially sorted to the recycling endosome or the lysosome in comparison to those receptors such as the EGF receptor that are predominantly sorted to the lysosome. RhoB can recruit proteins that may be involved in intracellular trafficking to endosomal membranes such as Dia1 (Fernandez-Borja et al., 2005) and PRK1 (Mellor et al., 1998). The recruitment of different effectors to RhoB may mediate the various responses elicited by RhoB.

Interestingly, the RhoB Q63L mutant impairs the ability of CXCR2 to enter the perinuclear recycling compartment but the receptor is still able to recycle back to the plasma membrane (Figure 20). The degradation of CXCR2 and co-localization of CXCR2 with lysosomal markers is also impaired when the Q63L mutant is expressed. This finding implicates not only the ability of RhoB to exchange GDP for GTP but also the ability of RhoB to hydrolyze GTP for proper function. It appears that GDP-bound RhoB specifies sorting to the Rab11a perinuclear recycling compartment while GTP-bound RhoB and subsequent GTP hydrolysis is necessary for lysosomal sorting.

The co-localization of CXCR2 with Rab4 and the mannose-6-phosphate receptor indicate that CXCR2 enters the sorting compartment and recycles back

to the plasma membrane through alternative recycling pathways. It is interesting that CXCR2 may enter the trans-Golgi network and recycle back to the plasma membrane through this compartment. Our data indicate that CXCR2 recycling is a default pathway, while degradation is largely CXCL8- or RhoB activation-mediated.

In summary, the dominant negative (T19N) RhoB mutant, the GTPase-deficient activated (Q63L) RhoB mutant, and siRNA directed against RhoB impair CXCR2-mediated chemotaxis. This impairment is accompanied by the failure of CXCR2 to traffic appropriately. The normal activity of RhoB is essential for CXCR2 degradation in the lysosome and recycling through the perinuclear Rab11a-positive compartment. We therefore propose that RhoB plays a role in the CXCR2 sorting decision. The ability of the cell to differentially sort chemokine receptors is critical for the chemotactic response. These results establish for the first time that RhoB plays a role in the differential sorting of a chemokine receptor.

CHAPTER III

IDENTIFICATION OF NOVEL CXCR2-INTERACTING PROTEINS THROUGH PROTEOMIC ANALYSES

Introduction

Chemokine receptors activate many intracellular signaling pathways through their coupling to G proteins. However, recent evidence suggests the importance of G protein-independent signaling pathways in the chemotactic response. The specific adaptor molecules that link activated chemokine receptors to these alternative signaling pathways are largely unknown. The importance of chemokine receptors in a number of pathological conditions such as inflammation, angiogenesis, and cancer make them ideal for therapeutic targeting. Proteomic screening for the identification of novel interacting proteins is an ideal technique because it allows components of large signaling complexes within the cell to be elucidated. The technology not only allows identification of the proteins but the conditions under which these proteins interact under physiological conditions.

In the current study, we describe identification of ligand-mediated receptor/protein interactions using immunoprecipitation followed by proteomics analysis. This approach has a number of benefits. First, proteins that bind CXCR2 indirectly can be identified using this method. Second, conformation-specific and modification-specific interactions can be identified. Third,

interactions mediated through other intracellular domains of the receptor in addition to the carboxyl-terminus can be identified. Finally, immunoprecipitation of CXCR2-associating proteins in cells stimulated with ligand allows identification of dynamic and transient interactions. Use of this approach led to the identification of several novel CXCR2-interacting proteins that may be involved in the intracellular trafficking of the receptor, initiation of the chemotactic response, and activation of signaling pathways.

IQGAP1 was identified as a novel CXCR2-interacting protein. It is a major scaffolding protein involved in cytoskeletal organization and signaling through regulation of a number of cellular functions including adhesion, migration, and integration of complex signaling pathways within the cell. IQGAP1 is large protein that contains multiple domains (Figure 21) and localizes to the leading edge in migrating cells where it cross-links actin filaments (Briggs and Sacks, 2003; Noritake et al., 2005). Interestingly, IQGAP1 contains a RasGAP homology domain but does not stimulate the GTPase activity. In fact, it inhibits the intrinsic GTPase activity of Rac1 and Cdc42, stabilizing them in their active forms (Hart et al., 1996; Ho et al., 1999). As expected, IQGAP1 has a fundamental role in cell motility. Expression of dominant negative IQGAP1, a form that is unable to bind Rac1 and Cdc42, or siRNA directed against IQGAP1 severely impairs cell motility and invasion (Mataraza et al., 2003). Specifically, it plays an essential role in polarization of a migrating cell through its interactions with Rac1/Cdc42, APC, and CLIP-170 (reviewed in (Noritake et al., 2005)). Not only does IQGAP1 play a fundamental role in cell migration, it also serves as a

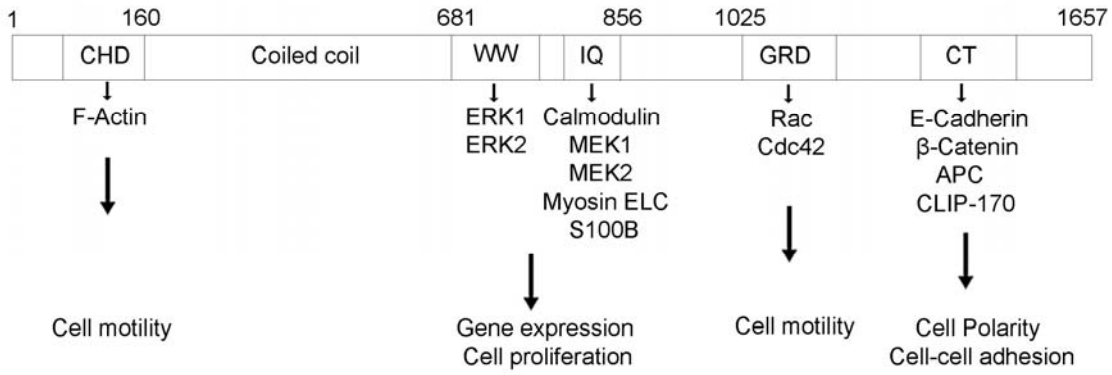

Figure 21: Schematic of domain structure of IQGAP1, interacting proteins, and cellular functions.
Domains: calponin homology domain (CHD), poly-proline protein–protein domain (WW), IQ motif (IQ), Ras GTPase-activating protein related domain (GRD) and C-terminus CT). Numbers represent amino acids.

scaffold for the MAP kinase signaling cascade (Roy et al., 2004; Roy et al., 2005), suggesting that it may also play an important role in cell proliferation (Figure 21).

Materials and Methods

Cell culture

For all described experiments HL-60 cells were differentiated along the neutrophilic lineage as described previously (Servant et al., 1999). Briefly, cells were cultured in RPMI 1640 medium supplemented with 25 mM HEPES (pH 7.4), 10% fetal bovine serum (Atlanta Biologicals, Atlanta, GA), L-glutamine, 100 units/ml pen/strep (Mediatech, Inc., Herndon, VA). Cells were subcultured every 3-4 days to a cell density of 1 X 10^6 cells/ml. To differentiate HL60 cells along the granulocytic lineage, cells were inoculated at a density of 2 x 10^5 cells/ml in antibiotic-free medium containing 1.3% Dimethyl sulfoxide (DMSO) (endotoxin-free, Sigma) and cultured for 6-7 days.

Immunoprecipitation of CXCR2 protein complexes

Normal rabbit IgG antibodies (Jackson Immunoresearch, West Grove, PA) and rabbit polyclonal anti-CXCR2 antibodies were coupled to NHS-activated Sepharose 4 Fast Flow matrix (GE Healthcare, Piscataway, NJ) at a 4:1 ratio (mg antibody: ml matrix). Anti-CXCR2 affinity purified polyclonal antibody was generated in our laboratory and described previously (Mueller et al., 1994).

Coupled antibody beads were blocked with ethanolamine (Sigma, St. Louis, MO) to minimize non-specific binding of proteins to matrix. For immunoprecipitations, HL-60 cells stably expressing CXCR2 were differentiated for 7 days in 1.3% DMSO and stimulated with vehicle (0.1% BSA/PBS) or 100 ng/ml CXCL8 for 1 minute. Cells were resuspended in lysis buffer (50mM Tris-HCl, pH 7.5, 0.05% Triton X-100, 300 mM NaCl), cleared by centrifugation, and pre-cleared with normal rabbit IgG-coupled beads. Precleared lysates were then incubated with normal rabbit IgG-coupled beads (Mock) or anti-CXCR2 rabbit antibody-coupled beads and associating proteins were eluted with 2X Laemmli sample buffer, heated for 55˚C for 10 minutes, loaded directly onto a 10% polyacrylamide gel with no stacker gel. The electrophoresis was continued until the dye front ran approximately 1 cm into the gel and proteins were stained with colloidal blue stain (Invitrogen, Carlsbad, CA**)**. Excised gel bands were subjected to in-gel trypsin digest (Manza et al., 2005) and tryptic peptides submitted for LC/MS/MS analysis.

LC/MS/MS analysis and protein identification

One dimensional LC/MS/MS analysis was performed as described previously (Lapierre et al., 2007). Briefly, analysis was performed using a Thermo Finnigan LTQ ion trap mass spectrometer and peptides were separated on a packed capillary tip (100µm X 11 cm) with C18 resin (Monitor C18, 5µm, 100Å, Column Engineering, ON, Canada). MS/MS spectra of peptides was performed using data-dependent scanning in which one full MS spectrum, using

a full mass range of 400-200 amu, was followed by 3 MS-MS spectra. Protein matches were preliminarily filtered using the criteria described previously (Lapierre et al., 2007). Once the peptides were filtered based on these criteria, all matches that had less than two peptide matches were eliminated. These filtering criteria achieved a false positive rate of <1% in all datasets.

Immunofluorescence staining and confocal microscopy

Cells in serum-free RPMI were seeded on glass coverslips coated with 100 µg/ml human fibronectin (BD Biosciences, San Diego, CA) and stimulated globally with vehicle (0.1% BSA/PBS) or 100 ng/ml CXCL8 diluted in 0.1% BSA/PBS at 37˚C for indicated times. Cells were fixed in 4% paraformaldehyde for 10 min, permeabilized in 0.2% Triton X-100/PBS for 5 min, blocked in 10% normal donkey serum for 30 min (Jackson Immunoresearch Laboratories, Inc., West Grove, PA). Anti-CXCR2 rabbit polyclonal (Mueller et al, 1994) and anti-IQGAP1 mouse monoclonal (Invitrogen, Carlsbad, CA) primary antibodies were added and incubated for 2 hours at room temperature. After washing three times with 0.1% Tween 20/PBS, the coverslips were incubated with fluorescence-conjugated secondary antibodies for 1 hour. After final three washes with 0.1% Tween 20/PBS, coverslips were mounted with ProLong Gold antifade reagent (Invitrogen, Carlsbad, CA). Confocal images were acquired using a LSM-510 Meta laser scanning microscope (Carl Zeiss, Thornwood, NY) with a 63X 1.3 numerical aperture oil immersion lens and images were processed by Photoshop software (Adobe Systems, San Jose, CA).

Construction of GST-IQGAP1 plasmids and preparation of recombinant GST-IQGAP1 protein from Escherichia coli

The pGEX-2T-IQGAP1-amino-terminus (NT) (aa 1-863) and –carboxyl-terminus (CT) (aa 864-1657) was a generous gift from Dr. David Sacks and were described previously (Hart et al., 1996). To prepare the cDNA for GST-IQGAP1 1-160 and GST-IQGAP1 1-265 PCR was performed on pGEX-2T-IQGAP1-NT using the forward primers containing a 5' BamHI site and a 3' XhoI site. The same forward primer was used to prepare both fragments. The following primers were used for 1-160 amplification: forward-5' ctctagggatccatgtccgccgcagacgaggtt 3' and reverse- 5' ctagctctcgagttagaacaggtacaaactgac 3'. The following reverse primer was used for 1-265 amplification: 5'ctagctctcgagttaagcctggtaaagtatat cctgg 3'. Fragments were amplified and digested with BamHI and XhoI, purified, and ligated into the pGEX-6P1 vector. All plasmids were purified using Sigma DNA maxiprep kits (Sigma, St. Louis, MO) according to the manufacturer's instructions. GST-fusion proteins were prepared from *Escherichia coli* as described previously. Briefly, cultures were inoculated and grown until OD600 = 0.6-0.8 and expression was induced with 10μM isopropyl β-D-1-thiogalactopyranoside (IPTG) (Sigma, St. Louis, MO) 4 hours at 30˚C. Bacteria were harvested, proteins extracted by sonication, and isolated by incubation with glutathione-agarose (Sigma, St. Louis, MO).

Direct binding of purified IQGAP1-NT and GST-CXCR2 carboxyl-terminus

The GST tag was cleaved from purified GST-IQGAP1-NT coupled to glutathione-agarose by incubating with thrombin (10 units/1mg total protein) (GE Healthcare, Piscataway, NJ) for 16 hours at 25˚C. Cleaved protein was incubated with Benzamidine sepharose 4 Fast Flow matrix (GE Healthcare, Piscataway, NJ) to remove thrombin. Glutathione agarose beads coupled to GST or GST-CXCR2 carboxyl-terminus and reaction tubes were blocked with 1% BSA for 1 hour at 25˚C prior to binding assay. 50µg total GST-fusion proteins on beads were incubated with 10µg purified IQGAP1-NT for 1 hour at 4˚C in binding buffer (50mM Tris-HCl, pH 7.5, 300 mM NaCl, 0.01% Triton X-100). Beads were washed four times with binding buffer. Bound proteins were eluted with 2X Laemmli sample buffer and subjected to SDS-PAGE and western blot analysis using an anti-IQGAP1 rabbit polyclonal antibody directed against the amino-terminus of the protein (Santa Cruz Biotechnology, Inc., Santa Cruz, CA)

Results

Development of a proteomics approach to identify novel CXCR2-interacting proteins

In order to identify proteins that differentially associate with the unstimulated receptor versus the activated receptor it was important to immunoprecipitate receptor-protein complexes from a physiologically relevant cell type. The analysis was conducted in the HL-60 cell line differentiated into the human neutrophil lineage because CXCR2 is essential for the inflammatory

response due to its involvement neutrophil recruitment. Differentiated HL-60 cells naturally express low levels of CXCR2, however, in order to maximize co-immunoprecipitating proteins, CXCR2 was stably over-expressed in the cell lines used in these experiments. An additional obstacle of performing these analyses is the presence of high amounts of IgG from immunprecipitation which makes it difficult to detect spectra of peptides from less abundant proteins. In order to address this problem, normal rabbit IgG and anti-CXCR2 rabbit antibodies were covalently coupled to sepharose beads. This allowed protein complexes to be eluted from the beads without IgG contamination.

Cells were stimulated with either vehicle or 100 ng/ml CXCL8 for 1 minute and lysed in a mild buffer in order to maintain weak interactions within protein complexes. Normal rabbit IgG- (mock control) and anti-CXCR2-coupled beads were then used to immunoprecipitate complexes from lysates and eluted using Laemmli sample buffer. Eluted proteins were then loaded directly onto a polyacrylamide resolving gel and allowed to run into the gel approximately 1 cm. Protein bands were stained with colloidal blue stain and excised from the gel. Tryptic peptides were generated by in-gel trypsin digest and subjected to LC/MS/MS analysis. Proteins were identified using the cluster version of the SEQUEST algorithm (Yates et al., 1995) using the human subset of the Uniref100 database (www.uniprot.org). Detailed methodology is described in the Materials and Methods section above. Unique proteins in each group were identified using an in-house Vanderbilt database program called CHIPS (Complete Hierarchical Integration of Protein Searches). This allowed non-

specific identifications from the mock control immunoprecipitations to be subtracted from the two experimental groups. A schematic of the approach used to identify novel CXCR2-interacting proteins is shown in Figure 22.

Identification of novel ligand-independent and -dependent CXCR2-interacting proteins

The proteomics analysis was repeated four times for reproducibility. Proteins were considered consistent identifications if present in at least three of the four experiments and for which the spectra for at least three tryptic peptides matched. It should be noted that a number of proteins identified in the yeast-2-hybrid experiments were identified in this proteomics approach including, PP2A, AP-2, cyclophilin A, and clathrin. Consistent identifications included eleven proteins with the unstimulated receptor, eight proteins with the activated receptor, and six proteins common to the unstimulated and activated receptor (Table 2). These proteins ranged in functionality from those involved in modification of the actin cytoskeleton (ie: VASP, gelsolin, Arp 2/3, and Lasp-1), intracellular trafficking (ie: annexin 1, dynein, and SCAMP2), and signaling scaffolding (ie: IQGAP1, 14-3-3 zeta, and LIN-41).

IQGAP1 is a novel CXCR2 interacting protein

The signaling scaffolding protein IQGAP1 was consistently identified with both the unstimulated and activated receptor immunoprecipitations using this approach. The interaction of IQGAP1 with CXCR2 was verified by immunoprecipation followed by western blot analysis. In support of the

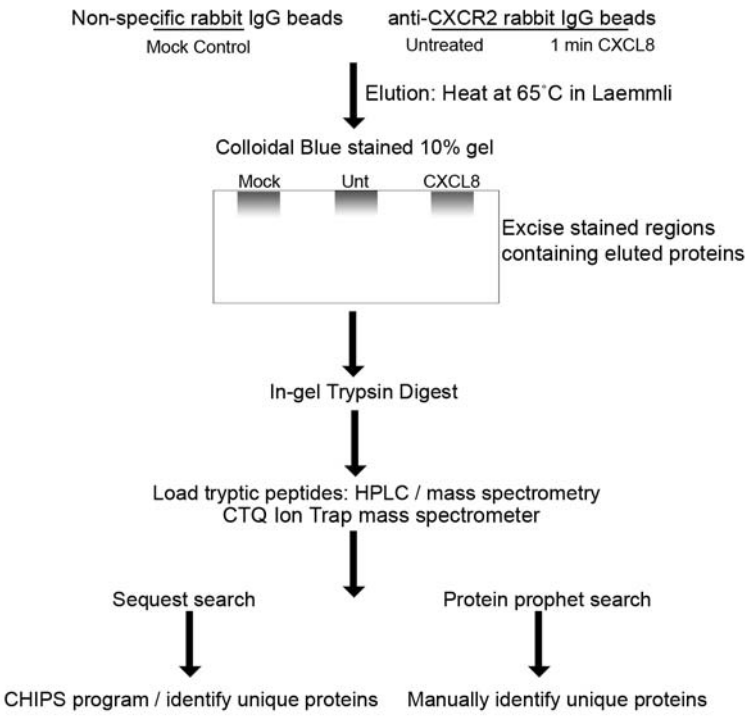

Figure 22: Schematic of representation of proteomics approach used to identify novel CXCR2-interacting proteins.

Table 2: List of identified proteins from untreated and CXCL8 stimulated cells in LC/MS/MS analysis.

	Untreated	CXCL8 treated	Both Untreated and CXCL8 treated
Actin cytoskeleton	p21-Arc	Vasodilator-stimulated phosphoprotein (VASP)	Talin1
	Gelsolin		Arp 2/3 subunit 2
	Plastin		Lasp-1
Intracellular trafficking	Rab7	Secretory carrier membrane protein 2 (SCAMP2)	Clathrin heavy chain 1
	Annexin 1	Nipsnap homolog 1	
	Kinesin light chain-2	Dynein heavy chain 5	
	Valosin-containing protein (VCP)		
Signaling scaffolding	14-3-3 gamma	Similar to LIN-41	YWHAZ (14-3-3 zeta)
			IQ motif-containing GTPase activating protein 1 (IQGAP1)
Other	Hsp 90	PSMA2 (proteosome subunit)	
	Hsp 75	26S proteosome subunit 9	
	Chaperonin TCP1		

proteomics analyses, western blot analysis shows an apparently equal amount of immunoreactive IQGAP1 co-IPs with CXCR2 in untreated cells and cells stimulated with CXCL8 for 1 minute. Interestingly, IQGAP1 no longer co-IPs with CXCR2 following 5 minutes of CXCL8 stimulation (Figure 23A). Intracellular localization of IQGAP1 was also examined upon CXCL8 stimulation by immunofluorescence staining and confocal microscopy. In unstimulated cells, IQGAP1 is localized just below the plasma membrane and accumulates in membrane ruffles with CXCR2 upon 1 minute of CXCL8 stimulation (Figure 23B). Consistent with the immunoprecipitation experiments, very little IQGAP1 localizes to membrane ruffles as the receptor internalizes after 5 minutes of CXCL8 stimulation (Figure 23B). These data suggest that IQGAP1 is important for early events (0-1 minutes) in response to ligand.

CXCR2 interacts with the amino-terminus of IQGAP1 specifically through amino acids 1-160

To determine the domain of IQGAP1 that interacts with CXCR2, GST-IQGAP1-amino-terminus (NT) (residues 1-863) and –carboxyl-terminus (CT) (residues 864-1657) fusion proteins were produced (Figure 24A). Pulldown reactions were performed using these proteins and lysates from differentiated HL-60 cells stably expressing CXCR2. As shown in Figure 24B, the amino terminus of IQGAP1 interacts with CXCR2 from HL-60 cells. GST fusion proteins of successively smaller domains within the amino-terminus of IQGAP1 were generated to further define the interaction domain. Amino acids 1-265 and 1-160 were both able to efficiently interact with CXCR2 from HL-60 cells (Figure 24C).

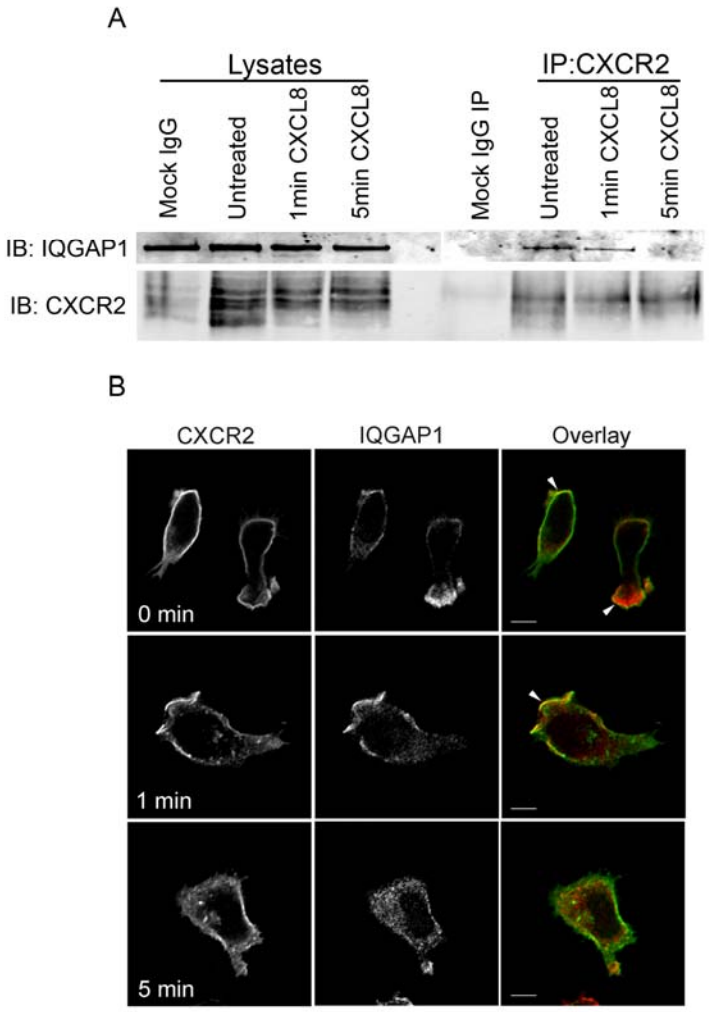

Figure 23: IQGAP1 is a novel CXCR2 interacting protein.
(A) IQGAP1 co-immunoprecipitates with CXCR2. Lysates from cells stimulated with vehicle (Mock, Untreated) or cells stimulated with 100 ng/ml CXCL8 for 1 min or 5 min were incubated with either normal rabbit IgG- (Mock IgG) or rabbit anti-CXCR2 antibody-coupled sepharose. Beads were washed and immunoprecipitated proteins were eluted with Laemmli sample buffer. Samples were analyzed by SDS-PAGE and western blot (IB) for CXCR2 and IQGAP1 (B) Co-localization of CXCR2 and IQGAP1. Immunofluorescence confocal images of CXCR2 and IQGAP1 staining in differentiated HL60 cells stably expressing CXCR2 and stimulated with vehicle (0 min) or 100 ng/ml of CXCL8 for 1 minute or 5 minutes. Cells were stained with rabbit polyclonal anti-CXCR2 and mouse monoclonal anti-IQGAP1 antibodies, and incubated with species specific Cy2- and Cy3-conjugated secondary antibodies. Co-localization is seen at 0 minutes and 1 minute stimulation. Overlay images are pseudocolored where green is CXCR2 and red is IQGAP1. Bars, 5μm. Data shown are representative of three separate experiments.

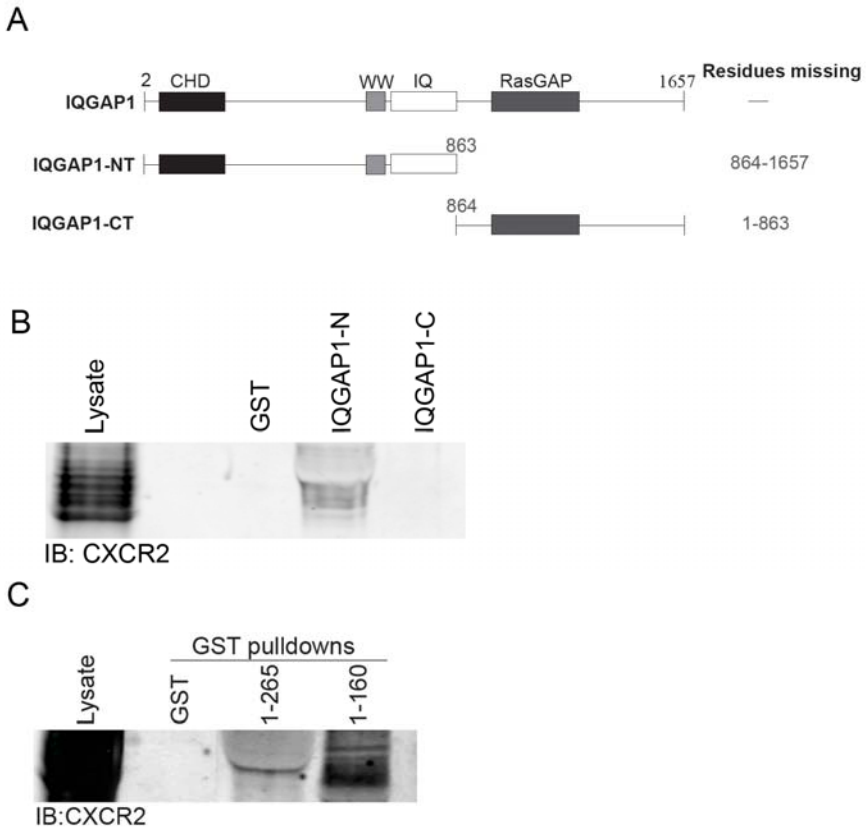

Figure 24: CXCR2 interacts with the amino-terminus of IQGAP1 specifically through amino acids 1-160.
(A) Domains contained in GST-IQGAP1 fusion constructs. Western blot analysis with anti-CXCR2 antibody of lysates (Input) and eluates from (B) GST, GST-IQGAP1-N-terminus (NT), and IQGAP1-C-terminus (CT) pulldown reactions and (C) GST, GST-IQGAP1-1-265, and -1-160. Data shown are representative of three separate experiments.

GST fusion proteins containing residues 1-44 and 160-431 were also generated and used in pulldown reactions. These two fusion proteins failed to interact with CXCR2. These data suggest that a region of IQGAP1 located between residues 44 and 160 is likely the CXCR2-interaction domain.

CXCR2 directly interacts with the amino-terminus of IQGAP1

We next sought to determine whether the IQGAP1 interaction with CXCR2 is direct or occurs through an intermediate adaptor protein. To investigate this, recombinant IQGAP1-amino-terminus (NT) and GST-CXCR2-carboxyl-terminus were purified. These proteins were then used in direct binding assays in order to assess whether the two proteins can interact in the absence of other cellular proteins. These assays demonstrated that purified IQGAP1-NT and GST-CXCR2 carboxyl-terminus are able to bind in vitro (Figure 25). These data suggest that CXCR2 directly interacts with the amino-terminus of IQGAP1.

Interaction of IQGAP1 with Cdc42 is enhanced by CXCL8 stimulation

A number of studies have demonstrated that the interaction of IQGAP1 with the small GTPases Rac and Cdc42 is affected by various different stimuli such as cell-cell adhesion (Fukata et al., 1999; Kuroda et al., 1999; Takahashi et al., 2006), cell-matrix adhesion (Takahashi and Suzuki, 2006), and Ca^{2+} signaling (Ho et al., 1999). Because Cdc42 is activated upon CXCR2 stimulation, we sought to investigate whether the association of Cdc42 with IQGAP1 was altered upon CXCL8 stimulation. We examined if the association of IQGAP1 with Cdc42

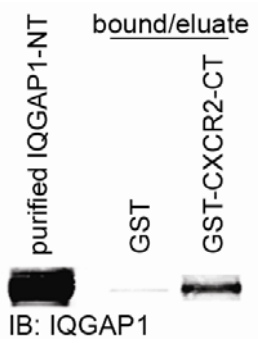

Figure 25: Purified IQGAP1/N-terminus binds directly to GST CXCR2/C-terminus.
Western blot analysis of purified IQGAP1/N-terminus (NT) and purified protein bound to glutathione sepharose beads with GST alone or GST-CXCR2/C-terminus (CT). Briefly, fusion protein-bound glutathione beads were blocked with 1% BSA for 1h at room temp and incubated for 1h at 4˚C with 10µg purified IQGAP1/N-terminus in binding buffer. Beads were washed 3X with binding buffer and bound protein eluted and analyzed by SDS-PAGE and western blot (IB) for IQGAP1. Data shown are representative of three separate experiments.

was altered upon CXCL8 stimulation. To investigate this, we immunoprecipitated IQGAP1 from differentiated HL-60 cells expressing CXCR2 stimulated with CXCL8 and examined association of Cdc42 by western blot analysis. These experiments demonstrated that co-immunoprecipitation of Cdc42 with IQGAP1 is slightly enhanced with CXCL8 stimulation (Figure 26A). This experiment was repeated twice with similar results demonstrating an average of a 1.23 fold (range = 0.06) increase in co-immunoprecipitated Cdc42 following 1 minute of CXCL8 stimulation (Figure 26B). This establishes a potential functional link between CXCR2 activation and modulation of IQGAP1 activities within the cell.

Discussion

We have developed a highly effective approach to identify novel dynamic chemokine receptor-interacting proteins. This approach allows protein complexes to be isolated from cells following various periods if ligand stimulation and has the potential to temporally define the components of chemokine receptor-associating complexes within the cell. This has important implications for the current understanding of the chemotactic response.

Among the proteins identified in the untreated samples was 14-3-3 gamma. 14-3-3 gamma is a signaling adaptor molecule that can bind regulators of G-protein signaling (RGS) proteins and inhibit their activity (Benzing et al., 2000; Niu et al., 2002). RGS proteins are GTPase activating proteins (GAPs) that specifically activate the Gα subunit (Ishii and Kurachi, 2003; Ross and Wilkie, 2000). It has been previously shown that RGS12 interacts with CXCR2

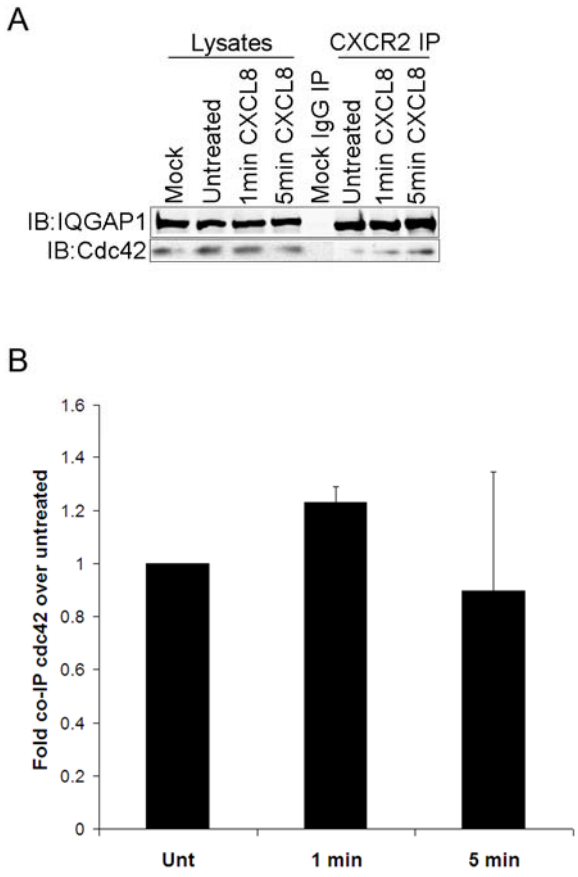

Figure 26: Interaction of IQGAP1 with Cdc42 is enhanced by CXCL8 stimulation.

Lysates from cells stimulated with vehicle (Mock, Untreated) or cells stimulated with 100 ng/ml CXCL8 for 1 min or 5 min were incubated with either normal rabbit IgG- (Mock IgG) or rabbit anti-IQGAP1 antibody and Protein A/G agarose beads. Beads were washed and immunoprecipitated proteins were eluted with Laemmli sample buffer. Samples were analyzed by SDS-PAGE and western blot (IB) for IQGAP1 and Cdc42. (A) Western blot is a representative from two separate experiments (B) Graph is an average fold increase of two separate experiments. Bars represent the range between the two experiments.

through its PDZ (PSD95/DlgA/ZO-1) domain (Snow et al., 1998). Therefore, the interaction of CXCR2 with 14-3-3 gamma represents a potential novel link to signaling pathways through its function as an adaptor molecule that is a known regulator of RGS proteins.

A number of proteins that regulate the actin cytoskeleton were also identified using this approach. p21-Arc is a subunit from the actin-related protein (Arp) 2/3 complex, which also localizes to sites of actin polymerization (Welch et al., 1997). In addition, another subunit from the Arp 2/3 complex was also identified with this approach. The Ena/VASP family of proteins can enhance actin polymerization by recruiting profilin-actin complexes to sites of acting remodeling, such as the lamellipodia in migrating cells (Krause et al., 2003; Sechi and Wehland, 2004). LIM and SH3 domain protein-1 (Lasp-1) is a component of the focal adhesion that has recently been shown to play an important role in cell migration and cell survival (Grunewald et al., 2006b; Grunewald et al., 2007; Lin et al., 2004). Each of these actin regulating proteins may provide a link between the activated chemokine receptor and the acting cytoskeleton.

Two components of microtubule motor proteins were also among the proteins identified with this approach. These proteins may play a role in the intracellular trafficking of chemokine receptors, as well as in signaling by transporting signaling proteins to appropriate cellular locations. For example, kinesins are microtubule motor proteins that are involved in transporting vesicles and organelles along microtubules. Interestingly, it was found that 14-3-3 interacts with kinesin light chain-2 in a phosphorylation-dependent manner

(Ichimura et al., 2002). Dynein heavy chain, another microtubule motor protein, was also identified in complexes from stimulated cells. Furthermore, microtubules are known to play a role in the endocytosis of other G protein-coupled receptors such as beta2-adrenoceptor (Vroon et al., 2007) and m3-muscarinic receptors (Popova and Rasenick, 2004). Additional proteins that may play a role in the intracellular sorting of internalized CXCR2 were among the novel CXCR2-interacting proteins. Valosin-containing protein is a molecular chaperone that is involved in the ubiquitin-proteosome degradation pathway (Brunger and DeLaBarre, 2003; Wang et al., 2004). Rab39 is a golgi-associated GTPase that can facilitate endocytosis (Chen et al., 2003a). Nipsnaps are a family of proteins that have a potential role in vesicular trafficking because of their homology to synaptosomal-associated proteins ((SNAP) (Seroussi et al., 1998). In addition, NIPSNAP4 was shown to interact with the *Salmonella enterica* factor SpiC, which inhibits lysosomal maturation (Lee et al., 2002).

IQGAP1 binds to CXCR2 in the absence of CXCL8 stimulation and no longer binds following prolonged stimulation. It is likely that once CXCR2 internalizes, IQGAP1 dissociates from the receptor. CXCL8 stimulation induces CXCR2 phosphorylation, Cdc42 activity, and a rise in intracellular Ca^{2+} levels. Activated Cdc42 and Ca^{2+}/calmodulin both modulate IQGAP1 activities and binding partners (reviewed in (Briggs and Sacks, 2003; Noritake et al., 2005)) . It has been previously demonstrated that inhibition of $Ca^{2+/}$calmodulin by the cell-permeable inhibitor CGS 9343B impairs the Ca^{2+}-dependent interaction of E-cadherin with IQGAP1 (Li et al., 1999). Therefore, we are interested in whether

CXCR2 phosphorylation, Cdc42 activity, and Ca^{2+}/calmodulin influence CXCR2/IQGAP1 binding. In the future, it will be of interest to express dominant negative and activated Cdc42 mutants and determine whether the interaction between CXCR2 and IQGAP1 is enhanced or disrupted. Additionally, investigation into the effects of inhibition of CXCR2 phosphorylation using phosphorylation-deficient receptor mutants and inhibition of Ca^{2+}/calmodulin through use of a cell-permeable calcium chelator on the CXCR2/IQGAP1 interaction will be of interest.

It is of interest that CXCR2 interacts with IQGAP1 between amino acids 44 and 160 because this region also contains the calponin homology domain (Figure 21). This region of IQGAP1 is necessary and sufficient for its high affinity interaction with F-actin (Mateer et al., 2004). Studies utilizing point mutations in the calponin homology domain demonstrated that the IQGAP1 interaction with F-actin is essential for its role in the promotion of cell motility (Mataraza et al., 2007). In addition, interaction of IQGAP1 with calmodulin has been shown to inhibit the binding of IQGAP1 to actin (Mateer et al., 2002). Therefore, it is possible that CXCR2 competes with actin for binding to the calponin homology domain of IQGAP1 similar to the phenomenon seen with calmodulin.

Investigation into the functional significance of the interaction between CXCR2 and IQGAP1 will also be of great interest in the future. We have identified amino acids 1-160 of IQGAP1 as the CXCR2 interaction domain. This domain can be utilized to specifically antagonize the CXCR2/IQGAP1 interaction in differentiated HL-60 cells. The effects of antagonizing the receptor/IQGAP1

interaction on CXCR2-mediated chemotaxis and CXCL8-mediated Rac/Cdc42 activation should be investigated. The effects on cell polarization in response to directional CXCL8 stimulation should be assessed by examining the ability of the cells to reorient the microtubule organizing center (MTOC) in the direction of the CXCL8 source. Because IQGAP1 has been shown to modulate activation of the MAP kinase pathway and cell proliferation, effects on CXCL8-mediated MAP kinase pathway activation and CXCL8-mediated cell proliferation will also be of interest to examine when the CXCR2/IQGAP1 interaction is antagonized.

We describe a novel and effective technique to identify components of dynamic chemokine receptor protein complexes within the cell. A number of interesting proteins have been identified that potentially regulate chemokine receptor function. These proteins range in function from intracellular trafficking and cytoskeletal modification. The characterization of these interactions will greatly impact or current understanding of how the chemotactic response is relayed from activated chemokine receptors to the cytoskeleton and intracellular signaling cascades.

CHAPTER IV

VASP IS A NOVEL CXCR2-INTERACTING PROTEIN THAT REGULATES CXCR2-MEDIATED LEUKOCYTE RECRUITMENT

Introduction

Chemokines mediate the chemotactic response through binding of their seven transmembrane G protein-coupled receptors. CXCR2-mediated chemotaxis is completely inhibited by treatment of pertussis toxin indicating that the majority of CXCR2 couples to Gαi (Jones et al., 1995). In addition, studies have demonstrated that specific Gβγ subunits coupled to the Gαi, but not the Gαi subunit itself is required for chemotaxis (Neptune et al., 1999). These data suggest that cAMP-protein kinase A (PKA)-mediated signaling pathways play a minimal role in the chemotactic response. These signaling pathways activated as a result of the uncoupling of the Gβγ subunit from the heterotrimeric complex involved in chemotaxis include activation of phospholipase Cβ (PLC-β), phosphatidylinositol 3 kinase (PI3K), and mitogen-activated proteins (MAPKs). Furthermore, these studies demonstrate that additional signaling pathways that mediate the chemotactic response may be activated via G protein-independent mechanisms, perhaps through novel receptor-interacting proteins (Luttrell et al., 1999; Richardson et al., 1998; Tilton et al., 2000).

Upon binding ligand, CXCR2 chemokine receptors are internalized largely through clathrin-mediated endocytosis. The proteins that mediate the

internalization of chemokine receptors and link activated receptors to signaling pathways are poorly defined. Of particular interest are the proteins that initiate and propagate the chemotactic response once a chemokine binds its receptor. In order to more completely understand these processes, the identification of protein complexes that associate with the receptor upon ligand binding is necessary.

Previous investigators in our laboratory have addressed this question by utilizing the carboxyl-terminal domain of CXCR2 in a yeast-2-hybrid analysis in order to identify interacting proteins (Fan et al., 2001a; Fan et al., 2002; Fan et al., 2001b). Although the yeast-2-hybrid analysis identified a number of important interacting proteins, this approach does not allow for identification of receptor/protein complexes that form upon ligand stimulation. We describe here the identification of a ligand-mediated receptor/protein interaction using immunoprecipitation followed by proteomics analysis. This approach has a number of benefits, including the ability to identify the dynamics of both direct and indirect receptor/protein interactions and those interactions that are conformation-specific, for example, dependent on phosphorylation.

One CXCR2-interacting protein identified by receptor immunoprecipitation followed by proteomics analysis is vasodilator-stimulated phosphoprotein (VASP). VASP is a member of the Ena/VASP family of proteins that mediate actin filament elongation (Sechi and Wehland, 2004). The Ena/VASP family members enhance actin filament elongation by recruiting profilin:actin complexes to sites of active actin remodeling, such as the lamellipodia and focal adhesions

(Kang et al., 1999; Korenbaum et al., 1998; Nyman et al., 2002). Localization of VASP at the barbed ends of actin filaments promotes filament elongation and prevents the binding of capping proteins (Barzik et al., 2005). In addition, VASP can enhance the activity of the Arp2/3 complex involved in actin filament nucleation (Samarin et al., 2003; Skoble et al., 2001). VASP contains two conserved EVH (Ena/VASP homology domains), a central proline rich region, and a number of conserved serine/threonine residues that can be phosphorylated by PKA and PKG (Eigenthaler et al., 1992; Gertler et al., 1996; Lambrechts et al., 2000) (Figure 27). Phosphorylation of Ena/VASP proteins at the conserved amino-terminal serine leads to a major conformational change which results in an electrophoretic mobility shift and alterations in protein-protein interactions (Gertler et al., 1996; Halbrugge et al., 1990; Lambrechts et al., 2000). VASP contains three phosphorylation sites, Ser157, Ser239, and Thr278 and phosphorylation at these residues influences the interaction of VASP with actin (Harbeck et al., 2000; Laurent et al., 1999). More specifically, in vitro phosphorylation of VASP at Ser239 decreases the anti-capping and filament bundling activity (Barzik et al., 2005). VASP Thr278 can be minimally phosphorylated in vitro by PKA and PKG (Butt et al., 1994) and recent studies identified VASP Thr278 as a substrate for AMP-activated protein kinase (AMPK) (Blume et al., 2007). However, the contribution of these kinases to Thr278 phosphorylation in vivo and the functional significance of this phosphorylation remain largely uncharacterized. Interestingly, phosphorylation of VASP at Thr278 is associated with decreased cellular F-actin content, suggesting that

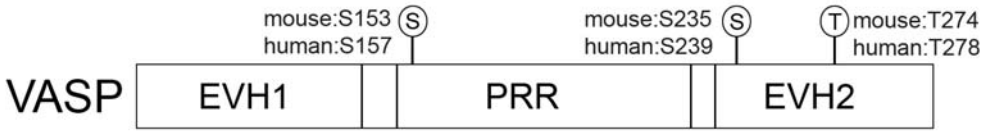

Figure 27: Schematic of VASP domain structure.
EVH1: Ena/VASP Homology 1, PRR: proline-rich region, EVH2: Ena/VASP Homology 2. Circled letters indicate phosphorylation sites (S-serine, T-threonine). The numbers indicate amino acid residues for phosphorylation sites in mouse and human proteins.

phosphorylation of this residue plays a negative role in the F-actin assembly (Blume et al., 2007). It is clear that differential phosphorylation of VASP at each of the three residues modulates its functional diversity, likely through differential cellular localization of various the phosphorylated forms of the protein.

Because of their roles in formation of actin-based structures essential for cell migration, Ena/VASP proteins have an obvious role in cell migration. However, the specific role may be cell type specific and vary depending on experimental conditions. Fibroblasts lacking either Mena or VASP move faster in random motility assays (Bear et al., 2000). Cardiac fibroblasts deficient in VASP exhibit sustained Rac activation (Garcia Arguinzonis et al., 2002). However, the role of VASP in persistent directional cell migration has not been extensively investigated. Futhermore, its role in the regulation of CXCR2-mediated neutrophil chemotaxis remains largely undefined.

In the current study, VASP was identified as a novel CXCR2-interacting protein in differentiated HL-60 cells using proteomic analysis. We show that CXCR2 directly interacts with VASP through the conserved EVH2 domain. In addition, we demonstrate that VASP is phosphorylated upon CXCL8 stimulation on serine residues 157 and 239. These phosphorylations occur via PKA- and PKC-dependent signaling pathways and modulate the interaction between CXCR2 and VASP. We have demonstrated for the first time that a chemokine receptor interacts with a member of the Ena/VASP family of proteins. We have also shown that VASP is phosphorylated in response to chemokine and this phosphorylation enhances the interaction.

Materials and Methods

Materials and Antibodies

Anti-CXCR2 affinity purified polyclonal antibody was generated in our laboratory and described previously (Mueller et al., 1994). Normal rabbit IgG was obtained from Jackson Immunoresearch, Inc. (West Grove, PA). Anti-VASP polyclonal, anti-VASP phospho-serine 157, and anti-VASP phospho-serine 239 monoclonal antibodies were purchased from Calbiochem (San Diego, CA). Anti-GFP polyclonal antibody was obtained from Abcam (Cambridge, MA). PKA inhibitor H-89, PKC inhibitor Ro-32-0432, and PKCδ inhibitor Rottlerin were acquired from Calbiochem (San Diego, CA). Phosphate buffered saline (PBS) was produced by dissolving 8g NaCl, 0.2g KCl, 1.44g Na_2HPO_4, and 0.24g KH_2PO_4 in 1L dH_2O and adjusting pH to 7.4. Bovine serum albumin (BSA) (Fraction V, ~99% purity, γ-globulin-free) was purchased from Sigma (St. Louis, MO)

Plasmids, cell culture, and transfection

Constructs for glutathione *S*-transferase (GST) fusion proteins of the C-terminal residues of CXCR2 were generated previously (Fan et al., 2001a) using PCR-amplified fragments. The HL-60 cell line stably expressing human CXCR2 was generated previously by retroviral infection (Sai et al., 2006). For all described experiments HL-60 cells were differentiated along the neutrophilic lineage as described previously (Servant et al., 1999). Briefly, cells were

cultured in RPMI 1640 medium (Invitrogen, Carlsbad, CA) supplemented with 25mM HEPES (pH 7.4) (Sigma, St. Louis, MO), 10% fetal bovine serum (Atlanta Biologicals, Atlanta, GA), L-glutamine, 100 units/ml pen/strep (Mediatech, Inc., Herndon, VA). Cells were subcultured every 3-4 days to a cell density of 1 X 10^6 cells/ml. To differentiate HL60 cells along the granulocytic lineage, cells were inoculated at a density of 2 X 10^5 cells/ml in antibiotic-free medium containing 1.3% Dimethyl sulfoxide (DMSO) (endotoxin-free, Sigma, St. Louis, MO) and cultured for 6-7 days.

MV^{D7} cells were cultured as described previously (Bear et al., 2000). Briefly, cells were grown at 32˚C in DMEM with 15% FBS, 100 units/ml pen/strep (Mediatech, Inc., Herndon, VA), L-glutamine, and 50 U/ml of mouse interferon-gamma (Sigma, St. Louis, MO).

CXCR2 immunoprecipitations and proteomics analyses

Purified normal rabbit IgG (Jackson Immunoresearch Laboratories, Inc., West Grove, PA) and anti-CXCR2 polyclonal antibodies were coupled to NHS-activated sepharose beads (GE Healthcare**,** Piscataway, NJ) following the manufacturer's protocol. For immunoprecipitations, HL-60 cells stably expressing CXCR2 were differentiated for 7 days in 1.3% DMSO and stimulated with vehicle (0.1% BSA/PBS) or 100 ng/ml CXCL8 for 1 minute. Cells were resuspended in lysis buffer (50mM Tris-HCl, pH 7.5, 0.05% Triton X-100, 300 mM NaCl), cleared by centrifugation, and pre-cleared with normal rabbit IgG-coupled beads. Pre-cleared lysates were then incubated with normal rabbit IgG-

coupled beads (Mock) or anti-CXCR2 rabbit antibody-coupled beads and associating proteins were eluted with Laemmli sample buffer, loaded onto a 10% polyacrylamide gel, stained with colloidal blue stain (Invitrogen, Carlsbad, CA) and bands were subjected to in-gel trypsin digest. Tryptic peptides were then analyzed by LC/MS/MS using a Thermo Finiigan LTQ ion trap mass spectrometer equipped with a Thermo MicroAS autosampler and Thermo Surveyor HPLC pump, Nanospray source, and Xcalibur 1.4 instrument control. Analysis and protein identification procedures were described previously (Lapierre et al., 2007). Unique proteins in each group were identified using an in-house database program called CHIPS (Complete Hierarchical Integration of Protein Searches). Only proteins identified in at least three of the four replicate experiments by multiple peptides were analyzed further.

Immunofluorescence staining and confocal microscopy

Cells in serum-free RPMI were seeded on glass coverslips coated with 100 µg/ml human fibronectin (BD Biosciences, San Diego, CA) and stimulated globally with vehicle (0.1% BSA/PBS) or 100 ng/ml CXCL8 diluted in 0.1% BSA/PBS at 37˚C for indicated times or directionally using a Zigmond chamber (Neuroprobe, Inc., Gaithersburg, MD). Cells were fixed in 4% paraformaldehyde for 10 minutes, permeabilized in 0.2% Triton X-100/PBS for 5 minutes, blocked in 10% normal donkey serum for 30 minutes (Jackson Immunoresearch Laboratories, Inc., West Grove, PA), primary antibodies were added and incubated for 2 hours at room temperature. After washing three times with 0.1%

Tween 20/PBS, the coverslips were incubated with fluorescence-conjugated secondary antibodies for 1 hour. After final three washes with 0.1% Tween 20/PBS, coverslips were mounted with ProLong Gold antifade reagent (Invitrogen, Carlsbad, CA). Confocal images were acquired using a LSM-510 Meta laser scanning microscope (Carl Zeiss, Thornwood, NY) with a 63X 1.3 numerical aperture oil immersion lens and images were processed by Photoshop software (Adobe Systems, San Jose, CA).

Recombinant protein expression and purification

Recombinant His_6-tagged full length and EVH2 domain of VASP were purified from *Escherichia coli* as described previously (Barzik et al., 2005). Recombinant GST and GST-CXCR2 carboxyl-terminus proteins were purified from *Escherichia coli.* Bacteria inoculated from glycerol stock encoding GST proteins were cultured overnight at 37˚C. The following morning, cultures were diluted 1:10 and grown until OD600 = 0.8 and protein expression was induced by incubating bacteria at 30˚C in the presence of 50μM isopropyl-1-thio-β-D-galactopyranoside (IPTG) for 2 hours. Bacteria was collected by centrifugation, washed with PBS, resuspended in 0.5% Triton X-100/PBS containing bacterial protease inhibitor cocktail (Sigma, St. Louis, MO), and sonicated. Lysates were cleared by centrifugation at 12,000 X g for 30 minutes and cleared lysates were incubated with glutathione agarose (Sigma, St Louis, MO) for 45 min at 4˚C. Agarose was washed three times with 0.5% Triton X-100/PBS and resuspended in PBS.

Direct binding of GST-CXCR2 331-355 and His_6-VASP

Assay was performed similarly to an assay previously described (Shimada et al., 2005). GST proteins were isolated as described above and eluted from glutathione agarose with an equal volume of elution buffer (50mM Tri-HCl, pH 8.0, 10 mM reduced glutathione). 96-well polyvinyl plates were coated with 3µg/ml eluted GST or GST-CXCR2 331-355, blocked with 0.5% Tween20/0.5% Triton X-100/PBS, and incubated with 15, 7.5, 3.25, 1.9, or 0.9 ng/µl His_6-VASP for 1 hour at room temperature. Plates were washed six times with 0.1% Tween20/PBS, incubated with 0.5µg/ml His-Probe-HRP (Pierce, Milwaukee, WI), and washed six more times with 0.1% Tween20/PBS. Peroxidase substrate solution [50 mM sodium citrate buffer, pH 4.2, 90 mM 2,2'-azino-bis (3-ethylbenzothiazoline-6-sulfonic acid) (ABTS) (Sigma, St. Louis, MO), 0.05 mM H_2O_2] was added to each well. Reactions were terminated with an equal volume of 1% Sodium dodecyl sulfate (SDS) (Sigma, St. Louis, MO) (w/v) solution. Substrate color intensities were measured at 405 nm using an $ELX800_{NB}$ plate reader (Bio-Tek Instruments, Winooski, VT). Assays were performed in triplicate.

Phosphorylation of His_6-VASP EVH2 with PKA

The His_6-VASP EVH2 domain was purified from *Escherichia coli* and protein was concentrated using Amicon Ultra centrifugal filter devices (MWCO 5,000 Da) (Millipore, Billerica, MA). 50µg purified His_6-VASP EVH2 was incubated with 2500 units cAMP-dependent Protein Kinase A (PKA) catalytic

subunit (New England Biolabs, Inc, Ipswich, MA) with 100 mM ATP for 30 minutes at 30˚C.

GST pulldown reactions with MV^{D7} cell lysates

GST or GST-CXCR2 carboxyl-terminus recombinant proteins were purified from *Escherichia coli* as described above. MV^{D7} cells were lysed in lysis buffer (50 mM Tris-HCl pH 7.5, 0.05% Triton X-100, 300 mM NaCl) containing mammalian protease inhibitor cocktail and phosphatase inhibitor cocktails I and II (Sigma-Aldrich, St. Louis, MO). Lysates were cleared by centrifugation and incubated with 50µg GST or GST-CXCR2 carboxyl-terminus coupled to glutathione agarose for 1 hour at 4˚C. Glutathione agarose was washed three times with lysis buffer, bound proteins were eluted with 2X Laemmli sample buffer, and subjected to SDS-PAGE and western blot analysis.

Statistical Analysis

Statistically significant differences between two groups were determined using the non-parametric two-tailed Mann Whitney U test (Wilcoxin rank sum test). All statistical analysis was performed using GraphPad Prism 5 software (GraphPad software, Inc., San Diego, CA).

Results

VASP is a novel CXCR2-interacting protein

Proteomics analysis was utilized to identify novel ligand-independent and –dependent CXCR2-interacting proteins. In order to identify physiologically relevant interacting proteins, HL-60 myeloid leukemia cells stably over-expressing human CXCR2 were differentiated into neutrophil-like cells. These cells were stimulated with vehicle or CXCL8 for 1 minute and CXCR2 was immunoprecipitated with associating proteins from lysates using rabbit polyclonal antibodies directed against the amino-terminus of the receptor coupled to sepharose beads. As a negative control, proteins were also immunopreciptated using normal rabbit IgG coupled to sepharose beads. Eluted proteins were digested with trypsin and the tryptic peptides were subjected to LC/MS/MS analysis. Spectra from tryptic peptides were compared to known spectra using the Sequest and Protein Prophet algorithms to identify proteins. Proteins identified from control rabbit IgG samples were subtracted from CXCR2 antibody samples. Detailed methodology is included in the Materials and Methods section of this manuscript. This analysis was repeated four times and proteins consistently identified were validated by immunoprecipitation assay.

Vasodilator-stimulated phosphoprotein (VASP) was consistently identified in CXCR2-immunoprecipitate samples from CXCL8 stimulated cells. Interaction of VASP with CXCR2 in differentiated HL-60 cells was confirmed by immunoprecipitation and western blot analysis. VASP co-immunoprecipitates

with CXCR2 in untreated cells and cells stimulated with CXCL8 for both 1 minute and 5 minutes (Figure 28A). Interestingly, VASP is phoshorylated upon CXCL8 stimulation, indicated by the electrophoretic mobility shift, and there is a significant increase in the amount of phosphorylated VASP that co-immunoprecipitates with CXCR2 (Figure 28B). In order to verify that CXCR2 and VASP were interacting in differentiated HL-60 cells we also performed the reverse immunoprecipitation experiment. We observed an electrophoretic mobility shift of CXCR2 upon CXCL8 stimulation indicating that the receptor is phosphorylated. However, these higher molecular weight bands are not clearly visible in the immunoprecipitation samples due to IgG heavy chain present at the same molecular weight obscuring the bands. Indeed, CXCR2 also associates with immunoprecipitated VASP from HL-60 cell lysates (Figure 28C).

To determine whether CXCR2 and VASP co-localize upon CXCL8 stimulation in differentiated HL-60 cells, we performed immunofluorescence staining and confocal imaging on cells stimulated with CXCL8 globally and directionally. As shown in Figure 29A, VASP primarily localizes to the cytoplasm and minimal plasma membrane localization is seen in vehicle stimulated cells. However, upon global stimulation with CXCL8, both VASP and CXCR2 localize to membrane ruffles. This localization is observed in cells stimulated for both 1 minute and 5 minutes, consistent with co-immunoprecipitation data. In addition, CXCR2 and VASP localize to the tips of F-actin-rich lamellipodia in the leading edge of the differentiated HL-60 cells that are directionally stimulated with

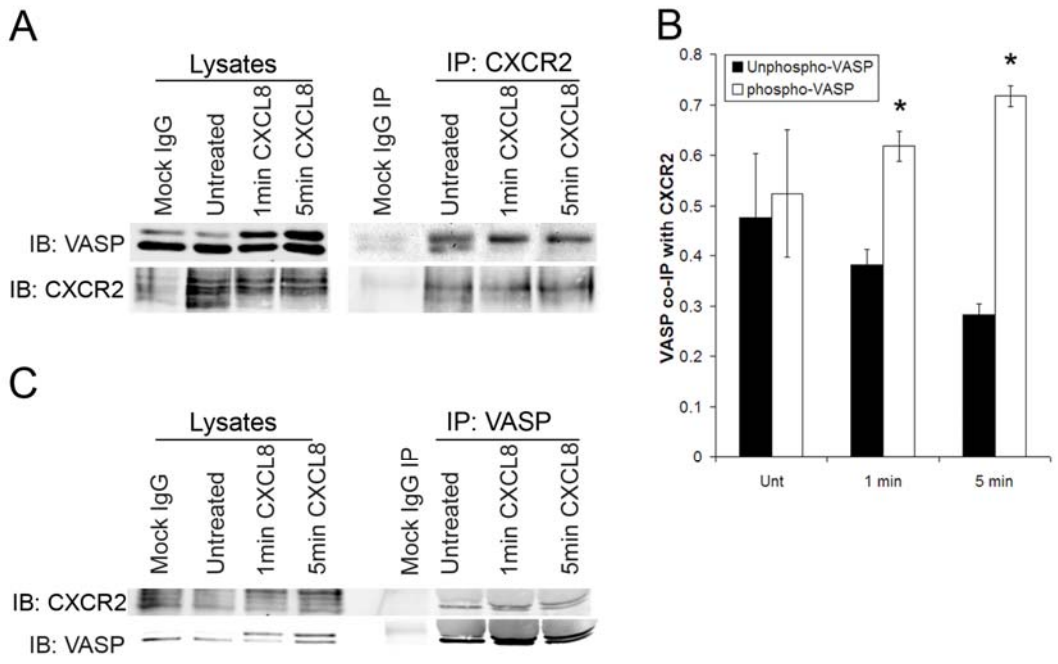

Figure 28: CXCR2 and VASP interact in differentiated HL-60 cells.
(A) VASP co-immunoprecipitates with CXCR2. Lysates from cells stimulated with vehicle (Mock, Unt) or cells stimulated with 100 ng/ml CXCL8 for 1 minute or 5 minutes were incubated with either normal rabbit IgG- (Mock IgG) or rabbit anti-CXCR2 antibody-coupled sepharose. Beads were washed and immunoprecipitated proteins were eluted with Laemmli sample buffer. Samples were analyzed by SDS-PAGE and western blot (IB) for CXCR2 and VASP (B) Quantitation of unphosphorylated (Unphospho-VASP) and phosphorylated (phospho-VASP) VASP that co-immunoprecipitates with CXCR2. Values are normalized to total VASP levels. Significant differences between the amount of unphosphorylated and phosphorylated VASP that co-IPs with CXCR2 are indicated by the asterisks (p-value ≤ 0.05, Mann Whitney U test) (C) CXCR2 co-immunoprecipitates with VASP. Cells were stimulated with vehicle (Mock, Unt) or 100 ng/ml CXCL8 for 1 minute or 5 minutes. Lysates were incubated with normal rabbit IgG (Mock IgG) or rabbit anti-VASP antibody. Immunoprecipitated proteins were immobilized on protein A/G agarose, eluted with Laemmli sample buffer, and subjected to SDS-PAGE and western blot analysis (IB) for VASP and CXCR2. Data shown are representative from three separate experiments.

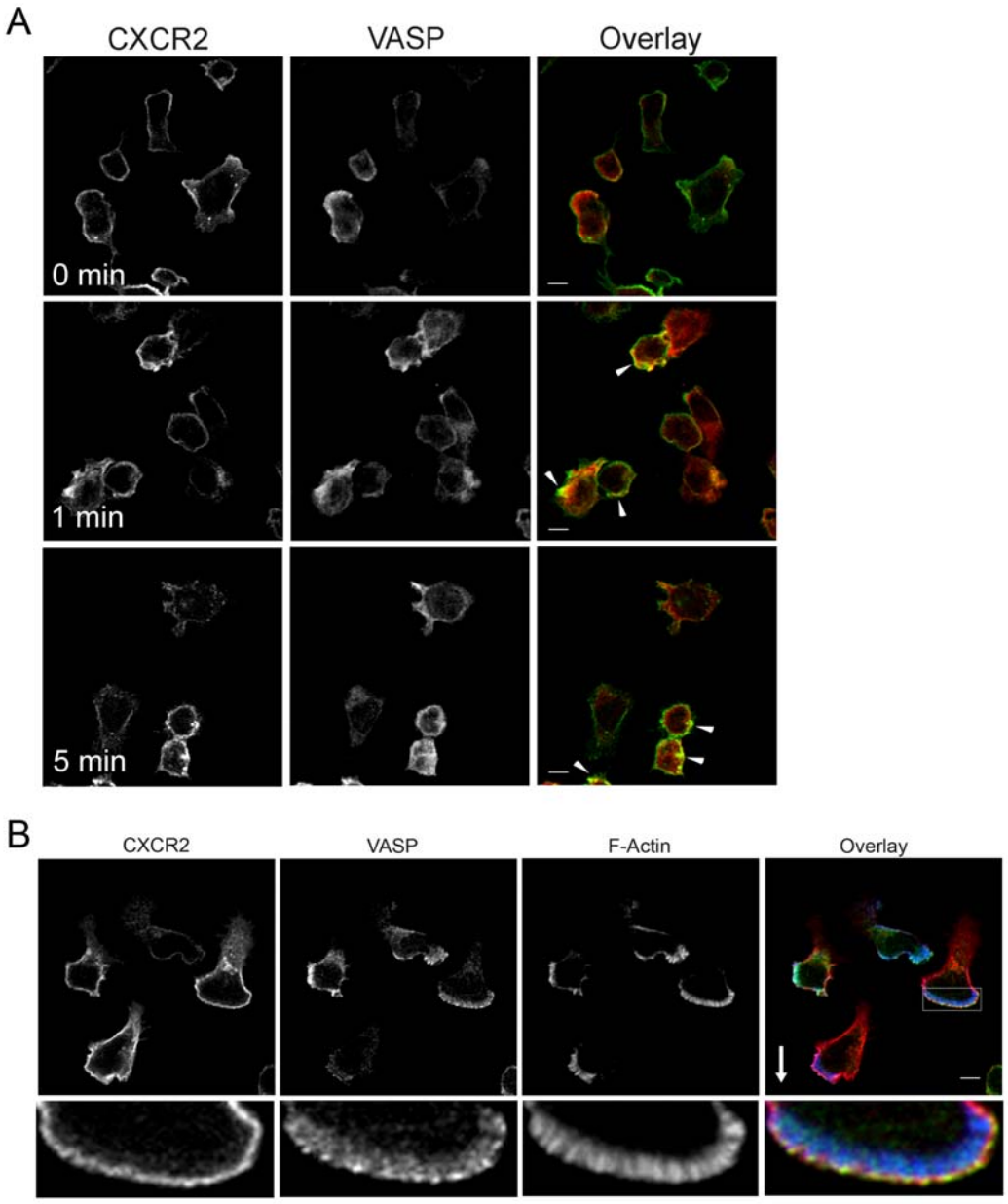

Figure 29: CXCR2 and VASP both localize to plasma membrane ruffles upon global and directional CXCL8 stimulation.
(A) Immunofluorescence confocal images of CXCR2 and VASP staining in differentiated HL-60 cells stably expressing CXCR2 and stimulated globally with vehicle (0 minutes) or 100 ng/ml of CXCL8 for 1 minute or 5 minutes. Overlay images are pseudocolored where green is CXCR2 and red is VASP (B) Immunofluorescence confocal images of CXCR2, VASP, and F-actin staining in differentiated HL-60 cells stably expressing CXCR2 and stimulated directionally with 50 ng/ml CXCL8 in Zigmond chamber for 5 minutes. Arrow indicates direction of CXCL8. Overlay image is pseudocolored where green is VASP, red is CXCR2, and blue is F-actin. Images were processed using Photoshop (Adobe Systems, San Jose, CA). Bars, 5μm.

CXCL8 in a Zigmond chamber (Figure 29B). VASP exhibits a punctate staining pattern in the lamellipodia with the most concentrated regions co-localizing with CXCR2. It is possible that these concentrated co-localizing regions represent the phosphorylated VASP that interacts strongly with CXCR2. These data indicate that VASP is a novel CXCR2-interacting protein that localizes with CXCR2 in the leading edge of cells stimulated with a CXCL8 gradient. These results suggest that the interaction of CXCR2 with VASP in the leading edge may play an important role in the organization of the actin cytoskeleton in response to chemokine.

CXCR2 directly interacts with VASP

The EVH2 domain of VASP interacts with a number of proteins including actin. Therefore, it was of interest to investigate whether the interaction between CXCR2 and VASP is direct or occurs indirectly through an additional protein. Purified regions of GST-CXCR2 carboxyl-terminus (residues 311-330 or 331-355) and full length His-tagged VASP were utilized in binding assays. Purified His-VASP interacts specifically with residues 331-355 from the carboxyl-terminus of CXCR2 (Figure 30). These results suggest that CXCR2 directly interacts with VASP and this interaction does not require additional adaptors.

VASP is phosphorylated on Ser157 and Ser239 in response to CXCL8 stimulation through PKA- and PKC-mediated signaling pathways

Immunoblotting for VASP following immunoprecipitation with CXCR2 antibody revealed an increased amount of the higher molecular weight band of

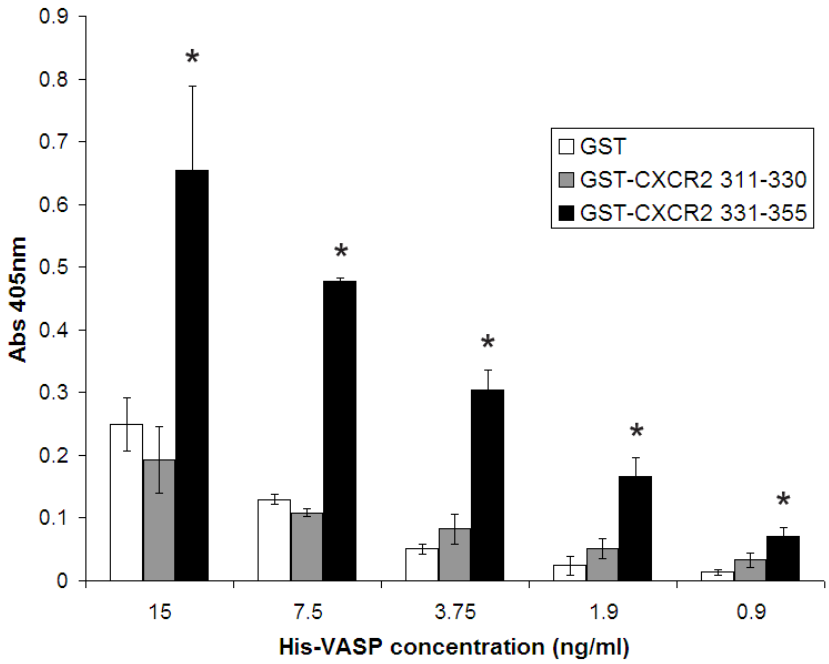

Figure 30: Purified His_6-VASP interacts specifically with amino acids 331-355 from the CXCR2 carboxyl-terminus.

96-well polystyrene plates were coated with 3µg/ml GST, GST-CXCR2 311-330, or GST-CXCR2 331-355. Wells were blocked with 0.5%Tween/0.5%TritonX-100/PBS and incubated with various concentrations of His-VASP (0.06 ng/ml-60 ng/ml). Bound His-VASP was detected using a nickel activated HRP. ABTS substrate was added and plates were read at 405nm. The assay was performed in triplicate. His-VASP binding to GST-CXCR2 331-355 was statistically higher than to GST alone or GST-CXCR2 311-330. Statistical significance in Abs 405nm of GST versus CXCR2 311-331 versus CXCR2 331-355 is indicated by the astericks (p-value ≤ 0.05, Mann Whitney U test). Data shown are representative of at least three separate experiments.

VASP present in immunoprecipitated samples, which represents VASP that is phosphorylated (Figure 28B). In addition, there is an increase in the overall amount of the phosphorylated form of VASP in samples stimulated with CXCL8, suggesting that VASP is phosphorylated in response to CXCL8 stimulation. To confirm that the higher molecular weight band was indeed representative of VASP phosphorylation upon CXCL8 stimulation, western blot analysis was performed on lysates from vehicle and CXCL8 stimulated cells using a phospho-Ser157 VASP-specific antibody (Figure 31A). In addition, VASP was phosphorylated on Ser239 in response to CXCL8 stimulation based upon western blot analysis and detection with a phosphor-serine 239-specific antibody (Figure 31B).

In order to determine what signaling pathways mediate the phosphorylation of VASP on Ser 157, phosphorylation was examined upon CXCL8 stimulation in cells treated with the PKA inhibitor, H89 or the broad classical PKC inhibitor Ro-32-0432. Basal phosphorylation of VASP is significantly inhibited by H89 treatment and CXCL8-induced VASP phosphorylation on Ser157 is also significantly inhibited by pretreatment with H89 (Figure 32A and 32B). Although not as striking, there is also inhibition of both basal and CXCL8-induced VASP phosphorylation at serine 157 upon treatment with Ro-32-0432 (Figure 32C and 32D). This suggests that basal phosphorylation at Ser157 is largely PKA-mediated and stimulation with CXCL8 activates PKA-mediated signaling pathways.

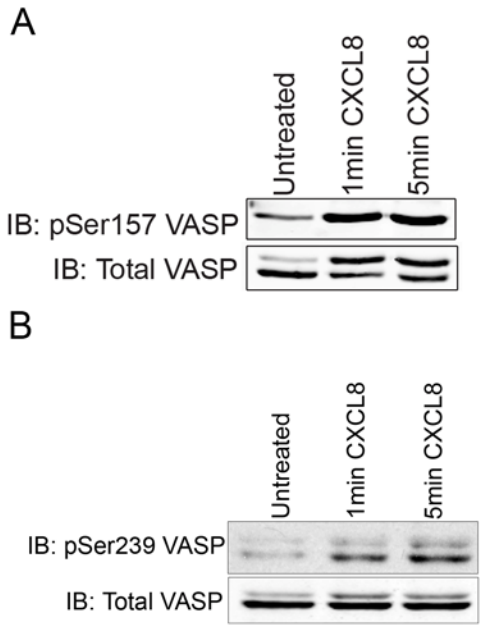

Figure 31: VASP is phosphorylated on Ser157 and Ser 239 in response to CXCL8 stimulation.
HL-60 cells stably expressing CXCR2 were stimulated with vehicle (Untreated) or 100 ng/ml CXCL8 for 1 minute or 5 minutes. Cell lysates were subjected to SDS-PAGE and western blot analysis (IB) using antibodies specific for VASP phospho-serine 157 (A) or VASP phosho-serine 239 (B). Data shown are representative of three separate experiments.

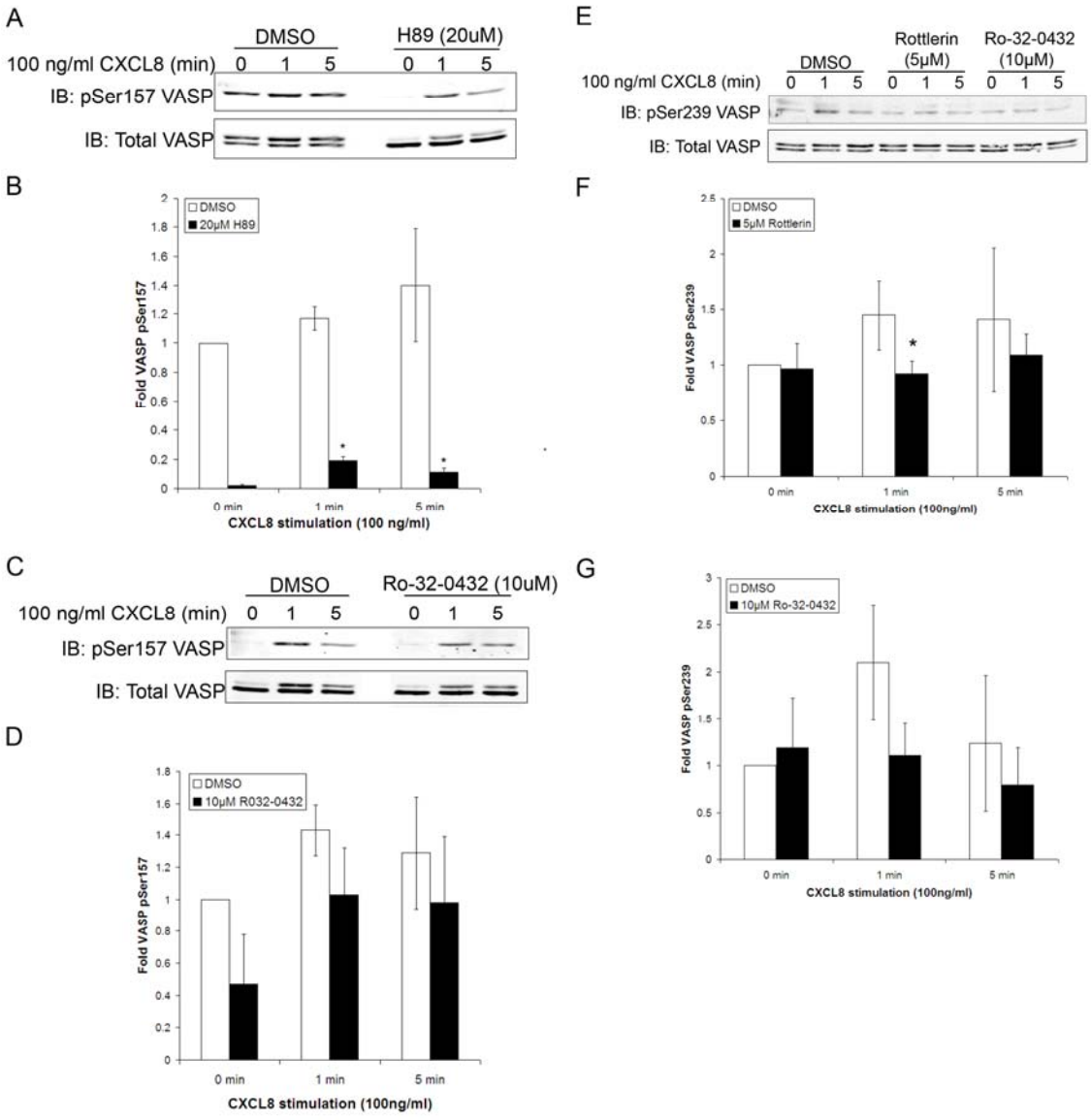
A
DMSO
H89 (20uM)
100 ng/ml CXCL8 (min) 0 1 5 0 1 5
IB: pSer157 VASP
IB: Total VASP
B
DMSO
20μM H89
Fold VASP pSer157
0 min
1 min
5 min
CXCL8 stimulation (100 ng/ml)
C
DMSO
Ro-32-0432 (10uM)
100 ng/ml CXCL8 (min) 0 1 5 0 1 5
IB: pSer157 VASP
IB: Total VASP
D
DMSO
10μM R032-0432
Fold VASP pSer157
0 min
1 min
5 min
CXCL8 stimulation (100ng/ml)
E
DMSO
Rottlerin (5μM)
Ro-32-0432 (10μM)
100 ng/ml CXCL8 (min) 0 1 5 0 1 5 0 1 5
IB: pSer239 VASP
IB: Total VASP
F
DMSO
5μM Rottlerin
Fold VASP pSer239
0 min
1 min
5 min
CXCL8 stimulation (100ng/ml)
G
DMSO
10μM Ro-32-0432
Fold VASP pSer239
0 min
1 min
5 min
CXCL8 stimulation (100ng/ml)

Figure 32: Phosphorylation of VASP upon CXCL8 stimulation is mediated through PKA and PKC.
(A) Western blot analysis of lysates from HL-60 cells stably expressing CXCR2 pretreated with DMSO (vehicle) or 20μM H89 for 60 minutes and stimulated with vehicle (0 minutes) or 100 ng/ml CXCL8 for 1 minute or 5 minutes using antibodies specific for VASP and VASP phospho-serine 157 (B) Quantitation of normalized density of VASP phospho-serine157 in DMSO treated samples versus 20μM H89 treated samples. Statistical significance of DMSO versus H89 treatment is indicated by the asterick (p-value ≤ 0.05, Mann Whitney U test) (C) Western blot analysis of lysates from HL-60 cells stably expressing CXCR2 pretreated with DMSO (vehicle) or 10 μM Ro-32-0432 for 30 minutes and stimulated with vehicle (0 minutes) or 100 ng/ml CXCL8 for 1 minute or 5 minutes using antibodies specific for VASP and VASP phospho-serine 157 (D) Quantitation of normalized density of VASP phospho-serine157 in DMSO treated samples versus 10μM R032-0432 treated samples (E) Western blot analysis of lysates from HL-60 cells stably expressing CXCR2 pretreated with DMSO (vehicle), 5 μM Rottlerin for 15 minutes, or 10 μM Ro-32-0432 for 30 minutes and stimulated with vehicle (0 minutes) or 100 ng/ml CXCL8 for 1 minute or 5 minutes using antibodies specific for VASP and VASP phospho-serine 239 (F) Quantitation of normalized density of VASP phospho-serine239 in DMSO treated samples versus 5μM Rottlerin treated samples. Statistical significance of DMSO versus Rottlerin treatment is indicated by the asterick (p-value ≤ 0.05, Mann Whitney U test) (G) Quantitation of normalized density of VASP phospho-serine239 in DMSO treated samples versus 10μM R032-0432 treated samples. Data shown are representative of at least three separate experiments.

The pathways that mediate the phosphorylation of VASP at Ser239 were also investigated using the PKA inhibitor H89, the broad classical PKC inhibitor Ro-32-0432, and the specific PKCδ inhibitor Rottlerin. No effect on basal or CXCL8-induced phosphorylation at Ser239 was observed with H89 treatment. In contrast, CXCL8-induced phosphorylation of VASP on Ser239 was almost completely ablated with pretreatment with the PKCδ-specific inhibitor Rottlerin (Figure 32E and 32F). The broad PKC inhibitor Ro-32-0432 (Figure 32E and 32G) also inhibited this phosphorylation although this was not significant. This suggests that phosphorylation of VASP on Ser239 occurs through a PKCδ-mediated signaling pathway.

These results indicate that CXCL8 stimulation of CXCR2 results in activation of both PKA and PKC which are responsible for phosphorylation of VASP at serine residues 157 and 239. In addition, phosphorylation of VASP on one or more of these residues may regulate the interaction between CXCR2 and VASP.

Phosphorylation of VASP on Serine 239 regulates the interaction between CXCR2 and VASP

Double homozygous mutant VASP/Mena mouse embryonic fibroblasts that also lack EVL expression (MV^{D7} cells) (Bear et al., 2000) were utilized in the following studies. These cells provide a valuable system in which to study Ena/VASP function because they lack expression of all Ena/VASP family members and various GFP-tagged murine VASP deletion mutants and domains

can be re-expressed in these cells to investigate the roles of the various domains. In order to determine whether phosphorylation of the serine and threonine residues in the EVH2 domain of VASP mediate its interaction with CXCR2, GST pull-down reactions were performed with lysates from MV^{D7} cells stably expressing GFP-tagged phosphorylation-deficient murine VASP. As shown in Figure 33A, mutation of both serine 235 and threonine 274 to alanine results in loss of GST-CXCR2 carboxyl-terminus binding. Interestingly, mutation of serine 153 in combination with either of the residues in the EVH2 domain does not result in loss of binding to GST-CXCR2 carboxyl-terminus, suggesting that phosphorylation of serine 235 and threonine 274 of VASP is important for CXCR2 binding.

We next sought to determine whether whether the phosphorylation induces a favorable conformational change necessary for interaction with CXCR2 or if the phosphorylated residues in the EVH2 domain actually serve as the interaction site. In order to distinguish between these possibilities, purified His_6-tagged VASP EVH2 domain was phosphorylated in vitro with the catalytic subunit of PKA. The phosphorylated VASP EVH2 domain was then used to determine the effects on binding to GST-CXCR2 331-355. Incubation of His_6-VASP EVH2 domain with the PKA catalytic subunit results in robust phosphorylation on serine 235 as indicated by western blot with a phospho-specific antibody (Figure 33B). Importantly, phosphorylation of the His_6-VASP EVH2 domain results in a significant increase in the binding of GST-CXCR2 331-355 (Figure 33C). These

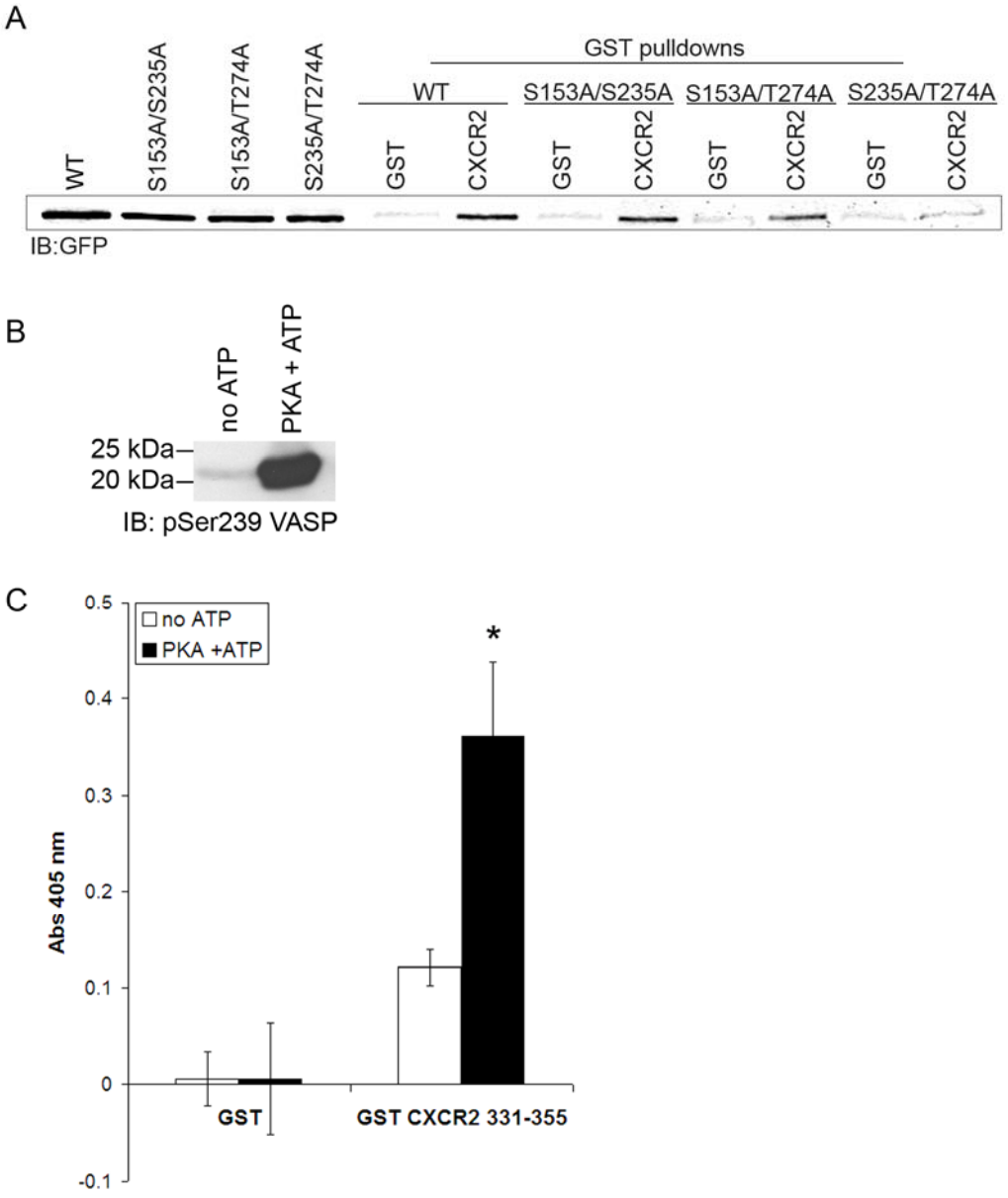

Figure 33: Phosphorylation of VASP on Serine 239 regulates the interaction between CXCR2 and VASP.

(A) Western blot analysis for GFP (IB) of GST pulldowns with GST or GST-CXCR2 carboxyl-terminus using lysates from MV^{D7} cells stably expressing GFP-VASP WT, S153A/S235A, S153/T274A, and S235A/T274A (B) Western blot analysis of purified His_6-VASP EVH2 domain incubated with catalytic subunit of PKA with and without ATP using a phospho-Ser235-specific antibody (C) Binding of His_6-VASP EVH2 domain incubated with and without ATP to either GST or GST-CXCR2 331-355. Binding was detected by measuring absorbance at 405 nm. Statistical significance of binding to GST-CXCR2 with ATP versus without ATP is indicated by the asterick (p-value ≤ 0.05, Mann Whitney U test). Data shown are representative of three separate experiments.

data demonstrate that phosphorylation of residues in the VASP EVH2 domain mediate the interaction with CXCR2.

CXCR2 carboxyl-terminus preferentially interacts with VASP over Mena and EVL

To more specifically identify the domain of VASP that is necessary for CXCR2 binding, GST pull-down experiments were performed using the purified CXCR2 carboxyl-terminus and lysates from MV^{D7} cells expressing GFP-VASP domains and deletion mutants. Because the EVH1 and EVH2 domains of the three Ena/VASP family members are highly conserved, we investigated whether the CXCR2 interaction was specific for VASP or could occur with other family members. GST pulldown experiments were performed using the carboxyl-terminus of CXCR2 and lysates from MV^{D7} stably expressing GFP-VASP, -Mena, or –EVL. CXCR2 preferentially interacted with GFP-VASP as compared to GFP-Mena and –EVL (Figure 34). This suggests that CXCR2 may interact with a domain specific for VASP and does not likely occur through a conserved region among the family members.

CXCR2 interaction with VASP occurs through the VASP EVH2 domain and requires the coiled-coil region

In order to determine the region of VASP that is necessary for the CXCR2 interaction, a series of GST pulldown reactions were performed using the carboxyl-terminus of CXCR2 and lysates from MV^{D7} cells stably expressing GFP-EVH1 or -EVH2 domains. Lysates from cells that express GFP-VASP in which

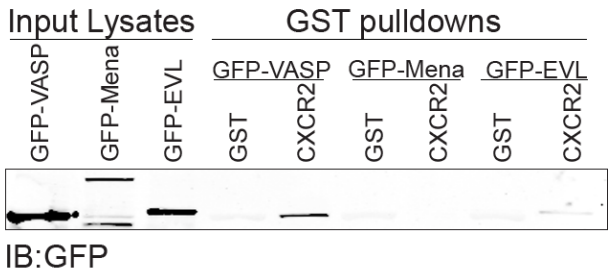

Figure 34: CXCR2 preferentially interacts with VASP as opposed to Mena or EVL.
Western blot analysis for GFP (IB) of GST pulldowns with GST or GST-CXCR2 carboxyl-terminus using lysates from MV^{D7} cells stably expressing GFP-VASP, -Mena, or –EVL. Data shown are representative of three separate experiments.

the central proline-rich region was deleted were also utilized in pulldown reactions. The GFP-EVH2 domain of VASP efficiently interacted with the GST-carboxyl-terminus of CXCR2 in pulldown reactions (Figure 35A). The EVH1 domain was not sufficient for binding and deletion of the proline-rich region of VASP did not ablate binding, suggesting that these regions are not important for the CXCR2 interaction.

In order to identify the precise region necessary for interaction with CXCR2, additional GST pulldown reactions were performed using lysates from MV^{D7} cells expressing GFP-VASP in which the F-actin binding (FAB) and tetramerization coiled-coil (COCO) regions were deleted. Deletion of the FAB region has no effect on GST-CXCR2 carboxyl-terminus binding (Figure 35B). In contrast, deletion of the tetramerization COCO region completely eliminates the interaction with CXCR2, suggesting that either tetramerization of VASP creates the actual binding site for CXCR2 or tetramerization maintains VASP in an orientation that is essential for the interaction with CXCR2. The latter is more likely the possibility since GST pulldown reactions with lysates from MV^{D7} cells expressing a reverse coiled-coil (LH COCO) VASP mutant also reveal a binding deficiency (Figure 35C). These results further suggest that phosphorylated residues in the EVH2 domain of VASP are sufficient to mediate the interaction with CXCR2 and establish that the right-handed coiled-coil conformation that mediates tetramerization of VASP is critical for the interaction with CXCR2.

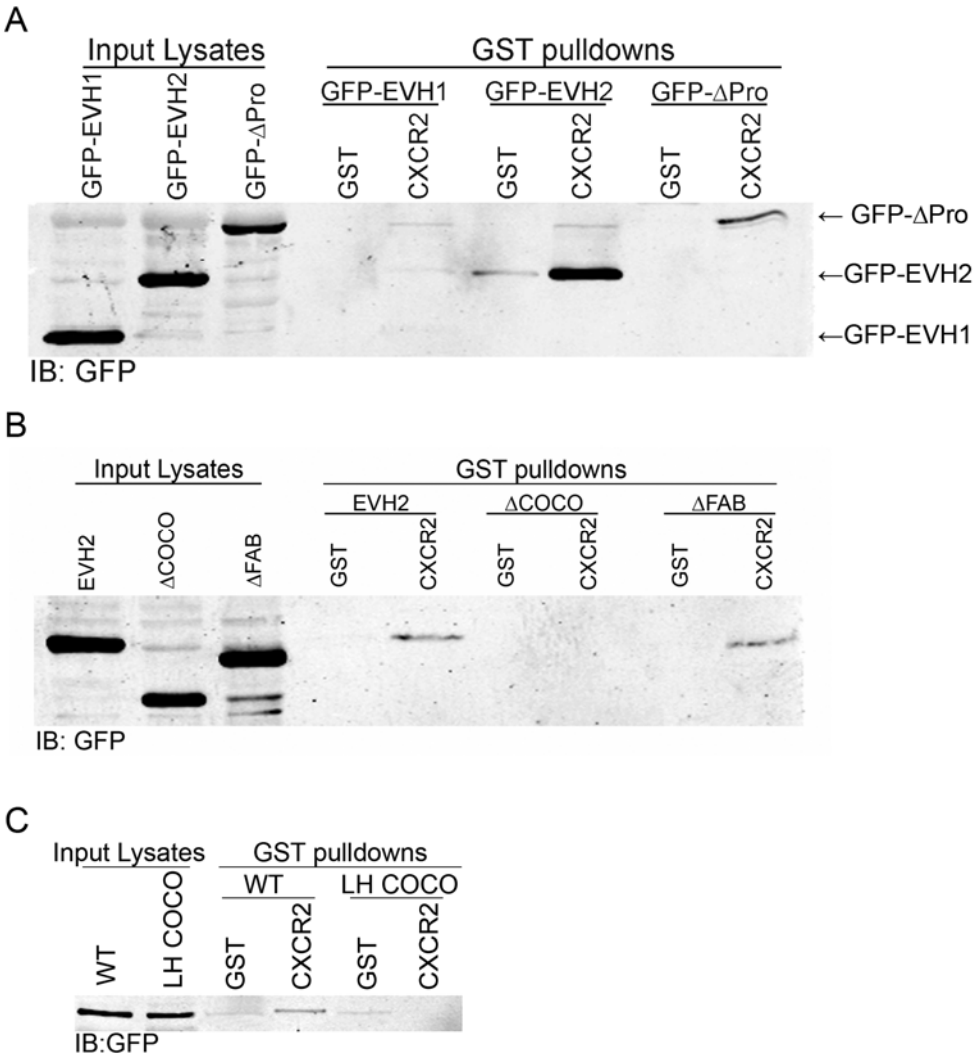

Figure 35: CXCR2 interaction with VASP occurs through the VASP-EVH2 domain and requires the coiled-coil region.
Western blot analysis for GFP (IB) to detect GFP-VASP of GST pulldowns with GST or GST-CXCR2 carboxyl-terminus using (A) lysates from MV^{D7} cells stably expressing GFP-VASP-EVH1, -VASP-EVH2, or –VASP-ΔPro (deletion of proline-rich region) (B) lysates from MV^{D7} cells stably expressing GFP-VASP-EVH2-WT, -ΔCOCO (coiled-coil deletion), or -ΔFAB (F-Actin binding domain deletion) (C) lysates from MV^{D7} cells stably expressing GFP-VASP-WT or –LHCOCO (reversed coiled-coil). Data shown are representative of three separate experiments.

F-Actin is necessary for localization of VASP to membrane ruffles and interaction with CXCR2

The phosphorylation of VASP on serine and threonine residues in the EVH2 domain interferes with its ability to interact with F-actin (Barzik et al., 2005; Harbeck et al., 2000; Laurent et al., 1999). In addition, we have shown that phosphorylation of VASP on serine residue 239 significantly enhances the VASP/CXCR2 interaction. These results suggested that CXCR2 and F-actin might be mutually exclusive in their binding to VASP. In order to investigate this hypothesis, we treated cells with Cytochalasin D to disrupt F-actin, immunoprecipitated CXCR2, and examined whether an increased amount of VASP was associated with CXCR2. In contrast to predicted results, Cytochalasin D treatment disrupts the CXCR2/VASP interaction (Figure 36A). Importantly, this disruption was not due to lack of VASP phosphorylation in response to CXCL8 as robust phosphorylation at serine residues 157 and 239 is still occurs with Cytochalasin D treatment (Figure 36B). These data indicate that not only is the VASP interaction with F-actin not competitive with CXCR2 but that the presence of F-actin is necessary for VASP to interact with CXCR2. Furthermore, pulldown experiments for which proper intracellular localization is not necessary, with the CXCR2 carboxyl-terminus and lysates from MV^{D7} cells expressing a VASP-FAB deletion mutant did not demonstrate a deficiency in binding. These data in combination suggest that the interaction of VASP with F-actin is necessary for proper VASP localization to membrane ruffles and subsequent interaction with CXCR2. In order to test this, we treated cells with

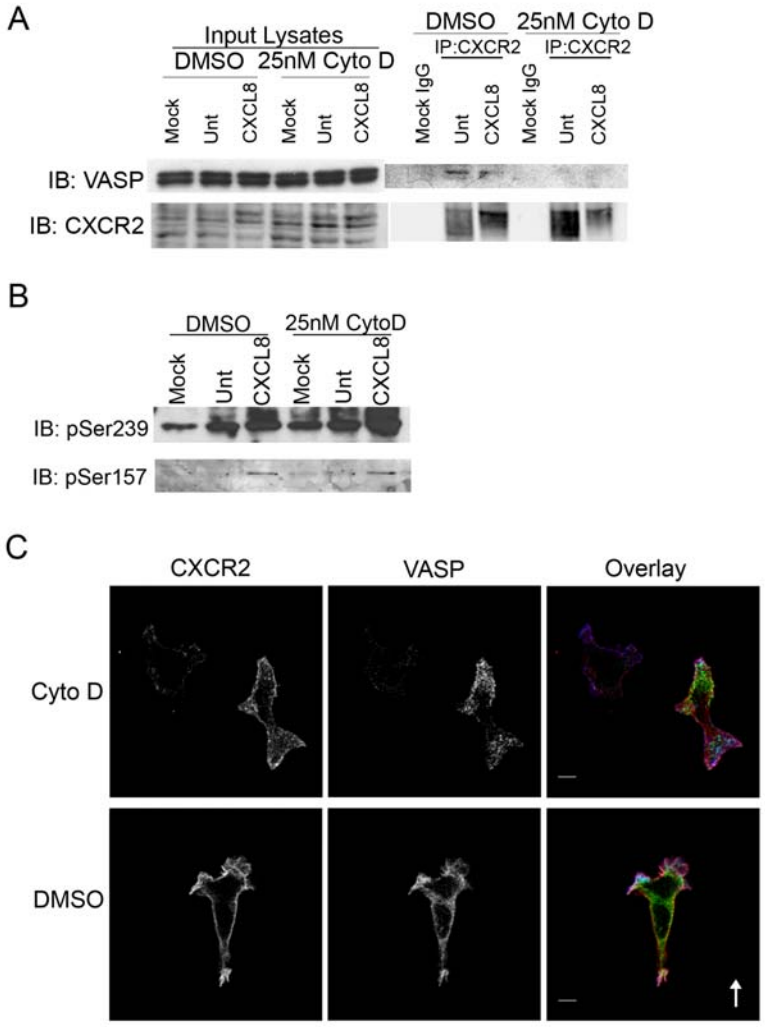

Figure 36: F-actin is necessary for localization of VASP to membrane ruffles and interaction with CXCR2.
Cells were pretreated for 30 minutes with 25 nM cytochalasin D (Cyto D) or DMSO (vehicle) and stimulated with vehicle (Mock, Unt) or 100 ng/ml CXCL8 for 1 minute (A) Lysates were incubated with normal rabbit IgG- (Mock IgG) or rabbit anti-CXCR2 antibody-coupled sepharose. Immunoprecipitated proteins were eluted with Laemmli sample buffer. Samples were analyzed by SDS-PAGE and western blot (IB) for CXCR2 and VASP (B) Western blot analysis (IB) using antibodies specific for VASP phospho-serine 157 or VASP phosho-serine 239 of lysates (C) Immunofluorescence confocal images of CXCR2, VASP, and F-Actin staining in differentiated HL-60 cells stably expressing CXCR2 and stimulated directionally with 50 ng/ml CXCL8 in Zigmond chamber for 5 minutes. The arrow indicates direction of CXCL8. Overlay image is pseudocolored where green is VASP, red is CXCR2, and blue is F-Actin. Images were processed using Photoshop (Adobe Systems, San Jose, CA). Bars, 5μm. Data shown are representative of three separate experiments.

Cytochalasin D, stimulated directionally with CXCL8, and examined localization of VASP. Cells treated with Cytochalasin D exhibited largely cytoplasmic VASP distribution and diminished recruitment of VASP to leading edge membrane ruffles with CXCR2 (Figure 36C). The requirement for F-actin to properly localize VASP for interaction with CXCR2 is illustrated by loss of co-immunoprecipitation and recruitment of VASP to membrane ruffles with Cytochalasin D treatment.

VASP is essential for efficient CXCL8-mediated leukocyte recruitment in vivo.

To assess the functional relevance of the CXCR2/VASP interaction in physiological processes, mice with a homozygous deletion of VASP were utilized in a peritoneal model of leukocyte recruitment. Three VASP -/- mice and three age-matched VASP +/+ mice were administered an intraperitoneal injection of 1ml sterile saline (0.85% NaCl) or 50 ng CXCL8. Four hours post-injection, peritoneal lavage was performed and the number of leukocytes from the lavage were counted with a hemacytometer. To distinguish between general defects in cell motility and defects in CXCL8-mediated chemotaxis, mice (three of each genotype) were also injected with 3% thioglycolate broth to induce peritoneal inflammation. VASP +/+ mice exhibited robust peritoneal leukocyte recruitment upon CXCL8 and thioglycolate injection (Table 3) (Figure 37). In contrast, peritoneal leukocyte recruitment in response to CXCL8 injection in VASP -/- mice was ablated. Interestingly, VASP -/- mice have a higher number of basal leukocytes in the peritoneal cavity (see saline control numbers in Table 3).

Table 3: VASP is essential for efficient CXCL8-mediated leukocyte recruitment in vivo.
Three VASP +/+ and VASP -/- mice were administered intraperitoneal injections with vehicle (sterile saline) 50 ng CXCL8 or 3% thioglycolate broth. Infiltrated cells were harvested by peritoneal lavage 4 hours post-injection and total cell numbers were counted. Values represent total cell numbers (10^6) ± SEM.

	Saline	CXCL8	Thioglycolate
VASP +/+	2.48 ± 1.15	7.45 ± 3.39	5.15 ± 1.8
VASP -/-	4.71 ± 2.19	3.98 ± 1.34	5.59 ± 2.06

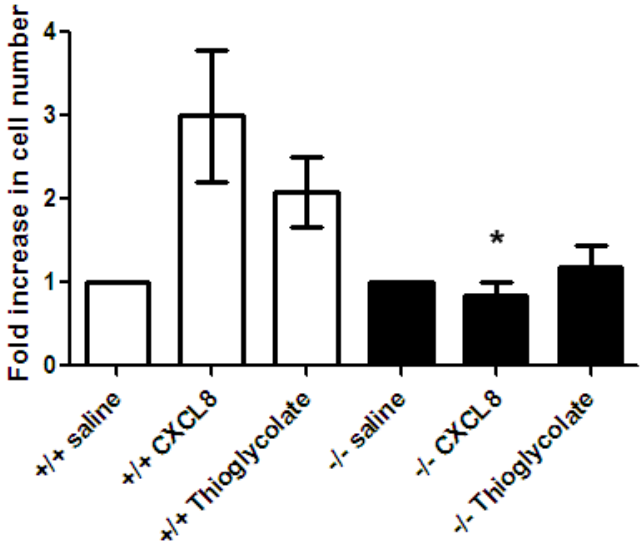

Figure 37: VASP -/- mice exhibit a significant decrease in CXCL8-mediated leukocyte recruitment.
Fold increase in total leukocyte number over saline control upon intraperitoneal injection of CXCL8 and thioglycolate. Statistical significance of CXCL8-mediated increase in total leukocyte number in VASP +/+ mice versus VASP -/- mice is indicated by the asterick (p-value ≤ 0.05, Mann Whitney U test). Data shown are the average from three animals of each genotype. Bars represent SEM.

Previous studies have shown that fibroblasts lacking Ena/VASP proteins exhibit enhanced random motility (Bear et al., 2000). In addition, introduction of Ena/VASP functional blocking peptides into primary human neutrophils induces F-actin in resting cells while F-actin formation and chemotaxis in response to fMLP was reduced (Anderson et al., 2003). Therefore, it is possible that random motility in leukocytes from VASP -/- mice is enhanced, while CXCR2-mediated chemotactic responses are impaired. Indeed, there was a statistically significant difference in the fold increase in leukocyte number over saline controls between VASP +/+ and VASP -/- animals (Figure 37). Peritoneal leukocyte recruitment in response to thioglycolate injection in VASP -/- was also impaired, although not as severely as in response to CXCL8 (Table 3). This suggests that other non-CXCL8-mediated mechanisms may be recruiting leukocytes with thioglycolate injection. We also examined the number of neutrophils present in the peritoneal lavages by measuring myeloperoxidase (MPO) activity. MPO is most abundant in neutrophil granules and measurement of MPO activity correlates to neutrophil number. A deficiency in the CXCL8-mediated neutrophil recruitment was observed in the VASP -/- mice as compared to the VASP +/+ mice (Table 4) (Figure 38). There was a trend for difference in the fold increase of MPO activity over saline controls between VASP +/+ and VASP -/- and upon examining additional animals, it is expected that these differences will be statistically significant. These results imply that CXCL8-mediated neutrophil responses specifically are largely dependent on VASP. While the number of mice available

Table 4: Number of peritoneal recruited neutrophils is decreased in VASP -/- mice.
Total neutrophil number quantitated by MPO assay.
Values represent MPO activity (abs 490 nm/time (min)) ± SEM.

	Saline	CXCL8
VASP +/+	0.0043 ± 0.0011	0.0162± 0.0095
VASP -/-	0.0126 ± 0.0075	0.0169 ± 0.0034

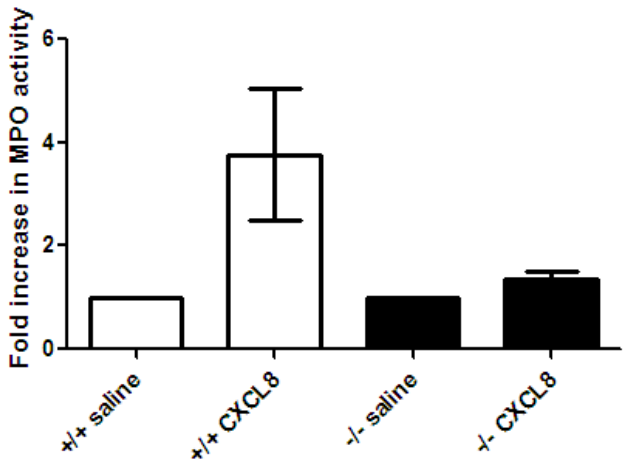

Figure 38: VASP -/- mice exhibit a decrease in CXCL8-mediated neutrophil recruitment.
Fold increase in MPO activity over saline control upon intraperitoneal injection of CXCL8. Data shown are the average from three animals of each genotype. Bars represent SEM.

for these studies was limited, these data suggest the CXCR2/VASP interaction has physiological importance in leukocyte trafficking to sites of inflammation.

Discussion

We have demonstrated for the first time a direct interaction between a chemokine receptor and a member of the Ena/VASP family of proteins. This interaction represents a direct link between CXCR2 and a regulator of the actin cytoskeleton and also potentially serves as a mechanism to link CXCR2 to other cellular signaling pathways, which has important implications for the current understanding of the chemotactic response. Upon CXCR2 activation by chemokine, a number of intracellular signaling pathways, such as the MAP kinase, PI3 kinase, and Ca^{2+}-dependent pathways are initiated through uncoupling of the G βγ subunits from the heterotrimeric complex. These signaling events are essential for the chemotactic response. Data from these studies indicate that VASP is a novel CXCR2-interacting protein.

We have also demonstrated that VASP is phosphorylated upon CXCL8 stimulation on serine residues through PKA- and PKC-mediated pathways. More specifically, VASP is phosphorylated on serine residue 239 by PKC-δ and this phosphorylation enhances the interaction with CXCR2. This suggests that PKC-δ is an important intermediate player in the CXCR2/VASP interaction. In addition, the fact that CXCL8-mediated leukocyte recruitment is severely impaired in VASP -/- mice suggests a novel essential role for PKC-δ-mediated signaling events in the chemotactic response.

The phosphorylation of VASP in the EVH2 domain mediates its interaction with actin. Phosphorylation of VASP in the EVH2 domain reduces its filament bundling activity (Barzik et al., 2005) and impairs actin fiber formation (Zhuang et al., 2004). Therefore, it is of great interest that CXCL8 stimulation induces VASP phosphorylation on serine residue 239 and that this affects the binding of CXCR2 to VASP. If binding of VASP to CXCR2 is mutually exclusive with the F-actin interaction, this presents perhaps a novel role for VASP in mediating the CXCR2-mediated chemotactic response. Alternatively, binding of phosphorylated VASP to CXCR2 may allow interaction with F-actin even when VASP is phosphorylated in the EVH2 domain. Our data using the VASP-ΔCOCO (coiled-coil) and -LH-COCO mutants in pulldown experiments suggest that the CXCR2 interaction domain is contained within this region and the requirement for phosphorylation in the EVH2 domain allows a favorable conformation for this interaction to occur via the COCO domain. This is a likely scenario as preliminary structural studies (unpublished results from Dr. Dorit Hanein at Burnham Institute) examining VASP interaction with F-actin place the coiled-coil domain in a freely accessible conformation (Figure 39). Recent studies have examined the role of phosphorylation of VASP on serine 239 on nitric oxide-induced lamellipodia protrusions (Lindsay et al., 2007). This study indicated that phosphorylation on serine 239 disrupts VASP localization to lamellipodial edge and retraction of lamellipodia. These observations in combination with our data present an intriguing possibility that CXCR2 interaction allows phosphorylated

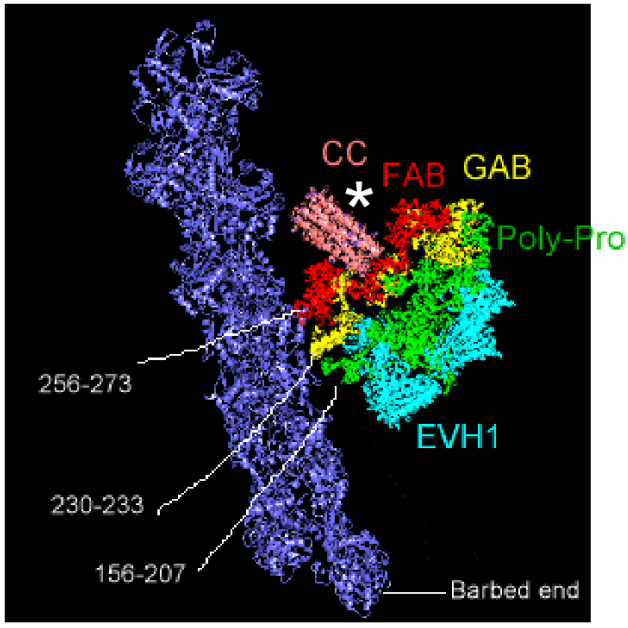

Figure 39: Structural model of VASP tetramer in complex with F-actin.
This is a preliminary model of the structure of VASP tetramer in complex with F-actin provided by Dr. Dorit Hanein at Burnham Institute. The numbers represent the amino acid residues of VASP. Colors represent different VASP domains where light blue is the EVH1 domain, green is the central poly-proline domain, yellow is the G-Actin binding (GAB) domain, red is the F-actin binding (FAB) domain, and pink is the coiled-coil (CC) domain. The dark blue represents F-actin and the position of the barbed end is indicated. Note the freely accessible coiled-coil domain. The * symbol indicates a possible interaction site for CXCR2.

VASP to remain localized to the plasma membrane. Currently, studies are underway to determine if the presence of the CXCR2 carboxyl-terminus enhances the filament bundling activity of the phosphorylated VASP EVH2 domain.

Furthermore it is unlikely that CXCR2 binding to VASP inhibits F-actin binding, representing competition between the two proteins. Our data demonstrate that treatment of cells with cytochalasin D ablates co-immunoprecipitation of VASP with CXCR2. In addition, VASP does not accumulate in plasma membrane ruffles with CXCR2 with cytochalasin D treatment. This finding is consistent with previously published results illustrating displacement of Ena/VASP proteins from the leading edge upon low dose cytochalasin D treatment (Bear et al., 2002). These results suggest that barbed ends of F-actin are required for targeting of VASP to the membrane where the interaction with CXCR2 takes place.

Due to its multi-domain structure VASP also has an important role as an adaptor molecule. VASP interacts with several proteins in the focal adhesions through its EVH1 domain and a number of SH3 domain-containing proteins through its proline-rich region. Not only does the interaction of VASP with CXCR2 represent a direct link to the actin cytoskeleton, which has important implications for the chemotactic response, but it may also serve as an adaptor linking CXCR2 to several additional potential mediators of the chemotactic response. For example, Ena/VASP proteins are known to interact with src homology 3 (SH3) domain-containing proteins, such as the Src family of kinases,

through their central proline-rich region (Ahern-Djamali et al., 1999; Gertler et al., 1995). Src tyrosine kinases play a role in the neutrophil chemotactic response (Di Cioccio et al., 2004; Montecucco et al., 2006; Zhang et al., 2005) (unpublished observations in Richmond laboratory). The EVH1 domains of Ena/VASP proteins are responsible for binding proteins that harbor a F/LPPPP motif, including several focal adhesion proteins (Brindle et al., 1996; Carl et al., 1999; Drees et al., 2000; Krause et al., 2000; Niebuhr et al., 1997) and recently lamellipodin (Lpd) (Krause et al., 2004). Lpd plays a crucial role in lamellipodial dynamics and is targeted to the leading edge in migrating cells through its PH domain that specifically interacts with phosphatidylinositol 3,4-bisphosphate (PI(3,4)P2) (Krause et al., 2004).

All Ena/VASP family members share a common domain structure with all three members containing EVH1, EVH2, and proline-rich regions as well as a conserved serine phosphorylation site flanking the proline-rich region. Moreover, all three members can hetero-tetramerize via their EVH2 domains (Bachmann et al., 1999). Therefore, the observation that CXCR2 specifically interacts with the EVH2 domain of VASP is surprising and suggests a unique characteristic of this region in VASP. Little is known regarding the role of the unique threonine phosphorylation site in the EVH2 domain of VASP. However, results from the pulldown reactions using lysates from MV^{D7} expressing the double S235/T274A mutation indicate a loss of CXCR2 binding to this mutant. This observation, combined with the fact that the CXCR2 interaction is highly specific for VASP, suggests that perhaps phosphorylation at both EVH2 domain sites is important

for the interaction. Lack of binding to EVL is not as surprising since it lacks the serine phosphorylation site in the EVH2 domain that we have shown enhances VASP interaction with CXCR2. It is intriguing that despite the presence of a phosphorylation site in the EVH2 domain of Mena, it also fails to interact with CXCR2. These findings, together with the observation of impaired leukocyte recruitment in VASP -/- mice, argue for a unique function of VASP in CXCR2-mediated responses in leukocytes. Unique roles for VASP in other cellular systems have been identified previously. For example, cardiac fibroblasts isolated from VASP -/- mice exhibit highly dynamic lamellipodia and increased cell spreading accompanied by sustained Rac activation and decreased cell motility (Garcia Arguinzonis et al., 2002). In addition, studies utilizing VASP knockdown by siRNA revealed that VASP is critical for migfilin-mediated regulation of cell migration in breast cancer cells (Zhang et al., 2006).

We have identified for the first time that VASP is a novel CXCR2-interacting protein. Moreover, we have demonstrated that VASP phosphorylation on two distinct sites is induced upon CXCL8 stimulation. These phosphorylations are mediated through PKA- and PKC-dependent signaling pathways initiated by ligand binding to receptor. Phosphorylation of VASP on serine 239 enhances CXCR2 interaction with VASP, which likely occurs through the coiled-coil domain. This interaction requires barbed-end F-actin to properly localize VASP to the plasma membrane. Our findings demonstrate a potentially novel role for CXCR2 in mediating interaction of phosphorylated VASP with F-actin. Finally,

VASP -/- mice exhibit a severely impaired CXCR2-mediated peritoneal leukocyte recruitment indicating a unique role for VASP in inflammatory responses.

CHAPTER V

DELETION OF THE CARBOXYL-TERMINUS OF CXCR4 LEADS TO CONSTIUTIVE RECYLCING AND INCREASED BREAST TUMOR GROWTH

Introduction

The CXCR4 chemokine receptor has recently been shown to be important in breast cancer metastasis (Chen et al., 2003b; Li et al., 2004; Liang et al., 2005; Muller et al., 2001). The expression of this receptor on tumor cells may mediate preferential metastasis to target organs that express the ligand for this receptor, stromal-derived factor-1 alpha (SDF-1α), also known as CXCL12. CXCR4 is upregulated in metastatic breast cancer cells and neutralization of the CXCR4/SDF-1α interaction with CXCR4-specific antibodies impairs the metastasis of breast cancer cell lines (Muller et al., 2001). In addition, both RNAi of CXCR4 and the synthetic polypeptide TN14003 that mimics SDF-1α have been shown to individually inhibit primary tumor growth and metastasis of the highly metastatic MDA-MB-231 breast cancer cell line (Chen et al., 2003b; Lapteva et al., 2005; Liang et al., 2005).

Although, the effectiveness of inhibitors of CXCR4 such as RNAi or small molecule inhibitors to reduce metastasis of aggressive breast cancer cell lines has been extensively characterized, the role of CXCR4 in the switch from an adenocarcinoma to a metastatic carcinoma remains to be elucidated. HER2 (neu) is a potent oncogene and plays a major role in the progression of a number

of human breast cancers (Slamon et al., 1989; Yarden and Sliwkowski, 2001; Yu and Hung, 2000). It has recently been reported that upregulation of CXCR4 is essential for human epidermal growth factor receptor (HER2)-mediated tumor metastasis (Li et al., 2004). In addition, SDF-1α stimulation of MDA-MB-231 breast cancer cells leads to activation of matrix metalloproteinases MMP-2 and MMP-9 (Fernandis et al., 2004). These findings further validate the possibility of targeting CXCR4 in the treatment of metastatic breast cancer.

CXCR4 antibodies have limited therapeutic potential because a majority of the antibodies are directed against conformation-specific epitopes of CXCR4. This may result in limited effectiveness in a clinical setting. Similarly, RNAi technology is not particularly stable and may prove to be a challenge as a feasible therapeutic modality. Therefore, it is necessary to develop novel approaches to target CXCR4 in metastatic breast cancer. The internalization of chemokine receptors plays an important role in chemotaxis and activation of intracellular signaling (Ben-Baruch et al., 1995; Kraft et al., 2001; Richardson et al., 2003; Richardson et al., 1998; Roland et al., 2003; Signoret et al., 1997; Zimmermann et al., 1999). Two adaptor molecules that are involved in CXCR4 internalization are β-arrestin and the heterotrimeric protein complex Adaptin-2. These two adaptors mediate the interaction of the receptor with clathrin and are necessary for clathrin-mediated endocytosis. Investigation into the development of alternative strategies to inhibit CXCR4 function has been limited. We hypothesize that targeting CXCR4 internalization by antagonizing its interaction with adaptor molecules will inhibit activation of MAP kinase and PI3 kinase

pathways, chemotaxis, and metastasis of breast cancer cells *in vivo*. We propose to target CXCR4 internalization by transducing a peptide derived from the carboxyl-terminal domain of CXCR4 containing the Adaptin-2 (AP-2) di-leucine binding motif into breast cancer cells. Previous studies using mutagenesis of residues in the carboxyl-terminus identified the di-leucine motif (Ile-328 and Leu-329) as essential for efficient SDF-1α-mediated CXCR4 internalization (Orsini et al., 1999). When these residues are mutated, CXCR4 internalization is severely impaired. This study also demonstrated that serine residues 324 and 325 were important for CXCR4 internalization (Orsini et al., 1999). Moreover, AP-2 binds clathrin and β-arrestin-2 during endocytosis (Laporte et al., 1999) and β-arrestin-2 is required for CXCR4-mediated MAP kinase activation and chemotaxis (Sun et al., 2002). Previous studies in our laboratory revealed that mutation of the di-leucine motif in the CXCR2 chemokine receptor impaired receptor internalization. As a result, CXCR2-mediated chemotaxis was also inhibited (Fan et al., 2001b). Interestingly, Hip (Hsc/Hsp70 Interacting Protein) also binds to the leucine rich domain in the CXCR2 carboxyl-terminus. Furthermore, CXCR2 and CXCR4 internalization are impaired in cells expressing a non-functional mutant of Hip (Fan et al., 2002). These data suggest that the di-leucine motif in the carboxyl-terminus may be important in a number of interactions that may regulate internalization.

These data support the idea that transduction of a peptide containing the di-leucine motif of CXCR4 may act as a dominant negative and serve as a novel inhibitor of CXCR4 function. In addition, it may be possible to deliver this peptide

in a cell-permeable form as a therapeutic agent in the treatment of metastatic breast cancer. The approach of using receptor domains as dominant negatives to interfere with protein-protein interactions has been successfully used in a number of instances. This includes G protein-coupled receptors such as beta-2 adrenergic receptor (Okamoto et al., 1991) and D2 dopamine receptor (George et al., 2003). Furthermore, it is possible to exogenously deliver the domain as a transactivator of transcription (TAT) fusion peptide (Fawell et al., 1994; Mann and Frankel, 1991), *Antennapedia* protein (Derossi et al., 1994), or membrane-permeable sequence peptide (Zhang et al., 1998). These peptides contain protein transduction domains (PTD). PTDs are short cationic peptide sequences that include the HIV-1 TAT protein. A number of TAT-fusion proteins have been successfully delivered into cells (reviewed in (Lindsay, 2002)). In addition, TAT-fusion peptides have the ability to enter non-dividing cells, have high transduction efficiency, and low toxicity. Transduction of peptides inhibits the function of biological targets both *in vitro* and *in vivo*. For example, delivery of phosphopeptides derived from fibroblast growth factor receptor (FGFR) inhibits FGF-stimulated phosphatidylinositol hydrolysis (Hall et al., 1996). Furthermore, the delivery of peptides that block the interaction of NEMO with the IKK complex to mice inhibits acute inflammatory responses (May et al., 2000). This offers a unique therapeutic opportunity and may represent an alternative strategy to the treatment of metastatic breast cancer.

In the current study, we sought to investigate whether expression of wild type CXCR4 in non-metastatic MCF-7 cells results in increased primary tumor

growth and metastatic capacity. Conversely, we investigated whether expression carboxyl-terminally-truncated CXCR4 in MCF-7 cells decreases primary tumor growth and metastatsis. The purpose of these studies was to evaluate the feasibility of using peptides derived from the carboxyl-terminus of CXCR4 as a novel therapeutic for metastatic breast cancer. Surprisingly, these studies revealed that truncation of the CXCR4 carboxyl-terminus results in enhanced proliferation, motility, and metastasis.

Materials and Methods

Cell culture and reagents

MCF-7 cells (purchased from the American Type Culture Collection, Manassas, VA) were maintained in DMEM supplemented with 10% heat-inactivated FCS and 2 mmol/L L-glutamine. Cells were incubated at 37°C in humidified air with 5% CO_2. All tissue culture reagents were from Life Technologies, Inc. (Rockville, MD).

Plasmid constructs

pBMN-IRES-EGFP-wild type CXCR4 and -ΔCTD CXCR4 plasmids were generated previously. MCF-7 cell lines stably expressing empty vector or these plasmids were also generated previously using retroviral infection (Ueda et al., 2006).

CXCR4-mediated chemotaxis assays

Chemotaxis was assessed using a modified Boyden chamber assay as previously described (Neel et al., 2007). Briefly, a 96-well chemotaxis chamber (Neuroprobe, Gaithersburg, MD) and 10μm pore size polycarbonate membranes (Neuroprobe, Gaithersburg, MD) coated on both sides with 20 μg/ml human collagen type IV were used for chemotaxis assays. The lower compartment of the chamber was loaded with 400μl of 1 mg/ml BSA/DMEM (chemotaxis buffer) or CXCL12 diluted in the chemotaxis buffer (2.5–250 ng/ml). Cells were lifted with enzyme-free cell dissociation buffer (Invitrogen, Carlsbad, CA), resuspended in chemotaxis buffer, and 1 X 10^5 cells were added to the top chamber. The chamber was then incubated for 4.5 hours at 37°C in a 5% CO_2 atmosphere. Cells on the top of the membrane were gently removed prior to fixation. The membrane was fixed with Diff-Quik® fixative (DADE Behring Inc, Miami, FL) and stained with 1% Crystal violet. The number of cells were counted in 20 microscope fields (20X objective).

Orthotopic nude mouse xenograft mammary fat pad injections

One week prior to injection MCF-7-wild type-CXCR4 and -ΔCTD-CXCR4 cells were sorted by FACS analysis for equivalent membrane receptor expression. Cells were dissociated using enzyme-free cell dissociation buffer (Invitrogen, Carlsbad, CA) and resuspended in sterile saline (0.85% NaCl). A total of 2 X 10^6 cells in a volume of 30 μl were injected into the cleared mammary fat pad of 4-6 week old female athymic nu/nu mice. A total of five mice were

injected for each cell line. Appearance of tumors was monitored by daily palpation and tumor growth was monitored by caliper measurements taken three times weekly. Tumor volume was calculated using the following equation: Volume (V) = (L X W^2) X 0.5 where L is the longest measurement and W is the shortest measurement of the tumor. Mice were sacrificed when any tumor dimension reached 1.5 cm. Primary tumors, kidneys, liver, and spleen were harvested. Lungs were perfused with Bouin's fixative, extracted, incubated for 48 hours in fixative, photographed to document surface metastases, washed with 50% ethanol, and embedded in paraffin for sectioning.

Tissue sectioning and immunohistochemical staining of paraffin embedded tissue

Tissue sections were deparaffinized with xylene, re-hydrated, and antigen retrieval was performed using 10mM sodium citrate buffer, pH 6.0 and boiling. Slides were then blocked with 10% normal donkey serum (Jackson Immunoresearch Laboratories, Inc., West Grove, PA) and incubated overnight at 4˚C in polyclonal rabbit anti-GFP antibody (Abcam, Cambridge, MA) or normal rabbit IgG isotype control antibody (Jackson Immunoresearch Laboratories, Inc., West Grove, PA). The slides were then incubated with a biotinylated secondary antibody and streptavidin-HRP in the R.T.U. *Elite* Vectastain ABC Kit (Vector Laboratories, Burlingame, CA). Staining was then detected using a 3,3'-diaminobenzidine (DAB) detection reagent (Vector Laboratories, Burlingame, CA). Slides were counterstained with hematoxylin (Sigma, St. Louis, MO).

Images were captured on a Zeiss Axiophot upright microscope (Carl Zeiss MicroImaging, Inc., Thornwood, NY).

Quantitation of GFP-positive immunohistochemical tissue staining

GFP-positive staining in lung sections from mice was quantitated in a total of 60 randomly selected 20X microscopic fields from all three mice from each group. Quantitation was performed using the Metamorph Imaging System software package (Molecular Devices Corporation, Sunnyvale, CA). Color threshold levels were kept consistent for analysis of all samples. Percent of total area positive for GFP staining was quantitated.

Immunofluorescent staining and confocal microscopy

Cells were immunostained as described previously (Neel et al, 2007). The primary antibodies used were monoclonal αCXCR4 (clone 12G5, MAB170, R&D Systems), αCXCR4 (clone 44708, MAB171, R&D Systems), and αRab11a (a gift from Dr. James Goldenring, Vanderbilt University Medical School, Nashville, TN). These proteins were visualized with appropriate fluorophore-conjugated secondary antibodies. Fluorescent images were captured on a LSM-510 Meta laser scanning microscope (Carl Zeiss MicroImaging, Inc., Thornwood, NY).

Fluorescence-activated cell sorting analysis

Cells were lifted with cell dissociation buffer (Invitrogen, Carlsbad, CA), labeled with αCXCR4 antibody (12G5, MAB170), and then incubated with

phycoerythrin (PE)–conjugated α-mouse IgG (Jackson ImmunoResearch, Westgrove, PA). To monitor background staining for the primary and secondary antibodies, cells were incubated with normal mouse IgG (Jackson ImmunoResearch, Westgrove, PA) followed by PE-conjugated α-mouse IgG. Cells were washed and a total of 20,000 stained cells were analyzed using a FACSCalibur flow cytometer (Becton Dickinson, Mansfield, MA).

Statistical Analysis

Statistically significant differences between two groups were determined using the non-parametric two-tailed Mann Whitney U test (Wilcoxin rank sum test). Significant differences between more than two groups were determined using non-parametric analysis of variance (ANOVA) (Kruskal-Wallis test). ANOVA was followed by the Dunn's post test to determine the p-value for the significance between two groups. All statistical analysis was performed using GraphPad Prism 5 software (GraphPad software, Inc., San Diego, CA).

Results

MCF-7 cells expressing ∆CTD (carboxyl-terminally deleted)-CXCR4 exhibit enhanced cell motility and lack of responsiveness to CXCL12

MCF-7 cells stably expressing empty vector, WT-CXCR4, or ∆CTD-CXCR4 were generated to assess the effects of CXCR4 truncation on breast cancer cells growth, signaling, motility, tumorigenesis, and metastasis. Expression of the CXCR4 receptor lacking the carboxyl-terminus results in

increased cell proliferation and constitutive MAPK signaling (Ueda et al., 2006). These data are in contrast to the predication that truncation of the carboxyl-terminus of CXCR4 would result in deficient CXCR4-mediated responses. Furthermore, these results suggest that the carboxyl-terminus of the receptor contains a region that may negatively regulate CXCR4-mediated signaling events.

CXCL12-mediated chemotaxis was examined in the cells expressing ΔCTD-CXCR4. As shown in Figure 38, cells expressing WT-CXCR4 exhibited a typical bell-shaped CXCL12-mediated chemotactic response. In contrast, cells expressing ΔCTD-CXCR4 displayed enhanced ligand-independent random motility that was not affected by presence of CXCL12 (Figure 40). These data suggest that ΔCTD-CXCR4 is constitutively active and insensitive to further stimulation by CXCL12.

Truncation of the cytoplasmic carboxyl-terminus of CXCR4 results in constitutive and accelerated CXCL12-mediated recycling

Binding of certain clathrin adaptor molecules such as β-Arrestin and AP-2 to serine residues and the di-leucine motif, respectively, in the carboxyl-terminus plays an important role in the internalization of CXCR4. In addition, sequences contained within the carboxyl-terminus may be important for mediating intracellular trafficking events. We sought to investigate whether the intracellular trafficking of the ΔCTD-CXCR4 receptor was altered.

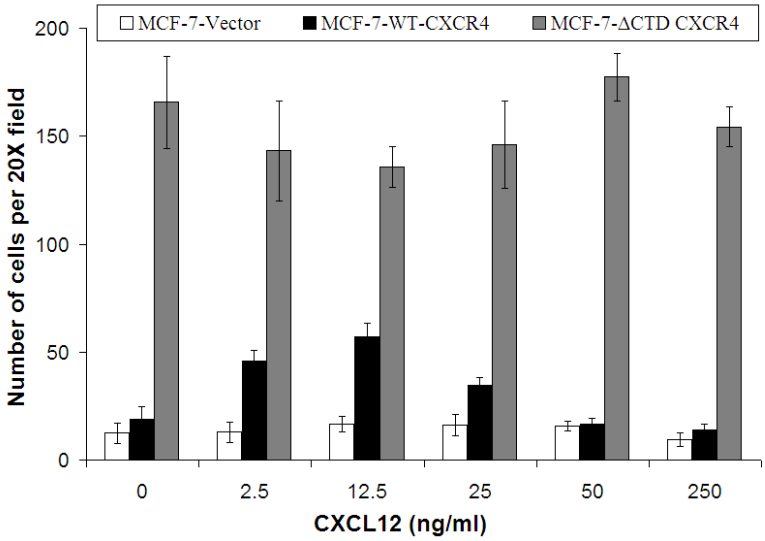

Figure 40: MCF-7 cells expressing ΔCTD (carboxyl-terminally deleted)-CXCR4 exhibit enhanced cell motility and lack of responsiveness to CXCL12.

Boyden chamber chemotaxis assay used to assess CXCL12-mediated chemotaxis in MCF-7-vector, -WT-CXCR4, and -ΔCTD-CXCR4 cells. The graph displays number of cells from twenty separate fields using the 20x objective lens ± S.E.M. Data shown are representative from three separate experiments.

CXCR4 recycling dynamics were examined by immunofluorescence staining for CXCR4 and the perinuclear recycling compartment marker Rab11a in MCF-7 cells stably expressing WT- and ΔCTD-CXCR4. In unstimulated cells, the majority of WT CXCR4 is localized to the plasma membrane. In contrast, a large percentage of ΔCTD-CXCR4 is localized to the Rab11a-positive perinuclear recycling compartment (Figure 41). Upon 30 minutes of CXCL12 stimulation, WT CXCR4 is internalized and exhibits a punctate endosomal staining pattern, while the majority of ΔCTD CXCR4 strongly co-localizes with Rab11a (Figure 41). Finally, WT CXCR4 is predominantly localized to the Rab11a compartment with minimal plasma membrane localization following 60 minutes of CXCL12 stimulation, while ΔCTD CXCR4 is displayed on the plasma membrane at this time point. These data suggest that ΔCTD CXCR4 exhibits constitutive recycling in the absence of CXCL12 and the CXCL12-induced recycling is accelerated.

MCF-7 cells expressing ΔCTD-CXCR4 exhibit enhanced tumor growth in vivo

In order to assess the potential role of the carboxyl-terminus of CXCR4 in primary tumorigenesis and metastasis, an orthotopic nude mouse mammary tumor model was employed. MCF-7 cells stably expressing empty vector, WT CXCR4, or ΔCTD CXCR4 were injected into the cleared mammary fat pad of female athymic nu/nu mice and primary tumor growth and metastasis to the lungs were examined.

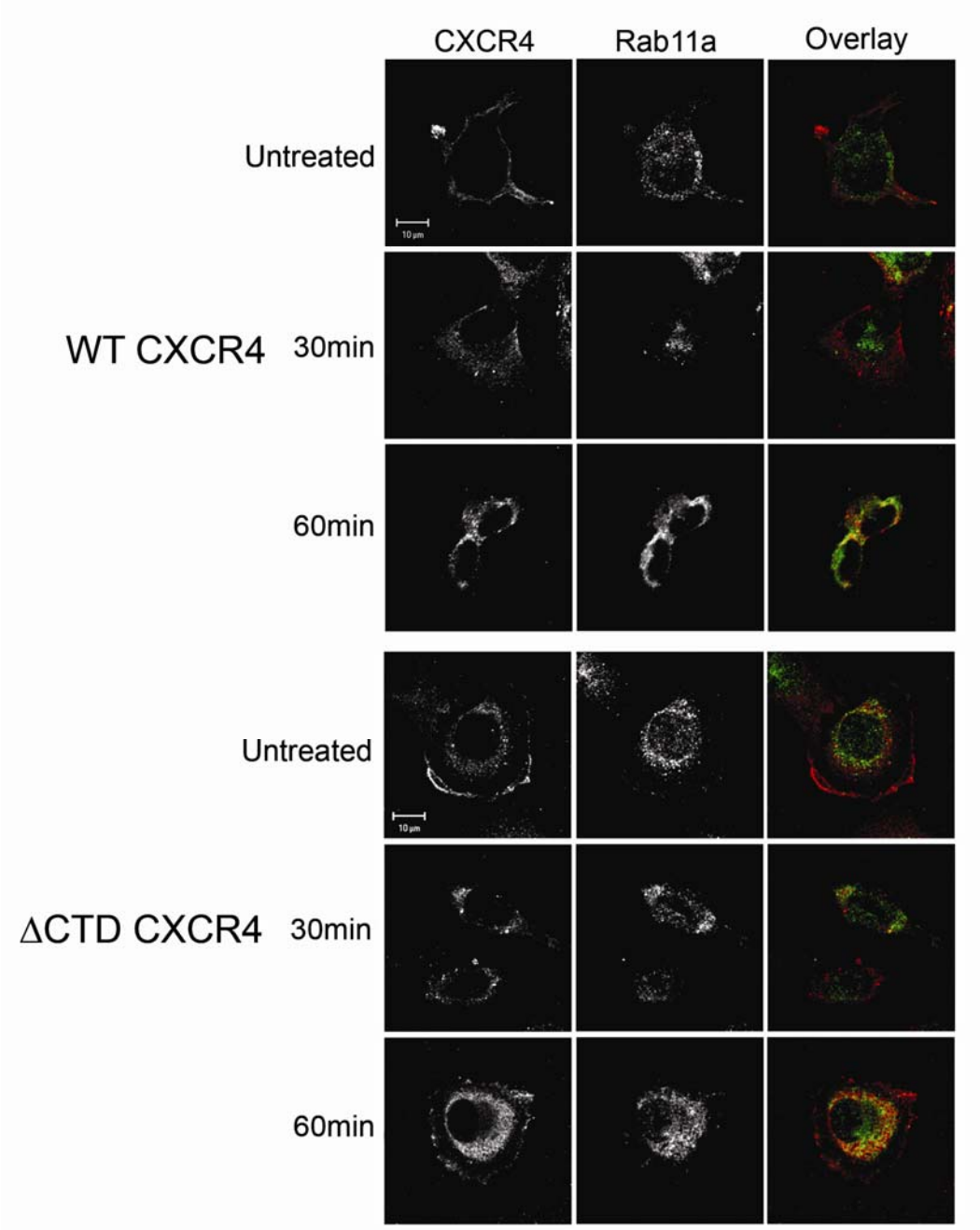

Figure 41: CXCR4 co-localization with Rab11a in the perinuclear recycling compartment following CXCL12 stimulation in MCF-7 cells expressing WT CXCR4, or ΔCTD CXCR4.
Cells were stimulated with vehicle (0.1% BSA/PBS) (Untreated) or 500ng/mL CXCL12 for 30min or 60min. Immunofluorescence staining for CXCR4 (MAb171) and Rab11a was performed and confocal images were taken with a slice thickness of 0.48μm. These images are representative of at least ten images for each cell type and treatment. Overlay images are pseudocolored where red is CXCR4 and green is Rab11a.

Tumor size was monitored over time by caliper measurements. As expected, mice injected with MCF-7 cells expressing ΔCTD-CXCR4 cells displayed palpable tumors only one week after injection, while mice injected with cells expressing empty vector or WT-CXCR4 had delayed onset of palpable tumors (Figure 42A). Furthermore, the average rate of tumor growth was significantly accelerated in mice injected with cells expressing ΔCTD-CXCR4 (Figure 42A).

All mice were sacrificed and tumors harvested when any dimension of the tumor reached 1.5 cm. However, analyzing final tumor volume by water displacement revealed that tumor final tumor volumes differed among the three groups of mice. Tumors from mice injected with WT-CXCR4 expressing cells showed a substantial increase in final tumor volume when compared to tumors from mice injected with vector expressing cells. Furthermore, tumors from mice injected with ΔCTD-CXCR4 expressing cells were significantly larger than those from mice in the vector expressing group (Figure 42B).

MCF-7 cells expressing ΔCTD-CXCR4 exhibit enhanced metastasis to the lung

Because MCF-7 parental cells normally exhibit a minimally invasive phenotype (Noel et al., 1991; Thompson et al., 1993), it was of interest to determine whether expression of WT- or ΔCTD-CXCR4 results in development of metastasis in an orthotopic in vivo model. These cells contain an IRES site that drives the simultaneous expression of GFP with the receptor. This allows metastatic lesions within secondary sites, such as the lung, to be easily identified

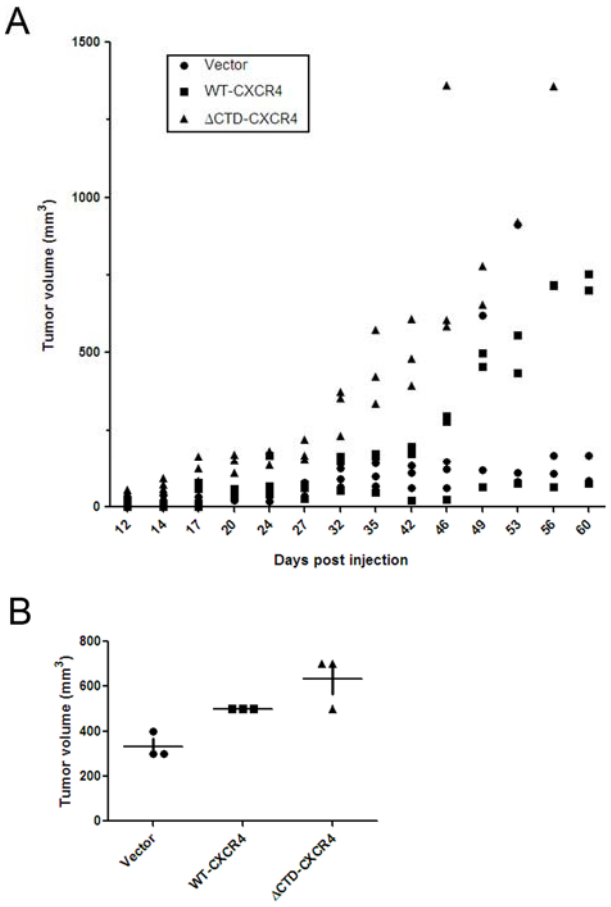

Figure 42: MCF-7 cells expressing ΔCTD-CXCR4 exhibit enhanced tumor growth in vivo.
Circles represent MCF-7-vector, squares represent MCF-7-WT-CXCR4, and triangles represent MCF-7-ΔCTD-CXCR4 expressing tumors. Each data point represents an individual mouse (A) Tumor volume over time. There is a statistically significant increase in the tumor growth rate of cells expressing ΔCTD-CXCR4 versus those cells expressing vector of WT-CXCR4 as determined by ANOVA (p-value < 0.05). (B) Final tumor volume. There is a statistically significant difference in final tumor volume of mice injected with cells expressing ΔCTD-CXCR4 versus those injected with cells expressing vector. Each group contains n=3.

in these studies. Lungs extracted from tumor bearing mice were infused with Bouin's fixative and examined for the presence of surface metastatic lesions prior to paraffin embedding and sectioning. As shown in Figure 43A, no surface metastatic lesions were visible upon gross examination of the lungs from any of the three groups. However, immunohistochemical staining of lung tissue sections with an anti-GFP antibody revealed the presence of micrometastic lesions in the lungs (Figure 43B). A statistically significant increase in GFP-positive staining (Figure 43C) and a greater from number of metastatic lesions (Table 5) were observed in lungs from mice injected with the MCF-7 cells expressing ΔCTD-CXCR4 when compared to mice injected with cells expressing vector or WT-CXCR4.

Discussion

These data reveal that truncation of the cytoplasmic carboxyl-terminus of CXCR4 results in constitutive, ligand-independent CXCR4 activity. This constitutive activation is accompanied by increased motility, proliferation, MAPK signaling, and recycling. These findings are quite surprising and are in contrast to our original hypothesis that this truncation would decrease CXCR4-mediated functions. However, a similar phenomenon does occur naturally in patients with a rare autosomal dominant immune deficiency disease known as WHIM (warts, hypogammaglobulinemia, infections, and myelokathexis) syndrome. This

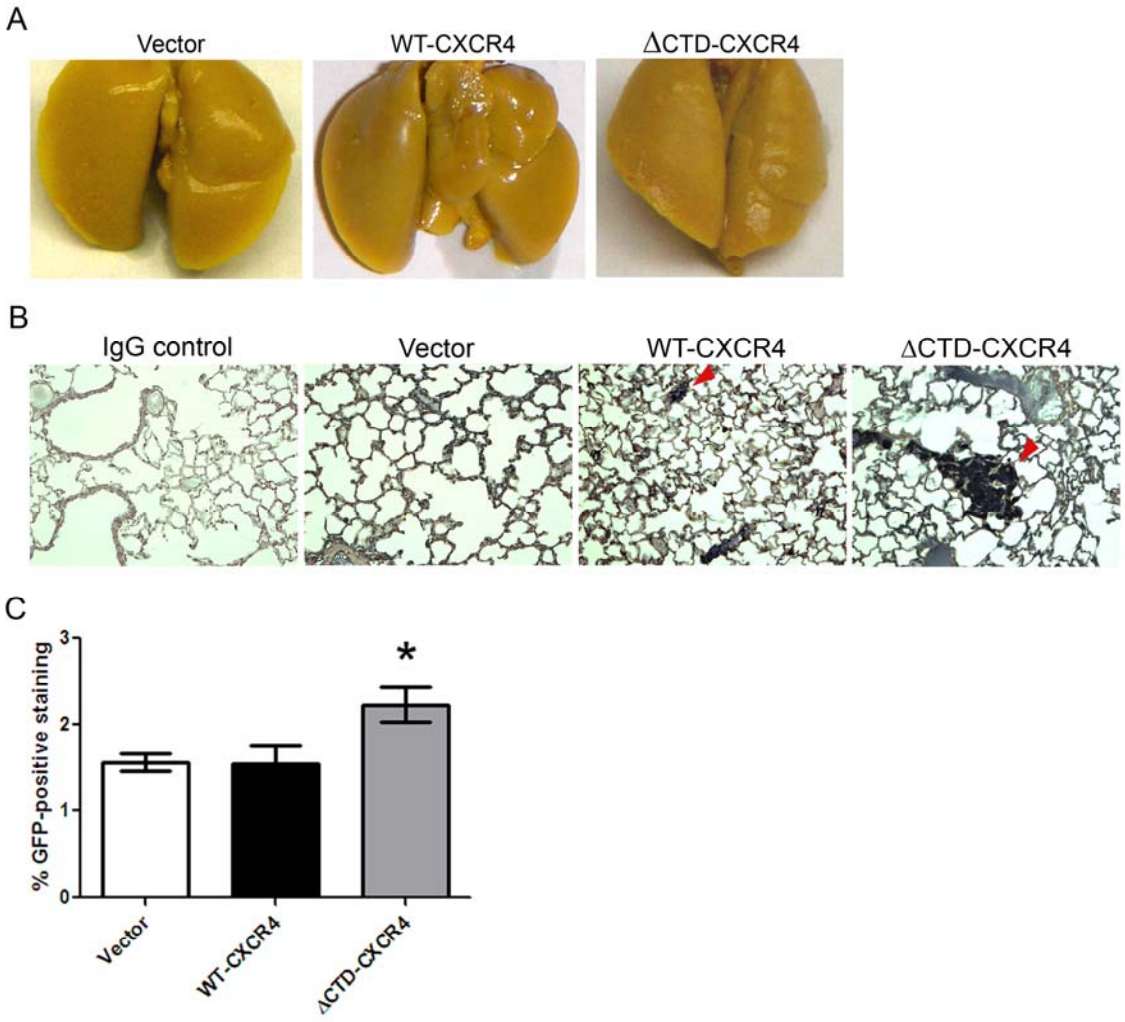

Figure 43: MCF-7 cells expressing ΔCTD-CXCR4 exhibit enhanced metastasis to the lung.
(A) Images of lungs extracted from mice injected with MCF-7 cells expressing empty vector, WT-CXCR4, or ΔCTD-CXCR4 cells and infused with Bouin's fixative. There were no visible macroscopic surface metastatic lesions on any of the lungs from any of the mice in all three groups (B) Images of immunohistochemical staining of lung sections using a rabbit IgG control antibody or an anti-GFP rabbit antibody taken with 20X objective. Red arrows indicate GFP-positive lesions that were quantitated for each group. Bars, 100μm (C) Quantitation of percent GFP-positive area of 60 randomly selected 20X microscopic fields of lung sections from mice injected with cells expressing vector, WT-CXCR4, or ΔCTD-CXCR4. Statistical significance between vector and WT-CXCR4 groups versus the ΔCTD-CXCR4 group is indicated by the asterick (p-value ≤ 0.05, Mann Whitney U test).

Table 5: **Lungs extracted from mice injected with MCF-7 cells expressing ΔCTD-CXCR4 exhibit an increased number of micrometastatic lesions.** Number of GFP-positive micrometastatic lesions in lung sections in 30 random 20X microscopic fields. Numbers represent Mean ±SD.

MCF-7-Vector	MCF-7-WT-CXCR4	MCF-7-ΔCTD-CXCR4
6 ± 1	8.7 ± 2.3	28 ± 3

disease causes severe neutropenia and is a result of truncation mutations in CXCR4. This mutant receptor leads to increased motility, calcium flux, and recycling in response to CXCL12 in primary human CD34+ cells (Kawai et al., 2005). These data are in contrast to our results in breast cancer cells expressing the truncated receptor, which exhibit constitutive activation and seem to be largely insensitive to further stimulation with CXCL12. These studies also found that there was decreased internalization of the truncated receptor, which the authors claim is the cause of enhanced and prolonged signaling. This discrepancy with our results may be a result of the methods used to detect receptor internalization. For example, it may be difficult to distinguish decreased internalization from rapid recycling back to the plasma membrane. In addition, it is well established that different monoclonal antibodies directed against CXCR4 only recognize specific receptor conformations and staining with these antibodies only represents a fraction of the total population of CXCR4 (Baribaud et al., 2001).

Cells expressing ΔCTD-CXCR4 exhibited enhanced migration and were non-responsive to further stimulation with CXCL12, suggesting ligand-independent signaling occurs. This hyper-motile phenotype in these cells is accompanied by gene expression changes associated with an epithelial-to-mesenchymal (EMT)-like transition. These cells demonstrate down-regulation of Zonula occludens (ZO-1) and E-cadherin expression. In addition, microarray analysis revealed upregulation of several mesenchymal markers in these cells

(Ueda et al., 2006). These cells also exhibit constitutive ERK 1/2 activation which may in part be contributing to the changes in gene expression.

These findings present a potential novel role for CXCR4 in the development of metastatic disease. The data suggest that not only can CXCR4 promote metastasis through the homing of cancer cells to secondary sites but may regulate gene expression of other proteins involved in the progression of metastatic disease. Recent evidence also suggests that CXCR4 cooperates with other tumor promoters to enhance the invasive phenotype. For example, it has been shown that CXCR4 can transactivate the epidermal growth factor receptor (EGFR) and this is involved in the proliferation of ovarian cancer cells (Porcile et al., 2005). In addition, studies have also demonstrated that upregulation of CXCR4 in breast cancer cells is essential for HER2-mediated tumor metastasis (Li et al., 2004). Further evidence indicates that crosstalk exists between CXCR4-mediated and BCR-ABL oncoprotein-mediated signaling through the src family of kinases in leukemia cells (Ptasznik et al., 2002). Because cells expressing ΔCTD-CXCR4 are significantly more metastatic than cells expressing WT-CXCR4 and the ΔCTD-CXCR4 receptor is constitutively active, it would be of interest to examine whether long-term stimulation with the CXCR4 ligand CXCL12 also leads to increases in the metastatic phenotype.

Overall, these data indicate that targeting the entire intracellular carboxyl-terminal domain of CXCR4 may not be the best approach for therapeutic intervention. However, the importance of this domain for receptor function and mediating pro-tumorigenic events is made apparent by these results. This region

of the receptor apparently contains residues that key for both positive and negative regulation of receptor function. These studies suggest that targeting specific receptor-protein interactions may be a more viable approach with which to target receptor-mediated functions. Therefore, further investigation into the regulation of receptor function through interacting proteins is warranted.

CHAPTER VI

CONCLUSIONS AND SIGNIFICANCE

The role of chemokines and their seven transmembrane G protein-coupled receptors in multiple aspects of tumorigenesis makes them ideal therapeutic targets for the treatment of cancer. The elucidation of mechanisms that mediate signaling initiated by activated chemokine receptors and the intracellular trafficking of chemokine receptors will identify novel therapeutic approaches.

The CXCR2 chemokine receptor is the major receptor for CXCL8 (Interleukin-8) and CXCL1 (MGSA/Gro-α). CXCL8 has a well established role in angiogenesis associated with malignancies, such as lung carcinoma (Arenberg et al., 1996; Smith et al., 1994; Yatsunami et al., 1997), ovarian carcinoma (Gawrychowski et al., 1998; Yoneda et al., 1998), melanoma (Luca et al., 1997; Singh et al., 1994), and gastrointestinal cancers (Kitadai et al., 1998; Wente et al., 2006). CXCL1 contributes to the tumorgenicity of melanoma (Balentien et al., 1991; Haghnegahdar et al., 2000; Owen et al., 1997) glioma (Zhou et al., 2005), colorectal carcinoma (Wang et al., 2006b), ovarian carcinoma (Furuya et al., 2007; Son et al., 2007; Yang et al., 2006) esophageal cancer (Wang et al., 2006a) and breast carcinoma (Yang et al., 2008). Moreover, CXCR2 is a major chemoattractive receptor expressed on neutrophils, which are key mediators of the inflammatory response and there is strong link between tumorigenesis and

chronic inflammation. In addition, CXCR2 expressed on endothelial cells plays a major role in tumor angiogenesis and thus tumor growth. Therefore, CXCR2 represents an attractive therapeutic target for multiple diseases.

CXCR4 was initially appreciated in disease for its role as a co-receptor in HIV infection (Feng et al, 1996) but recent evidence has established CXCR4 as an important mediator of metastasis (Zlotnik, 2006). It is also critically involved in the homing of recruited bone marrow-derived circulating cells (RBCCs) (Ruiz de Almodovar et al., 2006), a process that contributes significantly to tumor angiogenesis (Grunewald et al., 2006a). The CXCR4/CXCL12 axis is involved in the recruitment of Gr-1+CD11b+ myeloid cells into mammary tumors, which promote tumor metastasis (Yang et al., 2008). Testing of currently available CXCR4 inhibitors has proved successful in some preclinical animal models, however, the development of new modalities are needed for successful application in the clinic. Development of these novel targeting approaches will be more effective through understanding the regulation of the function of CXCR4.

We have demonstrated that RhoB plays an essential role in the proper intracellular trafficking of CXCR2 and as a consequence CXCR2-mediated functions. These studies not only emphasize the importance of recycling of CXCR2 to the plasma membrane but illustrate that the route of recycling is just as significant. This is supported by the finding that RhoB-Q63L mutant leads to recycling of CXCR2 through alternative pathways. Moreover, expression of this mutant severely impairs CXCR2-mediated chemotaxis. These data support our hypothesis that CXCR2 function is regulated by the small GTPase RhoB through

intracellular trafficking. These results are also suggestive that functional receptor not only exists at the plasma membrane but that intracellular signaling mediated by the receptor may be just as critical for the chemotactic response. This raises an entirely novel set of questions to be answered regarding the cellular functions mediated through chemokine receptors.

The components of the protein complex that accumulates at the cytoplasmic domains of chemokine receptors upon their activation are largely unknown. We propose that this chemokine receptor complex is analogous to the immune synapse in T-cells and focal adhesions. These structures are composed of dynamic and functional complexes that regulate the cellular responses elicited by these structures. We have developed a proteomics approach to identify novel ligand-dependent chemokine receptor interacting proteins. With this method, a number of interesting protein interactions have been identified that link CXCR2 to actin cytoskeleton, intracellular trafficking, and signaling pathways. Many of the identified proteins associate with the receptor in its unstimulated state, suggesting that these protein complexes are preformed within the cell. This represents a unique model for the association of proteins with the activated receptor. Previous experimental data suggested that the majority of chemokine receptor-associating proteins are actively recruited to activated chemokine receptors but our data indicate that this may not be the case for all mediators. Our data also support the notion that post-translational modifications, such as phosphorylation, of the receptor and its interacting proteins in response to ligand binding plays a critical role in regulating the chemotactic response.

Among the proteins identified is the multi-domain scaffolding protein IQGAP1. The interaction between CXCR2 and IQGAP1 may prove to be essential for the establishment of cell polarity during the chemotactic response. A key event in the establishment of cell polarity is the reorientation of the microtubule organizing center (MTOC), a process regulated by cdc42 and IQGAP1. IQGAP1 serves as a bridge between the actin cytoskeleton, through its interactions with the small GTPases rac and cdc42 and N-WASP, and the microtubule cytoskeleton via its interactions with cytoplasmic linker protein-170 (CLIP-170) and adenomatous polyposis coli (APC). The chemotactic response requires the proper coordination of these two systems in order for productive cell motility to occur. The protrusion of the dominant leading edge lamellipodia requires actin filament elongation and branching both of which are regulated by small GTPases and WAVE-2. Additionally, IQGAP1 may represent a direct link between CXCR2 and major signaling pathways involved in other cellular processes such as proliferation. In this manner, IQGAP1 serves as a central signaling “hub” to integrate multiple signaling pathways, particularly those initiated by chemokine receptors.

An additional protein identified in the proteomics screen for novel CXCR2 interacting proteins is the actin cytoskeletal modulator VASP. The Ena/VASP family of proteins are critical regulators of actin filament elongation and play a prominent role in the dynamics of lamellipodia. Interaction of CXCR2 specifically with VASP in a phosphorylation-dependent manner represents a direct link between CXCR2 and the actin cytoskeleton. Phosphorylation of VASP in the

EVH2 domain negatively regulates the interaction with F-actin (Barzik et al., 2005; Harbeck et al., 2000; Zhuang et al., 2004). Our studies demonstrate that the CXCR2/VASP interaction is enhanced by the EVH2 phosphorylation and F-actin is essential for the interaction. Therefore, our data suggests that VASP is able to interact with F-actin in the presence of CXCR2 and may have important implications for the mechanism of VASP binding to F-actin.

These studies establish the critical importance of the route of chemokine receptor recycling, regulated at least in part by RhoB, in maintaining a productive chemotactic response. Through these studies we have learned that there is an essential role for chemokine receptor-mediated endosomal signaling in chemotaxis. Previously, it was thought that recycling of a GPCR back to the plasma membrane was all that was required for resentization and as a result, continued cellular responses mediated by the receptor. However, our data and other recent evidence suggest that signaling that occurs on specific endocytic compartments is critical for the continued cellular response. Additionally, IQGAP1 and VASP have been identified as novel receptor-interacting proteins that link CXCR2 to the actin cytoskeleton and major signaling pathways. Furthermore, loss of VASP results in severely impaired CXCL8-mediated leukocyte trafficking in vivo. These studies provide knowledge for specific interruption of the CXCR2 interaction with VASP and IQGAP1 as a means of specifically targeting CXCR2 function.

We further demonstrate the importance of chemokine receptor trafficking on the biological function through our findings that constitutive recycling of a

truncated CXCR4 receptor leads to increased tumorigenesis and metastasis of breast cancer cells in vivo. Together these data ascertain the biological significance of chemokine receptor trafficking in the regulation of their function and implicate a new model for chemokine receptor-associated protein complexes in the cellular responses initiated by these receptors.

REFERENCES

Addison, C. L., Daniel, T. O., Burdick, M. D., Liu, H., Ehlert, J. E., Xue, Y. Y., Buechi, L., Walz, A., Richmond, A. and Strieter, R. M. (2000). The CXC chemokine receptor 2, CXCR2, is the putative receptor for ELR+ CXC chemokine-induced angiogenic activity. *J Immunol* **165**, 5269-77.

Ahern-Djamali, S. M., Bachmann, C., Hua, P., Reddy, S. K., Kastenmeier, A. S., Walter, U. and Hoffmann, F. M. (1999). Identification of profilin and src homology 3 domains as binding partners for Drosophila enabled. *Proc Natl Acad Sci U S A* **96**, 4977-82.

Akasaki, T., Koga, H. and Sumimoto, H. (1999). Phosphoinositide 3-kinase-dependent and -independent activation of the small GTPase Rac2 in human neutrophils. *J Biol Chem* **274**, 18055-9.

Anderson, S. I., Behrendt, B., Machesky, L. M., Insall, R. H. and Nash, G. B. (2003). Linked regulation of motility and integrin function in activated migrating neutrophils revealed by interference in remodelling of the cytoskeleton. *Cell Motil Cytoskeleton* **54**, 135-46.

Arenberg, D. A., Kunkel, S. L., Polverini, P. J., Glass, M., Burdick, M. D. and Strieter, R. M. (1996). Inhibition of interleukin-8 reduces tumorigenesis of human non-small cell lung cancer in SCID mice. *J Clin Invest* **97**, 2792-802.

Bachmann, C., Fischer, L., Walter, U. and Reinhard, M. (1999). The EVH2 domain of the vasodilator-stimulated phosphoprotein mediates tetramerization, F-actin binding, and actin bundle formation. *J Biol Chem* **274**, 23549-57.

Balentien, E., Mufson, B. E., Shattuck, R. L., Derynck, R. and Richmond, A. (1991). Effects of MGSA/GRO alpha on melanocyte transformation. *Oncogene* **6**, 1115-24.

Balkwill, F., Charles, K. A. and Mantovani, A. (2005). Smoldering and polarized inflammation in the initiation and promotion of malignant disease. *Cancer Cell* **7**, 211-7.

Baribaud, F., Edwards, T. G., Sharron, M., Brelot, A., Heveker, N., Price, K., Mortari, F., Alizon, M., Tsang, M. and Doms, R. W. (2001). Antigenically distinct conformations of CXCR4. *J Virol* **75**, 8957-67.

Barlic, J., Khandaker, M. H., Mahon, E., Andrews, J., DeVries, M. E., Mitchell, G. B., Rahimpour, R., Tan, C. M., Ferguson, S. S. and Kelvin, D. J.

(1999). beta-arrestins regulate interleukin-8-induced CXCR1 internalization. *J Biol Chem* **274**, 16287-94.

Barzik, M., Kotova, T. I., Higgs, H. N., Hazelwood, L., Hanein, D., Gertler, F. B. and Schafer, D. A. (2005). Ena/VASP proteins enhance actin polymerization in the presence of barbed end capping proteins. *J Biol Chem* **280**, 28653-62.

Bear, J. E., Loureiro, J. J., Libova, I., Fassler, R., Wehland, J. and Gertler, F. B. (2000). Negative regulation of fibroblast motility by Ena/VASP proteins. *Cell* **101**, 717-28.

Bear, J. E., Svitkina, T. M., Krause, M., Schafer, D. A., Loureiro, J. J., Strasser, G. A., Maly, I. V., Chaga, O. Y., Cooper, J. A., Borisy, G. G. et al. (2002). Antagonism between Ena/VASP proteins and actin filament capping regulates fibroblast motility. *Cell* **109**, 509-21.

Belperio, J. A., Keane, M. P., Arenberg, D. A., Addison, C. L., Ehlert, J. E., Burdick, M. D. and Strieter, R. M. (2000). CXC chemokines in angiogenesis. *J Leukoc Biol* **68**, 1-8.

Ben-Baruch, A., Bengali, K. M., Biragyn, A., Johnston, J. J., Wang, J. M., Kim, J., Chuntharapai, A., Michiel, D. F., Oppenheim, J. J. and Kelvin, D. J. (1995). Interleukin-8 receptor beta. The role of the carboxyl terminus in signal transduction. *J Biol Chem* **270**, 9121-8.

Benovic, J. L., Kuhn, H., Weyand, I., Codina, J., Caron, M. G. and Lefkowitz, R. J. (1987). Functional desensitization of the isolated beta-adrenergic receptor by the beta-adrenergic receptor kinase: potential role of an analog of the retinal protein arrestin (48-kDa protein). *Proc Natl Acad Sci U S A* **84**, 8879-82.

Benzing, T., Yaffe, M. B., Arnould, T., Sellin, L., Schermer, B., Schilling, B., Schreiber, R., Kunzelmann, K., Leparc, G. G., Kim, E. et al. (2000). 14-3-3 interacts with regulator of G protein signaling proteins and modulates their activity. *J Biol Chem* **275**, 28167-72.

Blume, C., Benz, P. M., Walter, U., Ha, J., Kemp, B. E. and Renne, T. (2007). AMP-activated protein kinase impairs endothelial actin cytoskeleton assembly by phosphorylating vasodilator-stimulated phosphoprotein. *J Biol Chem* **282**, 4601-12.

Briggs, M. W. and Sacks, D. B. (2003). IQGAP proteins are integral components of cytoskeletal regulation. *EMBO Rep* **4**, 571-4.

Brindle, N. P., Holt, M. R., Davies, J. E., Price, C. J. and Critchley, D. R. (1996). The focal-adhesion vasodilator-stimulated phosphoprotein (VASP) binds to the proline-rich domain in vinculin. *Biochem J* **318 (Pt 3)**, 753-7.

Brunger, A. T. and DeLaBarre, B. (2003). NSF and p97/VCP: similar at first, different at last. *FEBS Lett* **555**, 126-33.

Bucci, C., Parton, R. G., Mather, I. H., Stunnenberg, H., Simons, K., Hoflack, B. and Zerial, M. (1992). The small GTPase rab5 functions as a regulatory factor in the early endocytic pathway. *Cell* **70**, 715-28.

Butt, E., Abel, K., Krieger, M., Palm, D., Hoppe, V., Hoppe, J. and Walter, U. (1994). cAMP- and cGMP-dependent protein kinase phosphorylation sites of the focal adhesion vasodilator-stimulated phosphoprotein (VASP) in vitro and in intact human platelets. *J Biol Chem* **269**, 14509-17.

Carl, U. D., Pollmann, M., Orr, E., Gertlere, F. B., Chakraborty, T. and Wehland, J. (1999). Aromatic and basic residues within the EVH1 domain of VASP specify its interaction with proline-rich ligands. *Curr Biol* **9**, 715-8.

Casanova, J. E., Wang, X., Kumar, R., Bhartur, S. G., Navarre, J., Woodrum, J. E., Altschuler, Y., Ray, G. S. and Goldenring, J. R. (1999). Association of Rab25 and Rab11a with the apical recycling system of polarized Madin-Darby canine kidney cells. *Mol Biol Cell* **10**, 47-61.

Chen, T., Han, Y., Yang, M., Zhang, W., Li, N., Wan, T., Guo, J. and Cao, X. (2003a). Rab39, a novel Golgi-associated Rab GTPase from human dendritic cells involved in cellular endocytosis. *Biochem Biophys Res Commun* **303**, 1114-20.

Chen, Y., Stamatoyannopoulos, G. and Song, C. Z. (2003b). Down-regulation of CXCR4 by inducible small interfering RNA inhibits breast cancer cell invasion in vitro. *Cancer Res* **63**, 4801-4.

Cheng, Z. J., Zhao, J., Sun, Y., Hu, W., Wu, Y. L., Cen, B., Wu, G. X. and Pei, G. (2000). beta-arrestin differentially regulates the chemokine receptor CXCR4-mediated signaling and receptor internalization, and this implicates multiple interaction sites between beta-arrestin and CXCR4. *J Biol Chem* **275**, 2479-85.

Colvin, R. A., Campanella, G. S., Sun, J. and Luster, A. D. (2004). Intracellular domains of CXCR3 that mediate CXCL9, CXCL10, and CXCL11 function. *J Biol Chem* **279**, 30219-27.

Coussens, L. M., Raymond, W. W., Bergers, G., Laig-Webster, M., Behrendtsen, O., Werb, Z., Caughey, G. H. and Hanahan, D. (1999). Inflammatory mast cells up-regulate angiogenesis during squamous epithelial carcinogenesis. *Genes Dev* **13**, 1382-97.

Curiel, T. J., Coukos, G., Zou, L., Alvarez, X., Cheng, P., Mottram, P., Evdemon-Hogan, M., Conejo-Garcia, J. R., Zhang, L., Burow, M. et al. (2004). Specific recruitment of regulatory T cells in ovarian carcinoma fosters immune privilege and predicts reduced survival. *Nat Med* **10**, 942-9.

Dalgleish, A. G. and O'Byrne, K. (2006). Inflammation and cancer: the role of the immune response and angiogenesis. *Cancer Treat Res* **130**, 1-38.

del Pozo, M. A., Vicente-Manzanares, M., Tejedor, R., Serrador, J. M. and Sanchez-Madrid, F. (1999). Rho GTPases control migration and polarization of adhesion molecules and cytoskeletal ERM components in T lymphocytes. *Eur J Immunol* **29**, 3609-20.

Derossi, D., Joliot, A. H., Chassaing, G. and Prochiantz, A. (1994). The third helix of the Antennapedia homeodomain translocates through biological membranes. *J Biol Chem* **269**, 10444-50.

Di Cioccio, V., Strippoli, R., Bizzarri, C., Troiani, G., Cervellera, M. N., Gloaguen, I., Colagrande, A., Cattozzo, E. M., Pagliei, S., Santoni, A. et al. (2004). Key role of proline-rich tyrosine kinase 2 in interleukin-8 (CXCL8/IL-8)-mediated human neutrophil chemotaxis. *Immunology* **111**, 407-15.

Drees, B., Friederich, E., Fradelizi, J., Louvard, D., Beckerle, M. C. and Golsteyn, R. M. (2000). Characterization of the interaction between zyxin and members of the Ena/vasodilator-stimulated phosphoprotein family of proteins. *J Biol Chem* **275**, 22503-11.

Droese, J., Mokros, T., Hermosilla, R., Schulein, R., Lipp, M., Hopken, U. E. and Rehm, A. (2004). HCMV-encoded chemokine receptor US28 employs multiple routes for internalization. *Biochem Biophys Res Commun* **322**, 42-9.

Eigenthaler, M., Nolte, C., Halbrugge, M. and Walter, U. (1992). Concentration and regulation of cyclic nucleotides, cyclic-nucleotide-dependent protein kinases and one of their major substrates in human platelets. Estimating the rate of cAMP-regulated and cGMP-regulated protein phosphorylation in intact cells. *Eur J Biochem* **205**, 471-81.

Ernst, S., Zobiack, N., Boecker, K., Gerke, V. and Rescher, U. (2004). Agonist-induced trafficking of the low-affinity formyl peptide receptor FPRL1. *Cell Mol Life Sci* **61**, 1684-92.

Fan, G. H., Lapierre, L. A., Goldenring, J. R. and Richmond, A. (2003). Differential regulation of CXCR2 trafficking by Rab GTPases. *Blood* **101**, 2115-24.

Fan, G. H., Lapierre, L. A., Goldenring, J. R., Sai, J. and Richmond, A. (2004). Rab11-family interacting protein 2 and myosin Vb are required for CXCR2 recycling and receptor-mediated chemotaxis. *Mol Biol Cell* **15**, 2456-69.

Fan, G. H., Yang, W., Sai, J. and Richmond, A. (2001a). Phosphorylation-independent association of CXCR2 with the protein phosphatase 2A core enzyme. *J Biol Chem* **276**, 16960-8.

Fan, G. H., Yang, W., Sai, J. and Richmond, A. (2002). Hsc/Hsp70 interacting protein (hip) associates with CXCR2 and regulates the receptor signaling and trafficking. *J Biol Chem* **277**, 6590-7.

Fan, G. H., Yang, W., Wang, X. J., Qian, Q. and Richmond, A. (2001b). Identification of a motif in the carboxyl terminus of CXCR2 that is involved in adaptin 2 binding and receptor internalization. *Biochemistry* **40**, 791-800.

Fawell, S., Seery, J., Daikh, Y., Moore, C., Chen, L. L., Pepinsky, B. and Barsoum, J. (1994). Tat-mediated delivery of heterologous proteins into cells. *Proc Natl Acad Sci U S A* **91**, 664-8.

Ferguson, S. S. (2001). Evolving concepts in G protein-coupled receptor endocytosis: the role in receptor desensitization and signaling. *Pharmacol Rev* **53**, 1-24.

Ferguson, S. S., Downey, W. E., 3rd, Colapietro, A. M., Barak, L. S., Menard, L. and Caron, M. G. (1996). Role of beta-arrestin in mediating agonist-promoted G protein-coupled receptor internalization. *Science* **271**, 363-6.

Ferguson, S. S., Zhang, J., Barak, L. S. and Caron, M. G. (1998). Molecular mechanisms of G protein-coupled receptor desensitization and resensitization. *Life Sci* **62**, 1561-5.

Fernandez-Borja, M., Janssen, L., Verwoerd, D., Hordijk, P. and Neefjes, J. (2005). RhoB regulates endosome transport by promoting actin assembly on endosomal membranes through Dia1. *J Cell Sci* **118**, 2661-70.

Fernandis, A. Z., Prasad, A., Band, H., Klosel, R. and Ganju, R. K. (2004). Regulation of CXCR4-mediated chemotaxis and chemoinvasion of breast cancer cells. *Oncogene* **23**, 157-67.

Freedman, N. J. and Lefkowitz, R. J. (1996). Desensitization of G protein-coupled receptors. *Recent Prog Horm Res* **51**, 319-51; discussion 352-3.

Fukata, M., Kuroda, S., Nakagawa, M., Kawajiri, A., Itoh, N., Shoji, I., Matsuura, Y., Yonehara, S., Fujisawa, H., Kikuchi, A. et al. (1999). Cdc42 and

Rac1 regulate the interaction of IQGAP1 with beta-catenin. *J Biol Chem* **274**, 26044-50.

Fukata, M., Watanabe, T., Noritake, J., Nakagawa, M., Yamaga, M., Kuroda, S., Matsuura, Y., Iwamatsu, A., Perez, F. and Kaibuchi, K. (2002). Rac1 and Cdc42 capture microtubules through IQGAP1 and CLIP-170. *Cell* **109**, 873-85.

Fukui, Y., Hashimoto, O., Sanui, T., Oono, T., Koga, H., Abe, M., Inayoshi, A., Noda, M., Oike, M., Shirai, T. et al. (2001). Haematopoietic cell-specific CDM family protein DOCK2 is essential for lymphocyte migration. *Nature* **412**, 826-31.

Furuya, M., Suyama, T., Usui, H., Kasuya, Y., Nishiyama, M., Tanaka, N., Ishiwata, I., Nagai, Y., Shozu, M. and Kimura, S. (2007). Up-regulation of CXC chemokines and their receptors: implications for proinflammatory microenvironments of ovarian carcinomas and endometriosis. *Hum Pathol* **38**, 1676-87.

Gampel, A. and Mellor, H. (2002). Small interfering RNAs as a tool to assign Rho GTPase exchange-factor function in vivo. *Biochem J* **366**, 393-8.

Gampel, A., Parker, P. J. and Mellor, H. (1999). Regulation of epidermal growth factor receptor traffic by the small GTPase rhoB. *Curr Biol* **9**, 955-8.

Garcia Arguinzonis, M. I., Galler, A. B., Walter, U., Reinhard, M. and Simm, A. (2002). Increased spreading, Rac/p21-activated kinase (PAK) activity, and compromised cell motility in cells deficient in vasodilator-stimulated phosphoprotein (VASP). *J Biol Chem* **277**, 45604-10.

Gawrychowski, K., Skopinska-Rozewska, E., Barcz, E., Sommer, E., Szaniawska, B., Roszkowska-Purska, K., Janik, P. and Zielinski, J. (1998). Angiogenic activity and interleukin-8 content of human ovarian cancer ascites. *Eur J Gynaecol Oncol* **19**, 262-4.

George, S. R., Ng, G. Y., Lee, S. P., Fan, T., Varghese, G., Wang, C., Deber, C. M., Seeman, P. and O'Dowd, B. F. (2003). Blockade of G protein-coupled receptors and the dopamine transporter by a transmembrane domain peptide: novel strategy for functional inhibition of membrane proteins in vivo. *J Pharmacol Exp Ther* **307**, 481-9.

Gertler, F. B., Comer, A. R., Juang, J. L., Ahern, S. M., Clark, M. J., Liebl, E. C. and Hoffmann, F. M. (1995). enabled, a dosage-sensitive suppressor of mutations in the Drosophila Abl tyrosine kinase, encodes an Abl substrate with SH3 domain-binding properties. *Genes Dev* **9**, 521-33.

Gertler, F. B., Niebuhr, K., Reinhard, M., Wehland, J. and Soriano, P. (1996). Mena, a relative of VASP and Drosophila Enabled, is implicated in the control of microfilament dynamics. *Cell* **87**, 227-39.

Ghosh, P., Dahms, N. M. and Kornfeld, S. (2003). Mannose 6-phosphate receptors: new twists in the tale. *Nat Rev Mol Cell Biol* **4**, 202-12.

Goldenring, J. R., Ray, G. S. and Lee, J. R. (1999). Rab11 in dysplasia of Barrett's epithelia. *Yale J Biol Med* **72**, 113-20.

Goodman, O. B., Jr., Krupnick, J. G., Santini, F., Gurevich, V. V., Penn, R. B., Gagnon, A. W., Keen, J. H. and Benovic, J. L. (1996). Beta-arrestin acts as a clathrin adaptor in endocytosis of the beta2-adrenergic receptor. *Nature* **383**, 447-50.

Gorvel, J. P., Chavrier, P., Zerial, M. and Gruenberg, J. (1991). rab5 controls early endosome fusion in vitro. *Cell* **64**, 915-25.

Green, E. G., Ramm, E., Riley, N. M., Spiro, D. J., Goldenring, J. R. and Wessling-Resnick, M. (1997). Rab11 is associated with transferrin-containing recycling compartments in K562 cells. *Biochem Biophys Res Commun* **239**, 612-6.

Grunewald, M., Avraham, I., Dor, Y., Bachar-Lustig, E., Itin, A., Jung, S., Chimenti, S., Landsman, L., Abramovitch, R. and Keshet, E. (2006a). VEGF-induced adult neovascularization: recruitment, retention, and role of accessory cells. *Cell* **124**, 175-89.

Grunewald, T. G., Kammerer, U., Schulze, E., Schindler, D., Honig, A., Zimmer, M. and Butt, E. (2006b). Silencing of LASP-1 influences zyxin localization, inhibits proliferation and reduces migration in breast cancer cells. *Exp Cell Res* **312**, 974-82.

Grunewald, T. G., Kammerer, U., Winkler, C., Schindler, D., Sickmann, A., Honig, A. and Butt, E. (2007). Overexpression of LASP-1 mediates migration and proliferation of human ovarian cancer cells and influences zyxin localisation. *Br J Cancer* **96**, 296-305.

Haghnegahdar, H., Du, J., Wang, D., Strieter, R. M., Burdick, M. D., Nanney, L. B., Cardwell, N., Luan, J., Shattuck-Brandt, R. and Richmond, A. (2000). The tumorigenic and angiogenic effects of MGSA/GRO proteins in melanoma. *J Leukoc Biol* **67**, 53-62.

Halbrugge, M., Friedrich, C., Eigenthaler, M., Schanzenbacher, P. and Walter, U. (1990). Stoichiometric and reversible phosphorylation of a 46-kDa

protein in human platelets in response to cGMP- and cAMP-elevating vasodilators. *J Biol Chem* **265**, 3088-93.

Hales, C. M., Vaerman, J. P. and Goldenring, J. R. (2002). Rab11 family interacting protein 2 associates with Myosin Vb and regulates plasma membrane recycling. *J Biol Chem* **277**, 50415-21.

Hall, H., Williams, E. J., Moore, S. E., Walsh, F. S., Prochiantz, A. and Doherty, P. (1996). Inhibition of FGF-stimulated phosphatidylinositol hydrolysis and neurite outgrowth by a cell-membrane permeable phosphopeptide. *Curr Biol* **6**, 580-7.

Harbeck, B., Huttelmaier, S., Schluter, K., Jockusch, B. M. and Illenberger, S. (2000). Phosphorylation of the vasodilator-stimulated phosphoprotein regulates its interaction with actin. *J Biol Chem* **275**, 30817-25.

Hart, M. J., Callow, M. G., Souza, B. and Polakis, P. (1996). IQGAP1, a calmodulin-binding protein with a rasGAP-related domain, is a potential effector for cdc42Hs. *Embo J* **15**, 2997-3005.

Heilker, R., Manning-Krieg, U., Zuber, J. F. and Spiess, M. (1996). In vitro binding of clathrin adaptors to sorting signals correlates with endocytosis and basolateral sorting. *Embo J* **15**, 2893-9.

Hille-Rehfeld, A. (1995). Mannose 6-phosphate receptors in sorting and transport of lysosomal enzymes. *Biochim Biophys Acta* **1241**, 177-94.

Hirsch, E., Katanaev, V. L., Garlanda, C., Azzolino, O., Pirola, L., Silengo, L., Sozzani, S., Mantovani, A., Altruda, F. and Wymann, M. P. (2000). Central role for G protein-coupled phosphoinositide 3-kinase gamma in inflammation. *Science* **287**, 1049-53.

Ho, Y. D., Joyal, J. L., Li, Z. and Sacks, D. B. (1999). IQGAP1 integrates Ca2+/calmodulin and Cdc42 signaling. *J Biol Chem* **274**, 464-70.

Horton, L. W., Yu, Y., Zaja-Milatovic, S., Strieter, R. M. and Richmond, A. (2007). Opposing roles of murine duffy antigen receptor for chemokine and murine CXC chemokine receptor-2 receptors in murine melanoma tumor growth. *Cancer Res* **67**, 9791-9.

Hunyady, L., Baukal, A. J., Gaborik, Z., Olivares-Reyes, J. A., Bor, M., Szaszak, M., Lodge, R., Catt, K. J. and Balla, T. (2002). Differential PI 3-kinase dependence of early and late phases of recycling of the internalized AT1 angiotensin receptor. *J Cell Biol* **157**, 1211-22.

Huttenrauch, F., Nitzki, A., Lin, F. T., Honing, S. and Oppermann, M. (2002). Beta-arrestin binding to CC chemokine receptor 5 requires multiple C-terminal receptor phosphorylation sites and involves a conserved Asp-Arg-Tyr sequence motif. *J Biol Chem* **277**, 30769-77.

Ichimura, T., Wakamiya-Tsuruta, A., Itagaki, C., Taoka, M., Hayano, T., Natsume, T. and Isobe, T. (2002). Phosphorylation-dependent interaction of kinesin light chain 2 and the 14-3-3 protein. *Biochemistry* **41**, 5566-72.

Ishii, M. and Kurachi, Y. (2003). Physiological actions of regulators of G-protein signaling (RGS) proteins. *Life Sci* **74**, 163-71.

Jimenez-Sainz, M. C., Fast, B., Mayor, F., Jr. and Aragay, A. M. (2003). Signaling pathways for monocyte chemoattractant protein 1-mediated extracellular signal-regulated kinase activation. *Mol Pharmacol* **64**, 773-82.

Jones, S. A., Moser, B. and Thelen, M. (1995). A comparison of post-receptor signal transduction events in Jurkat cells transfected with either IL-8R1 or IL-8R2. Chemokine mediated activation of p42/p44 MAP-kinase (ERK-2). *FEBS Lett* **364**, 211-4.

Jordens, I., Fernandez-Borja, M., Marsman, M., Dusseljee, S., Janssen, L., Calafat, J., Janssen, H., Wubbolts, R. and Neefjes, J. (2001). The Rab7 effector protein RILP controls lysosomal transport by inducing the recruitment of dynein-dynactin motors. *Curr Biol* **11**, 1680-5.

Kang, F., Purich, D. L. and Southwick, F. S. (1999). Profilin promotes barbed-end actin filament assembly without lowering the critical concentration. *J Biol Chem* **274**, 36963-72.

Kawai, T., Choi, U., Whiting-Theobald, N. L., Linton, G. F., Brenner, S., Sechler, J. M., Murphy, P. M. and Malech, H. L. (2005). Enhanced function with decreased internalization of carboxy-terminus truncated CXCR4 responsible for WHIM syndrome. *Exp Hematol* **33**, 460-8.

Keane, M. P., Belperio, J. A., Xue, Y. Y., Burdick, M. D. and Strieter, R. M. (2004). Depletion of CXCR2 inhibits tumor growth and angiogenesis in a murine model of lung cancer. *J Immunol* **172**, 2853-60.

Kitadai, Y., Haruma, K., Sumii, K., Yamamoto, S., Ue, T., Yokozaki, H., Yasui, W., Ohmoto, Y., Kajiyama, G., Fidler, I. J. et al. (1998). Expression of interleukin-8 correlates with vascularity in human gastric carcinomas. *Am J Pathol* **152**, 93-100.

Korenbaum, E., Nordberg, P., Bjorkegren-Sjogren, C., Schutt, C. E., Lindberg, U. and Karlsson, R. (1998). The role of profilin in actin polymerization and nucleotide exchange. *Biochemistry* **37**, 9274-83.

Kraft, K., Olbrich, H., Majoul, I., Mack, M., Proudfoot, A. and Oppermann, M. (2001). Characterization of sequence determinants within the carboxyl-terminal domain of chemokine receptor CCR5 that regulate signaling and receptor internalization. *J Biol Chem* **276**, 34408-18.

Krause, M., Dent, E. W., Bear, J. E., Loureiro, J. J. and Gertler, F. B. (2003). Ena/VASP proteins: regulators of the actin cytoskeleton and cell migration. *Annu Rev Cell Dev Biol* **19**, 541-64.

Krause, M., Leslie, J. D., Stewart, M., Lafuente, E. M., Valderrama, F., Jagannathan, R., Strasser, G. A., Rubinson, D. A., Liu, H., Way, M. et al. (2004). Lamellipodin, an Ena/VASP ligand, is implicated in the regulation of lamellipodial dynamics. *Dev Cell* **7**, 571-83.

Krause, M., Sechi, A. S., Konradt, M., Monner, D., Gertler, F. B. and Wehland, J. (2000). Fyn-binding protein (Fyb)/SLP-76-associated protein (SLAP), Ena/vasodilator-stimulated phosphoprotein (VASP) proteins and the Arp2/3 complex link T cell receptor (TCR) signaling to the actin cytoskeleton. *J Cell Biol* **149**, 181-94.

Krupnick, J. G. and Benovic, J. L. (1998). The role of receptor kinases and arrestins in G protein-coupled receptor regulation. *Annu Rev Pharmacol Toxicol* **38**, 289-319.

Kuroda, S., Fukata, M., Nakagawa, M. and Kaibuchi, K. (1999). Cdc42, Rac1, and their effector IQGAP1 as molecular switches for cadherin-mediated cell-cell adhesion. *Biochem Biophys Res Commun* **262**, 1-6.

Lambrechts, A., Kwiatkowski, A. V., Lanier, L. M., Bear, J. E., Vandekerckhove, J., Ampe, C. and Gertler, F. B. (2000). cAMP-dependent protein kinase phosphorylation of EVL, a Mena/VASP relative, regulates its interaction with actin and SH3 domains. *J Biol Chem* **275**, 36143-51.

Lapierre, L. A., Avant, K. M., Caldwell, C. M., Ham, A. J., Hill, S., Williams, J. A., Smolka, A. J. and Goldenring, J. R. (2007). Characterization of immunoisolated human gastric parietal cells tubulovesicles: identification of regulators of apical recycling. *Am J Physiol Gastrointest Liver Physiol* **292**, G1249-62.

Lapierre, L. A., Kumar, R., Hales, C. M., Navarre, J., Bhartur, S. G., Burnette, J. O., Provance, D. W., Jr., Mercer, J. A., Bahler, M. and Goldenring, J. R.

(2001). Myosin vb is associated with plasma membrane recycling systems. *Mol Biol Cell* **12**, 1843-57.

Laporte, S. A., Oakley, R. H., Zhang, J., Holt, J. A., Ferguson, S. S., Caron, M. G. and Barak, L. S. (1999). The beta2-adrenergic receptor/betaarrestin complex recruits the clathrin adaptor AP-2 during endocytosis. *Proc Natl Acad Sci U S A* **96**, 3712-7.

Lapteva, N., Yang, A. G., Sanders, D. E., Strube, R. W. and Chen, S. Y. (2005). CXCR4 knockdown by small interfering RNA abrogates breast tumor growth in vivo. *Cancer Gene Ther* **12**, 84-9.

Laurent, V., Loisel, T. P., Harbeck, B., Wehman, A., Grobe, L., Jockusch, B. M., Wehland, J., Gertler, F. B. and Carlier, M. F. (1999). Role of proteins of the Ena/VASP family in actin-based motility of Listeria monocytogenes. *J Cell Biol* **144**, 1245-58.

Le Borgne, R. and Hoflack, B. (1998). Protein transport from the secretory to the endocytic pathway in mammalian cells. *Biochim Biophys Acta* **1404**, 195-209.

Lee, A. H., Zareei, M. P. and Daefler, S. (2002). Identification of a NIPSNAP homologue as host cell target for Salmonella virulence protein SpiC. *Cell Microbiol* **4**, 739-50.

Lee, W. J., Kim, D. U., Lee, M. Y. and Choi, K. Y. (2007). Identification of proteins interacting with the catalytic subunit of PP2A by proteomics. *Proteomics* **7**, 206-14.

Li, Y. M., Pan, Y., Wei, Y., Cheng, X., Zhou, B. P., Tan, M., Zhou, X., Xia, W., Hortobagyi, G. N., Yu, D. et al. (2004). Upregulation of CXCR4 is essential for HER2-mediated tumor metastasis. *Cancer Cell* **6**, 459-69.

Li, Z., Kim, S. H., Higgins, J. M., Brenner, M. B. and Sacks, D. B. (1999). IQGAP1 and calmodulin modulate E-cadherin function. *J Biol Chem* **274**, 37885-92.

Liang, Z., Yoon, Y., Votaw, J., Goodman, M. M., Williams, L. and Shim, H. (2005). Silencing of CXCR4 blocks breast cancer metastasis. *Cancer Res* **65**, 967-71.

Lin, Y. H., Park, Z. Y., Lin, D., Brahmbhatt, A. A., Rio, M. C., Yates, J. R., 3rd and Klemke, R. L. (2004). Regulation of cell migration and survival by focal adhesion targeting of Lasp-1. *J Cell Biol* **165**, 421-32.

Lindsay, M. A. (2002). Peptide-mediated cell delivery: application in protein target validation. *Curr Opin Pharmacol* **2**, 587-94.

Lindsay, S. L., Ramsey, S., Aitchison, M., Renne, T. and Evans, T. J. (2007). Modulation of lamellipodial structure and dynamics by NO-dependent phosphorylation of VASP Ser239. *J Cell Sci* **120**, 3011-21.

Loberg, R. D., Ying, C., Craig, M., Yan, L., Snyder, L. A. and Pienta, K. J. (2007). CCL2 as an important mediator of prostate cancer growth in vivo through the regulation of macrophage infiltration. *Neoplasia* **9**, 556-62.

Lohse, M. J., Benovic, J. L., Codina, J., Caron, M. G. and Lefkowitz, R. J. (1990). beta-Arrestin: a protein that regulates beta-adrenergic receptor function. *Science* **248**, 1547-50.

Luca, M., Huang, S., Gershenwald, J. E., Singh, R. K., Reich, R. and Bar-Eli, M. (1997). Expression of interleukin-8 by human melanoma cells up-regulates MMP-2 activity and increases tumor growth and metastasis. *Am J Pathol* **151**, 1105-13.

Luttrell, L. M., Daaka, Y. and Lefkowitz, R. J. (1999). Regulation of tyrosine kinase cascades by G-protein-coupled receptors. *Curr Opin Cell Biol* **11**, 177-83.

Mack, M., Luckow, B., Nelson, P. J., Cihak, J., Simmons, G., Clapham, P. R., Signoret, N., Marsh, M., Stangassinger, M., Borlat, F. et al. (1998). Aminooxypentane-RANTES induces CCR5 internalization but inhibits recycling: a novel inhibitory mechanism of HIV infectivity. *J Exp Med* **187**, 1215-24.

Mann, D. A. and Frankel, A. D. (1991). Endocytosis and targeting of exogenous HIV-1 Tat protein. *Embo J* **10**, 1733-9.

Manza, L. L., Stamer, S. L., Ham, A. J., Codreanu, S. G. and Liebler, D. C. (2005). Sample preparation and digestion for proteomic analyses using spin filters. *Proteomics* **5**, 1742-5.

Marchese, A. and Benovic, J. L. (2001). Agonist-promoted ubiquitination of the G protein-coupled receptor CXCR4 mediates lysosomal sorting. *J Biol Chem* **276**, 45509-12.

Mataraza, J. M., Briggs, M. W., Li, Z., Entwistle, A., Ridley, A. J. and Sacks, D. B. (2003). IQGAP1 promotes cell motility and invasion. *J Biol Chem* **278**, 41237-45.

Mataraza, J. M., Li, Z., Jeong, H. W., Brown, M. D. and Sacks, D. B. (2007). Multiple proteins mediate IQGAP1-stimulated cell migration. *Cell Signal* **19**, 1857-65.

Mateer, S. C., McDaniel, A. E., Nicolas, V., Habermacher, G. M., Lin, M. J., Cromer, D. A., King, M. E. and Bloom, G. S. (2002). The mechanism for regulation of the F-actin binding activity of IQGAP1 by calcium/calmodulin. *J Biol Chem* **277**, 12324-33.

Mateer, S. C., Morris, L. E., Cromer, D. A., Bensenor, L. B. and Bloom, G. S. (2004). Actin filament binding by a monomeric IQGAP1 fragment with a single calponin homology domain. *Cell Motil Cytoskeleton* **58**, 231-41.

May, M. J., D'Acquisto, F., Madge, L. A., Glockner, J., Pober, J. S. and Ghosh, S. (2000). Selective inhibition of NF-kappaB activation by a peptide that blocks the interaction of NEMO with the IkappaB kinase complex. *Science* **289**, 1550-4.

Mellor, H., Flynn, P., Nobes, C. D., Hall, A. and Parker, P. J. (1998). PRK1 is targeted to endosomes by the small GTPase, RhoB. *J Biol Chem* **273**, 4811-4.

Meresse, S., Gorvel, J. P. and Chavrier, P. (1995). The rab7 GTPase resides on a vesicular compartment connected to lysosomes. *J Cell Sci* **108 (Pt 11)**, 3349-58.

Merlot, S. and Firtel, R. A. (2003). Leading the way: Directional sensing through phosphatidylinositol 3-kinase and other signaling pathways. *J Cell Sci* **116**, 3471-8.

Miaczynska, M. and Zerial, M. (2002). Mosaic organization of the endocytic pathway. *Exp Cell Res* **272**, 8-14.

Michaelson, D., Silletti, J., Murphy, G., D'Eustachio, P., Rush, M. and Philips, M. R. (2001). Differential localization of Rho GTPases in live cells: regulation by hypervariable regions and RhoGDI binding. *J Cell Biol* **152**, 111-26.

Minamide, L. S., Painter, W. B., Schevzov, G., Gunning, P. and Bamburg, J. R. (1997). Differential regulation of actin depolymerizing factor and cofilin in response to alterations in the actin monomer pool. *J Biol Chem* **272**, 8303-9.

Montecucco, F., Bianchi, G., Gnerre, P., Bertolotto, M., Dallegri, F. and Ottonello, L. (2006). Induction of neutrophil chemotaxis by leptin: crucial role for p38 and Src kinases. *Ann N Y Acad Sci* **1069**, 463-71.

Moss, S. F. and Blaser, M. J. (2005). Mechanisms of disease: Inflammation and the origins of cancer. *Nat Clin Pract Oncol* **2**, 90-7; quiz 1 p following 113.

Mueller, S. G., Schraw, W. P. and Richmond, A. (1994). Melanoma growth stimulatory activity enhances the phosphorylation of the class II interleukin-8 receptor in non-hematopoietic cells. *J Biol Chem* **269**, 1973-80.

Mueller, S. G., White, J. R., Schraw, W. P., Lam, V. and Richmond, A. (1997). Ligand-induced desensitization of the human CXC chemokine receptor-2 is modulated by multiple serine residues in the carboxyl-terminal domain of the receptor. *J Biol Chem* **272**, 8207-14.

Muller, A., Homey, B., Soto, H., Ge, N., Catron, D., Buchanan, M. E., McClanahan, T., Murphy, E., Yuan, W., Wagner, S. N. et al. (2001). Involvement of chemokine receptors in breast cancer metastasis. *Nature* **410**, 50-6.

Murphy, P. M., Baggiolini, M., Charo, I. F., Hebert, C. A., Horuk, R., Matsushima, K., Miller, L. H., Oppenheim, J. J. and Power, C. A. (2000). International union of pharmacology. XXII. Nomenclature for chemokine receptors. *Pharmacol Rev* **52**, 145-76.

Neel, N. F., Lapierre, L. A., Goldenring, J. R. and Richmond, A. (2007). RhoB plays an essential role in CXCR2 sorting decisions. *J Cell Sci* **120**, 1559-71.

Neel, N. F., Schutyser, E., Sai, J., Fan, G. H. and Richmond, A. (2005). Chemokine receptor internalization and intracellular trafficking. *Cytokine Growth Factor Rev* **16**, 637-58.

Negus, R. P., Stamp, G. W., Relf, M. G., Burke, F., Malik, S. T., Bernasconi, S., Allavena, P., Sozzani, S., Mantovani, A. and Balkwill, F. R. (1995). The detection and localization of monocyte chemoattractant protein-1 (MCP-1) in human ovarian cancer. *J Clin Invest* **95**, 2391-6.

Neptune, E. R., Iiri, T. and Bourne, H. R. (1999). Galphai is not required for chemotaxis mediated by Gi-coupled receptors. *J Biol Chem* **274**, 2824-8.

Niebuhr, K., Ebel, F., Frank, R., Reinhard, M., Domann, E., Carl, U. D., Walter, U., Gertler, F. B., Wehland, J. and Chakraborty, T. (1997). A novel proline-rich motif present in ActA of Listeria monocytogenes and cytoskeletal proteins is the ligand for the EVH1 domain, a protein module present in the Ena/VASP family. *Embo J* **16**, 5433-44.

Nielsen, E., Christoforidis, S., Uttenweiler-Joseph, S., Miaczynska, M., Dewitte, F., Wilm, M., Hoflack, B. and Zerial, M. (2000). Rabenosyn-5, a novel Rab5 effector, is complexed with hVPS45 and recruited to endosomes through a FYVE finger domain. *J Cell Biol* **151**, 601-12.

Niu, J., Scheschonka, A., Druey, K. M., Davis, A., Reed, E., Kolenko, V., Bodnar, R., Voyno-Yasenetskaya, T., Du, X., Kehrl, J. et al. (2002). RGS3 interacts with 14-3-3 via the N-terminal region distinct from the RGS (regulator of G-protein signalling) domain. *Biochem J* **365**, 677-84.

Noel, A. C., Calle, A., Emonard, H. P., Nusgens, B. V., Simar, L., Foidart, J., Lapiere, C. M. and Foidart, J. M. (1991). Invasion of reconstituted basement membrane matrix is not correlated to the malignant metastatic cell phenotype. *Cancer Res* **51**, 405-14.

Noritake, J., Watanabe, T., Sato, K., Wang, S. and Kaibuchi, K. (2005). IQGAP1: a key regulator of adhesion and migration. *J Cell Sci* **118**, 2085-92.

Nyman, T., Page, R., Schutt, C. E., Karlsson, R. and Lindberg, U. (2002). A cross-linked profilin-actin heterodimer interferes with elongation at the fast-growing end of F-actin. *J Biol Chem* **277**, 15828-33.

Okamoto, T., Murayama, Y., Hayashi, Y., Inagaki, M., Ogata, E. and Nishimoto, I. (1991). Identification of a Gs activator region of the beta 2-adrenergic receptor that is autoregulated via protein kinase A-dependent phosphorylation. *Cell* **67**, 723-30.

Orsini, M. J., Parent, J. L., Mundell, S. J., Benovic, J. L. and Marchese, A. (1999). Trafficking of the HIV coreceptor CXCR4. Role of arrestins and identification of residues in the c-terminal tail that mediate receptor internalization. *J Biol Chem* **274**, 31076-86.

Owen, J. D., Strieter, R., Burdick, M., Haghnegahdar, H., Nanney, L., Shattuck-Brandt, R. and Richmond, A. (1997). Enhanced tumor-forming capacity for immortalized melanocytes expressing melanoma growth stimulatory activity/growth-regulated cytokine beta and gamma proteins. *Int J Cancer* **73**, 94-103.

Pereira-Leal, J. B. and Seabra, M. C. (2000). The mammalian Rab family of small GTPases: definition of family and subfamily sequence motifs suggests a mechanism for functional specificity in the Ras superfamily. *J Mol Biol* **301**, 1077-87.

Pippig, S., Andexinger, S., Daniel, K., Puzicha, M., Caron, M. G., Lefkowitz, R. J. and Lohse, M. J. (1993). Overexpression of beta-arrestin and beta-adrenergic receptor kinase augment desensitization of beta 2-adrenergic receptors. *J Biol Chem* **268**, 3201-8.

Pollard, J. W. (2004). Tumour-educated macrophages promote tumour progression and metastasis. *Nat Rev Cancer* **4**, 71-8.

Polverini, P. J., Cotran, P. S., Gimbrone, M. A., Jr. and Unanue, E. R. (1977). Activated macrophages induce vascular proliferation. *Nature* **269**, 804-6.

Popova, J. S. and Rasenick, M. M. (2004). Clathrin-mediated endocytosis of m3 muscarinic receptors. Roles for Gbetagamma and tubulin. *J Biol Chem* **279**, 30410-8.

Porcile, C., Bajetto, A., Barbieri, F., Barbero, S., Bonavia, R., Biglieri, M., Pirani, P., Florio, T. and Schettini, G. (2005). Stromal cell-derived factor-1alpha (SDF-1alpha/CXCL12) stimulates ovarian cancer cell growth through the EGF receptor transactivation. *Exp Cell Res* **308**, 241-53.

Proudfoot, A. E., Buser, R., Borlat, F., Alouani, S., Soler, D., Offord, R. E., Schroder, J. M., Power, C. A. and Wells, T. N. (1999). Amino-terminally modified RANTES analogues demonstrate differential effects on RANTES receptors. *J Biol Chem* **274**, 32478-85.

Ptasznik, A., Urbanowska, E., Chinta, S., Costa, M. A., Katz, B. A., Stanislaus, M. A., Demir, G., Linnekin, D., Pan, Z. K. and Gewirtz, A. M. (2002). Crosstalk between BCR/ABL oncoprotein and CXCR4 signaling through a Src family kinase in human leukemia cells. *J Exp Med* **196**, 667-78.

Reif, K. and Cyster, J. (2002). The CDM protein DOCK2 in lymphocyte migration. *Trends Cell Biol* **12**, 368-73.

Ren, M., Xu, G., Zeng, J., De Lemos-Chiarandini, C., Adesnik, M. and Sabatini, D. D. (1998). Hydrolysis of GTP on rab11 is required for the direct delivery of transferrin from the pericentriolar recycling compartment to the cell surface but not from sorting endosomes. *Proc Natl Acad Sci U S A* **95**, 6187-92.

Ren, X. D. and Schwartz, M. A. (2000). Determination of GTP loading on Rho. *Methods Enzymol* **325**, 264-72.

Richardson, R. M., Marjoram, R. J., Barak, L. S. and Snyderman, R. (2003). Role of the cytoplasmic tails of CXCR1 and CXCR2 in mediating leukocyte migration, activation, and regulation. *J Immunol* **170**, 2904-11.

Richardson, R. M., Pridgen, B. C., Haribabu, B., Ali, H. and Snyderman, R. (1998). Differential cross-regulation of the human chemokine receptors CXCR1 and CXCR2. Evidence for time-dependent signal generation. *J Biol Chem* **273**, 23830-6.

Ridley, A. J. (2001). Rho proteins: linking signaling with membrane trafficking. *Traffic* **2**, 303-10.

Rojas, R., Ruiz, W. G., Wang, E., Kinlough, C. L., Poland, P. A., Hughey, R. P., Dunn, K. W. and Apodaca, G. (2004). RhoB-dependent modulation of early endocytic traffic in Madin-Darby canine kidney cells. *J Biol Chem*.

Roland, J., Murphy, B. J., Ahr, B., Robert-Hebmann, V., Delauzun, V., Nye, K. E., Devaux, C. and Biard-Piechaczyk, M. (2003). Role of the intracellular domains of CXCR4 in SDF-1-mediated signaling. *Blood* **101**, 399-406.

Rosenberg, S. A. (2001). Progress in human tumour immunology and immunotherapy. *Nature* **411**, 380-4.

Ross, E. M. and Wilkie, T. M. (2000). GTPase-activating proteins for heterotrimeric G proteins: regulators of G protein signaling (RGS) and RGS-like proteins. *Annu Rev Biochem* **69**, 795-827.

Roy, M., Li, Z. and Sacks, D. B. (2004). IQGAP1 binds ERK2 and modulates its activity. *J Biol Chem* **279**, 17329-37.

Roy, M., Li, Z. and Sacks, D. B. (2005). IQGAP1 is a scaffold for mitogen-activated protein kinase signaling. *Mol Cell Biol* **25**, 7940-52.

Ruiz de Almodovar, C., Luttun, A. and Carmeliet, P. (2006). An SDF-1 trap for myeloid cells stimulates angiogenesis. *Cell* **124**, 18-21.

Sai, J., Walker, G., Wikswo, J. and Richmond, A. (2006). The IL sequence in the LLKIL motif in CXCR2 is required for full ligand-induced activation of Erk, Akt, and chemotaxis in HL60 cells. *J Biol Chem* **281**, 35931-41.

Samarin, S., Romero, S., Kocks, C., Didry, D., Pantaloni, D. and Carlier, M. F. (2003). How VASP enhances actin-based motility. *J Cell Biol* **163**, 131-42.

Sandilands, E., Cans, C., Fincham, V. J., Brunton, V. G., Mellor, H., Prendergast, G. C., Norman, J. C., Superti-Furga, G. and Frame, M. C. (2004). RhoB and actin polymerization coordinate Src activation with endosome-mediated delivery to the membrane. *Dev Cell* **7**, 855-69.

Sechi, A. S. and Wehland, J. (2004). ENA/VASP proteins: multifunctional regulators of actin cytoskeleton dynamics. *Front Biosci* **9**, 1294-310.

Seroussi, E., Pan, H. Q., Kedra, D., Roe, B. A. and Dumanski, J. P. (1998). Characterization of the human NIPSNAP1 gene from 22q12: a member of a novel gene family. *Gene* **212**, 13-20.

Servant, G., Weiner, O. D., Neptune, E. R., Sedat, J. W. and Bourne, H. R. (1999). Dynamics of a chemoattractant receptor in living neutrophils during chemotaxis. *Mol Biol Cell* **10**, 1163-78.

Sheff, D. R., Daro, E. A., Hull, M. and Mellman, I. (1999). The receptor recycling pathway contains two distinct populations of early endosomes with different sorting functions. *J Cell Biol* **145**, 123-39.

Shimada, T., Mernaugh, R. L. and Guengerich, F. P. (2005). Interactions of mammalian cytochrome P450, NADPH-cytochrome P450 reductase, and cytochrome b(5) enzymes. *Arch Biochem Biophys* **435**, 207-16.

Signoret, N., Hewlett, L., Wavre, S., Pelchen-Matthews, A., Oppermann, M. and Marsh, M. (2005). Agonist-induced endocytosis of CC chemokine receptor 5 is clathrin dependent. *Mol Biol Cell* **16**, 902-17.

Signoret, N., Oldridge, J., Pelchen-Matthews, A., Klasse, P. J., Tran, T., Brass, L. F., Rosenkilde, M. M., Schwartz, T. W., Holmes, W., Dallas, W. et al. (1997). Phorbol esters and SDF-1 induce rapid endocytosis and down modulation of the chemokine receptor CXCR4. *J Cell Biol* **139**, 651-64.

Signoret, N., Pelchen-Matthews, A., Mack, M., Proudfoot, A. E. and Marsh, M. (2000). Endocytosis and recycling of the HIV coreceptor CCR5. *J Cell Biol* **151**, 1281-94.

Singh, R. K., Gutman, M., Radinsky, R., Bucana, C. D. and Fidler, I. J. (1994). Expression of interleukin 8 correlates with the metastatic potential of human melanoma cells in nude mice. *Cancer Res* **54**, 3242-7.

Skoble, J., Auerbuch, V., Goley, E. D., Welch, M. D. and Portnoy, D. A. (2001). Pivotal role of VASP in Arp2/3 complex-mediated actin nucleation, actin branch-formation, and Listeria monocytogenes motility. *J Cell Biol* **155**, 89-100.

Slamon, D. J., Godolphin, W., Jones, L. A., Holt, J. A., Wong, S. G., Keith, D. E., Levin, W. J., Stuart, S. G., Udove, J., Ullrich, A. et al. (1989). Studies of the HER-2/neu proto-oncogene in human breast and ovarian cancer. *Science* **244**, 707-12.

Smith, D. R., Polverini, P. J., Kunkel, S. L., Orringer, M. B., Whyte, R. I., Burdick, M. D., Wilke, C. A. and Strieter, R. M. (1994). Inhibition of interleukin 8 attenuates angiogenesis in bronchogenic carcinoma. *J Exp Med* **179**, 1409-15.

Snow, B. E., Hall, R. A., Krumins, A. M., Brothers, G. M., Bouchard, D., Brothers, C. A., Chung, S., Mangion, J., Gilman, A. G., Lefkowitz, R. J. et al. (1998). GTPase activating specificity of RGS12 and binding specificity of an alternatively spliced PDZ (PSD-95/Dlg/ZO-1) domain. *J Biol Chem* **273**, 17749-55.

Soldati, T., Rancano, C., Geissler, H. and Pfeffer, S. R. (1995). Rab7 and Rab9 are recruited onto late endosomes by biochemically distinguishable processes. *J Biol Chem* **270**, 25541-8.

Son, D. S., Parl, A. K., Rice, V. M. and Khabele, D. (2007). Keratinocyte chemoattractant (KC)/human growth-regulated oncogene (GRO) chemokines and pro-inflammatory chemokine networks in mouse and human ovarian epithelial cancer cells. *Cancer Biol Ther* **6**, 1302-12.

Sonnichsen, B., De Renzis, S., Nielsen, E., Rietdorf, J. and Zerial, M. (2000). Distinct membrane domains on endosomes in the recycling pathway visualized by multicolor imaging of Rab4, Rab5, and Rab11. *J Cell Biol* **149**, 901-14.

Stenmark, H., Parton, R. G., Steele-Mortimer, O., Lutcke, A., Gruenberg, J. and Zerial, M. (1994). Inhibition of rab5 GTPase activity stimulates membrane fusion in endocytosis. *Embo J* **13**, 1287-96.

Steuve, S., Devosse, T., Lauwers, E., Vanderwinden, J. M., Andre, B., Courtoy, P. J. and Pirson, I. (2006). Rhophilin-2 is targeted to late-endosomal structures of the vesicular machinery in the presence of activated RhoB. *Exp Cell Res* **312**, 3981-9.

Stradal, T. E., Rottner, K., Disanza, A., Confalonieri, S., Innocenti, M. and Scita, G. (2004). Regulation of actin dynamics by WASP and WAVE family proteins. *Trends Cell Biol* **14**, 303-11.

Strieter, R. M., Polverini, P. J., Arenberg, D. A., Walz, A., Opdenakker, G., Van Damme, J. and Kunkel, S. L. (1995). Role of C-X-C chemokines as regulators of angiogenesis in lung cancer. *J Leukoc Biol* **57**, 752-62.

Sun, Y., Cheng, Z., Ma, L. and Pei, G. (2002). Beta-arrestin2 is critically involved in CXCR4-mediated chemotaxis, and this is mediated by its enhancement of p38 MAPK activation. *J Biol Chem* **277**, 49212-9.

Takahashi, K., Nakajima, E. and Suzuki, K. (2006). Involvement of protein phosphatase 2A in the maintenance of E-cadherin-mediated cell-cell adhesion through recruitment of IQGAP1. *J Cell Physiol* **206**, 814-20.

Takahashi, K. and Suzuki, K. (2006). Regulation of protein phosphatase 2A-mediated recruitment of IQGAP1 to beta1 integrin by EGF through activation of Ca2+/calmodulin-dependent protein kinase II. *J Cell Physiol* **208**, 213-9.

Takenawa, T. and Suetsugu, S. (2007). The WASP-WAVE protein network: connecting the membrane to the cytoskeleton. *Nat Rev Mol Cell Biol* **8**, 37-48.

Thompson, E. W., Brunner, N., Torri, J., Johnson, M. D., Boulay, V., Wright, A., Lippman, M. E., Steeg, P. S. and Clarke, R. (1993). The invasive and metastatic properties of hormone-independent but hormone-responsive variants of MCF-7 human breast cancer cells. *Clin Exp Metastasis* **11**, 15-26.

Tilton, B., Ho, L., Oberlin, E., Loetscher, P., Baleux, F., Clark-Lewis, I. and Thelen, M. (2000). Signal transduction by CXC chemokine receptor 4. Stromal cell-derived factor 1 stimulates prolonged protein kinase B and extracellular signal-regulated kinase 2 activation in T lymphocytes. *J Exp Med* **192**, 313-24.

Ueda, Y., Neel, N. F., Schutyser, E., Raman, D. and Richmond, A. (2006). Deletion of the COOH-terminal domain of CXC chemokine receptor 4 leads to the down-regulation of cell-to-cell contact, enhanced motility and proliferation in breast carcinoma cells. *Cancer Res* **66**, 5665-75.

Ullrich, O., Reinsch, S., Urbe, S., Zerial, M. and Parton, R. G. (1996). Rab11 regulates recycling through the pericentriolar recycling endosome. *J Cell Biol* **135**, 913-24.

van der Bliek, A. M., Redelmeier, T. E., Damke, H., Tisdale, E. J., Meyerowitz, E. M. and Schmid, S. L. (1993). Mutations in human dynamin block an intermediate stage in coated vesicle formation. *J Cell Biol* **122**, 553-63.

van der Sluijs, P., Hull, M., Webster, P., Male, P., Goud, B. and Mellman, I. (1992). The small GTP-binding protein rab4 controls an early sorting event on the endocytic pathway. *Cell* **70**, 729-40.

Venkatesan, S., Rose, J. J., Lodge, R., Murphy, P. M. and Foley, J. F. (2003). Distinct mechanisms of agonist-induced endocytosis for human chemokine receptors CCR5 and CXCR4. *Mol Biol Cell* **14**, 3305-24.

Vicari, A. P., Vanbervliet, B., Massacrier, C., Chiodoni, C., Vaure, C., Ait-Yahia, S., Dercamp, C., Matsos, F., Reynard, O., Taverne, C. et al. (2004). In vivo manipulation of dendritic cell migration and activation to elicit antitumour immunity. *Novartis Found Symp* **256**, 241-54; discussion 254-69.

Vila-Coro, A. J., Mellado, M., Martin de Ana, A., Martinez, A. C. and Rodriguez-Frade, J. M. (1999). Characterization of RANTES- and aminooxypentane-RANTES-triggered desensitization signals reveals differences in recruitment of the G protein-coupled receptor complex. *J Immunol* **163**, 3037-44.

Vroon, A., Lombardi, M. S., Kavelaars, A. and Heijnen, C. J. (2007). Taxol normalizes the impaired agonist-induced beta2-adrenoceptor internalization in splenocytes from GRK2+/- mice. *Eur J Pharmacol* **560**, 9-16.

Wang, B., Hendricks, D. T., Wamunyokoli, F. and Parker, M. I. (2006a). A growth-related oncogene/CXC chemokine receptor 2 autocrine loop contributes to cellular proliferation in esophageal cancer. *Cancer Res* **66**, 3071-7.

Wang, D., Wang, H., Brown, J., Daikoku, T., Ning, W., Shi, Q., Richmond, A., Strieter, R., Dey, S. K. and DuBois, R. N. (2006b). CXCL1 induced by prostaglandin E2 promotes angiogenesis in colorectal cancer. *J Exp Med* **203**, 941-51.

Wang, Q., Song, C. and Li, C. C. (2004). Molecular perspectives on p97-VCP: progress in understanding its structure and diverse biological functions. *J Struct Biol* **146**, 44-57.

Watanabe, T., Wang, S., Noritake, J., Sato, K., Fukata, M., Takefuji, M., Nakagawa, M., Izumi, N., Akiyama, T. and Kaibuchi, K. (2004). Interaction with IQGAP1 links APC to Rac1, Cdc42, and actin filaments during cell polarization and migration. *Dev Cell* **7**, 871-83.

Weber, M., Blair, E., Simpson, C. V., O'Hara, M., Blackburn, P. E., Rot, A., Graham, G. J. and Nibbs, R. J. (2004). The chemokine receptor D6 constitutively traffics to and from the cell surface to internalize and degrade chemokines. *Mol Biol Cell* **15**, 2492-508.

Weiner, O. D. (2002). Rac activation: P-Rex1 - a convergence point for PIP(3) and Gbetagamma? *Curr Biol* **12**, R429-31.

Welch, M. D., DePace, A. H., Verma, S., Iwamatsu, A. and Mitchison, T. J. (1997). The human Arp2/3 complex is composed of evolutionarily conserved subunits and is localized to cellular regions of dynamic actin filament assembly. *J Cell Biol* **138**, 375-84.

Wennerberg, K. and Der, C. J. (2004). Rho-family GTPases: it's not only Rac and Rho (and I like it). *J Cell Sci* **117**, 1301-12.

Wente, M. N., Keane, M. P., Burdick, M. D., Friess, H., Buchler, M. W., Ceyhan, G. O., Reber, H. A., Strieter, R. M. and Hines, O. J. (2006). Blockade of the chemokine receptor CXCR2 inhibits pancreatic cancer cell-induced angiogenesis. *Cancer Lett* **241**, 221-7.

Wheeler, A. P. and Ridley, A. J. (2004). Why three Rho proteins? RhoA, RhoB, RhoC, and cell motility. *Exp Cell Res* **301**, 43-9.

Wherlock, M., Gampel, A., Futter, C. and Mellor, H. (2004). Farnesyltransferase inhibitors disrupt EGF receptor traffic through modulation of the RhoB GTPase. *J Cell Sci* **117**, 3221-31.

Worthylake, R. A., Lemoine, S., Watson, J. M. and Burridge, K. (2001). RhoA is required for monocyte tail retraction during transendothelial migration. *J Cell Biol* **154**, 147-60.

Yang, G., Rosen, D. G., Zhang, Z., Bast, R. C., Jr., Mills, G. B., Colacino, J. A., Mercado-Uribe, I. and Liu, J. (2006). The chemokine growth-regulated oncogene 1 (Gro-1) links RAS signaling to the senescence of stromal fibroblasts and ovarian tumorigenesis. *Proc Natl Acad Sci U S A* **103**, 16472-7.

Yang, L., Huang, J., Ren, X., Gorska, A. E., Chytil, A., Aakre, M., Carbone, D. P., Matrisian, L. M., Richmond, A., Lin, P. C. et al. (2008). Abrogation of TGFbeta Signaling in Mammary Carcinomas Recruits Gr-1+CD11b+ Myeloid Cells that Promote Metastasis. *Cancer Cell* **13**, 23-35.

Yang, W., Wang, D. and Richmond, A. (1999). Role of clathrin-mediated endocytosis in CXCR2 sequestration, resensitization, and signal transduction. *J Biol Chem* **274**, 11328-33.

Yarden, Y. and Sliwkowski, M. X. (2001). Untangling the ErbB signalling network. *Nat Rev Mol Cell Biol* **2**, 127-37.

Yates, J. R., 3rd, Eng, J. K., McCormack, A. L. and Schieltz, D. (1995). Method to correlate tandem mass spectra of modified peptides to amino acid sequences in the protein database. *Anal Chem* **67**, 1426-36.

Yatsunami, J., Tsuruta, N., Ogata, K., Wakamatsu, K., Takayama, K., Kawasaki, M., Nakanishi, Y., Hara, N. and Hayashi, S. (1997). Interleukin-8 participates in angiogenesis in non-small cell, but not small cell carcinoma of the lung. *Cancer Lett* **120**, 101-8.

Yoneda, J., Kuniyasu, H., Crispens, M. A., Price, J. E., Bucana, C. D. and Fidler, I. J. (1998). Expression of angiogenesis-related genes and progression of human ovarian carcinomas in nude mice. *J Natl Cancer Inst* **90**, 447-54.

Yu, D. and Hung, M. C. (2000). Overexpression of ErbB2 in cancer and ErbB2-targeting strategies. *Oncogene* **19**, 6115-21.

Zaslaver, A., Feniger-Barish, R. and Ben-Baruch, A. (2001). Actin filaments are involved in the regulation of trafficking of two closely related chemokine receptors, CXCR1 and CXCR2. *J Immunol* **166**, 1272-84.

Zerial, M. and McBride, H. (2001). Rab proteins as membrane organizers. *Nat Rev Mol Cell Biol* **2**, 107-17.

Zhang, H., Meng, F., Chu, C. L., Takai, T. and Lowell, C. A. (2005). The Src family kinases Hck and Fgr negatively regulate neutrophil and dendritic cell chemokine signaling via PIR-B. *Immunity* **22**, 235-46.

Zhang, L., Torgerson, T. R., Liu, X. Y., Timmons, S., Colosia, A. D., Hawiger, J. and Tam, J. P. (1998). Preparation of functionally active cell-permeable

peptides by single-step ligation of two peptide modules. *Proc Natl Acad Sci U S A* **95**, 9184-9.

Zhang, Y., Tu, Y., Gkretsi, V. and Wu, C. (2006). Migfilin interacts with vasodilator-stimulated phosphoprotein (VASP) and regulates VASP localization to cell-matrix adhesions and migration. *J Biol Chem* **281**, 12397-407.

Zhou, Y., Zhang, J., Liu, Q., Bell, R., Muruve, D. A., Forsyth, P., Arcellana-Panlilio, M., Robbins, S. and Yong, V. W. (2005). The chemokine GRO-alpha (CXCL1) confers increased tumorigenicity to glioma cells. *Carcinogenesis* **26**, 2058-68.

Zhuang, S., Nguyen, G. T., Chen, Y., Gudi, T., Eigenthaler, M., Jarchau, T., Walter, U., Boss, G. R. and Pilz, R. B. (2004). Vasodilator-stimulated phosphoprotein activation of serum-response element-dependent transcription occurs downstream of RhoA and is inhibited by cGMP-dependent protein kinase phosphorylation. *J Biol Chem* **279**, 10397-407.

Zimmermann, N., Conkright, J. J. and Rothenberg, M. E. (1999). CC chemokine receptor-3 undergoes prolonged ligand-induced internalization. *J Biol Chem* **274**, 12611-8.

Zlotnik, A. (2006). Involvement of chemokine receptors in organ-specific metastasis. *Contrib Microbiol* **13**, 191-9.

Zou, W. (2005). Immunosuppressive networks in the tumour environment and their therapeutic relevance. *Nat Rev Cancer* **5**, 263-74.